

HDL-DS-89-1

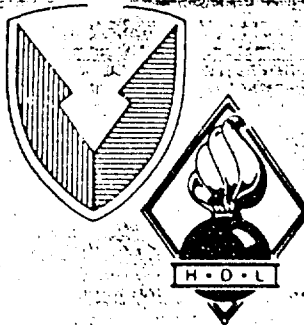
September 1989

Host Materials for Transition-Metal Ions

by Clyde A. Morrison

AD-A213 605

DTIC
ELECTED
OCT 24 1989
S D
Dcs



U.S. Army Laboratory Command
Harry Diamond Laboratories
Adelphi, MD 20783-1197

Approved for public release; distribution unlimited.

89 10 23 087

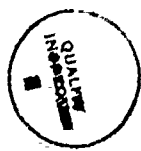
UNCLASSIFIED

SECURITY CLASSIFICATION OF THIS PAGE

REPORT DOCUMENTATION PAGE				Form Approved OMB No. 0704-0188
1a. REPORT SECURITY CLASSIFICATION Unclassified		1b. RESTRICTIVE MARKINGS		
2a. SECURITY CLASSIFICATION AUTHORITY		3. DISTRIBUTION/AVAILABILITY OF REPORT Approved for public release; distribution unlimited.		
2b. DECLASSIFICATION/DOWNGRADING SCHEDULE				
4. PERFORMING ORGANIZATION REPORT NUMBER(S) HDL-DS-89-1		5. MONITORING ORGANIZATION REPORT NUMBER(S)		
6a. NAME OF PERFORMING ORGANIZATION Harry Diamond Laboratories	6b. OFFICE SYMBOL (if applicable) SLCHD-ST-AP	7a. NAME OF MONITORING ORGANIZATION		
6c. ADDRESS (City, State, and ZIP Code) 2800 Powder Mill Road Adelphi, MD 20783-1197		7b. ADDRESS (City, State, and ZIP Code)		
8a. NAME OF FUNDING/SPONSORING ORGANIZATION Night-Vision and Electro-Optics Lab	8b. OFFICE SYMBOL (if applicable)	9. PROCUREMENT INSTRUMENT IDENTIFICATION NUMBER		
8c. ADDRESS (City, State, and ZIP Code) Fort Belvoir, VA 22060		10. SOURCE OF FUNDING NUMBERS PROGRAM ELEMENT NO. P611102. H440011	PROJECT NO. H44	TASK NO. WORK UNIT ACCESSION NO.
11. TITLE (Include Security Classification) Host Materials for Transition-Metal Ions				
12. PERSONAL AUTHOR(S) Clyde A. Morrison				
13a. TYPE OF REPORT Interim	13b. TIME COVERED FROM July 83 TO July 88	14. DATE OF REPORT (Year, Month, Day) September 1989	15. PAGE COUNT 164	
16. SUPPLEMENTARY NOTATION AMS code: 61102.H440011, HDL project: AE1951				
17. COSATI CODES		18. SUBJECT TERMS (Continue on reverse if necessary and identify by block number) Transition metal ions, crystal-field parameters, crystal-field components, spectra		
FIELD	GROUP	SUB-GROUP		
19. ABSTRACT (Continue on reverse if necessary and identify by block number) Data are given on host materials for lasers that use the transition-metal ions. Included in each section are the crystallographic data, x-ray data, crystal-field components A_{nm} , crystal field parameters $B_{nm}(Dq)$, and spin-orbit constants (ζ) . One section contains the phenomenological free-ion parameters $F^{(k)}$, ζ , and α , which have been obtained by fitting the reported free-ion data. There is a bibliography for each host which, depending on the host, is more or less complete. The data contained on each host material will be updated periodically, and data on new host materials will be added.				
20. DISTRIBUTION/AVAILABILITY OF ABSTRACT <input checked="" type="checkbox"/> UNCLASSIFIED/UNLIMITED <input type="checkbox"/> SAME AS RPT. <input type="checkbox"/> DTIC USERS			21. ABSTRACT SECURITY CLASSIFICATION Unclassified	
22a. NAME OF RESPONSIBLE INDIVIDUAL Clyde A. Morrison			22b. TELEPHONE (Include Area Code) (202) 394-2042	22c. OFFICE SYMBOL SLCHD-ST-AP

CONTENTS

	<u>Page</u>
1. INTRODUCTION	13
2. PRESENTATION OF DATA	24
2.1 Crystallographic Data	24
2.2 Crystal-Field Components, A_{nm} , and Parameters, B_{nm}	24
2.3 Experimental Results	25
2.3.1 Relation of Dq with B_{40}	25
2.3.2 Relation between Slater and Racah parameters	28
2.4 Bibliographies and Reference Lists	30
2.5 References	30
3. $Y_3Al_5O_{12}$ (YAG)	32
3.1 Crystallographic Data on $Y_3Al_5O_{12}$	32
3.2 Crystal Fields for 24(d) (S_4) Site	32
3.2.1 Crystal-field components, A_{nm} , for Al_2 (S_4) site	32
3.2.2 Theoretical crystal-field parameters, B_{nm} , for Al_2 (S_4) site for transition-metal ions with electronic configuration $3d^N$	33
3.3 Crystal Fields for 16(a) (C_{3i}) Site	34
3.3.1 Crystal-field components, A_{nm} , for Al_1 (C_{3i}) site	34
3.3.2 Theoretical crystal-field parameters, B_{nm} , for Al_1 (C_{3i}) site	35
3.4 Experimental Values of B_{40} , $F^{(2)}$, and $F^{(4)}$ for nd^N Ions	36
3.5 Bibliography and References	37
4. K_2NaAlF_6	40
4.1 Crystallographic Data on Two Forms of K_2NaAlF_6	40
4.1.1 Cubic T_h^6 (Pa3), 205, $Z = 4$, elpasoite	40
4.1.2 Cubic O_h^5 (Fm3m), 225, $Z = 4$, elpasolite	40



by	
Distribution /	
Availability Codes	
Dist	Avy
A-1	

CONTENTS (cont'd)

	<u>Page</u>
4.2 Crystal Fields for $\text{Pa}\bar{3}$ Form	40
4.2.1 Crystal-field components, A_{nm} , for Al (C_{3i}) site	40
4.2.2 Theoretical crystal-field parameters, B_{nm} , for monopole A_{nm} for Al (C_{3i}) site	41
4.3 Crystal Fields for $\text{Fm}\bar{3}m$ Form	42
4.3.1 Crystal-field components, A_{nm} , for Al (O_h) site	42
4.3.2 Theoretical crystal-field parameters, B_{nm} , for A_{nm} of Al (O_h) site	43
4.4 Bibliography and References	44
5. Cs_2TiF_6	45
5.1 Crystallographic Data on Two Forms of Cs_2TiF_6	45
5.1.1 Cubic O_h^5 ($\text{Fm}\bar{3}m$), 225, $Z = 4$	45
5.1.2 Hexagonal D_{3d}^3 ($\text{P}\bar{3}m1$), 164, $Z = 1$	45
5.2 Crystal Fields for O_h Site	45
5.2.1 Crystal-field components, A_{nm} , for Ti (O_h) site	45
5.2.2 Theoretical crystal-field parameters, B_{nm} , for A_{nm} of Ti (O_h) site	46
5.3 Crystal Fields for D_{3d} Site	47
5.3.1 Crystal-field components, A_{nm} , for Ti (D_{3d}) site	47
5.3.2 Theoretical crystal-field parameters, B_{nm} , for A_{nm} of Ti (D_{3d}) site	48
5.4 Bibliography and References	49
6. $\text{NH}_4\text{Al}(\text{SO}_4)_2$	50
6.1 Crystallographic Data on $\text{NH}_4\text{Al}(\text{SO}_4)_2$	50
6.2 Crystal Fields for Al (D_2) Site	50
6.2.1 Crystal-field components, A_{nm} , for Al (D_2) site	50
6.2.2 Theoretical crystal-field parameters, B_{nm} , for A_{nm} of Al (D_2) site	51
6.3 Experimental Parameters	51
6.4 Bibliography and References	52

CONTENTS (cont'd)

	<u>Page</u>
7. MgF_2	53
7.1 Crystallographic Data on MgF_2	53
7.2 Crystal Fields for Mg (D_{2h}) Site	53
7.2.1 Crystal-field components, A_{nm} , for Mg (D_{2h}) site	53
7.2.2 Theoretical crystal-field parameters, B_{nm} , for A_{nm} of Mg (D_{2h}) site	54
7.3 Experimental Parameters	55
7.4 Bibliography and References	56
8. MnF_2	58
8.1 Crystallographic Data on MnF_2	58
8.2 Crystal Fields for Mn (D_{2h}) Site	58
8.2.1 Crystal-field components, A_{nm} , for Mn (D_{2h}) site	58
8.2.2 Theoretical crystal-field parameters, B_{nm} , for A_{nm} of Mn (D_{2h}) site	59
8.3 Experimental Parameters	61
8.4 References	61
9. ZnF_2	63
9.1 Crystallographic Data on ZnF_2	63
9.2 Crystal Fields for Zn (D_{2h}) Site	63
9.2.1 Crystal-field components, A_{nm} , for Zn (D_{2h}) site	63
9.2.2 Theoretical crystal-field parameters, B_{nm} , for A_{nm} of Zn (D_{2h}) site	64
9.3 Experimental Parameters	65
9.4 Bibliography and References	66
10. MgO	67
10.1 Crystallographic Data on MgO	67
10.2 Crystal Fields for Mg (O_h) site	67
10.2.1 Crystal-field components, A_{nm} , for Mg (O_h) site	67
10.2.2 Theoretical crystal-field parameters, B_{nm} , for A_{nm} of Mg (O_h) site	68
10.3 Experimental Parameters	69
10.4 Bibliography and References	69

CONTENTS (cont'd)

	<u>Page</u>
11. $\text{Be}_3\text{Al}_2(\text{SiO}_3)_6$ (Beryl, Emerald)	74
11.1 Crystallographic and X-Ray Data on $\text{Be}_3\text{Al}_2(\text{SiO}_3)_6$	74
11.2 Crystal Fields for Al (D_3) Site	74
11.2.1 Crystal-field components, A_{nm} , for Al (D_3) site	74
11.2.2 Theoretical crystal-field parameters, B_{nm} , for A_{nm} of Al (D_3) site	75
11.3 Experimental Parameters	75
11.4 Bibliography	76
12. $\text{Na}_3\text{M}_2\text{Li}_3\text{F}_{12}$ (Fluoride Garnets)	77
12.1 Crystallographic Data on $\text{Na}_3\text{M}_2\text{Li}_3\text{F}_{12}$	77
12.2 X-Ray Data on $\text{Na}_3\text{M}_2\text{Li}_3\text{F}_{12}$	77
12.3 Crystal-Field Data	78
12.3.1 Crystal-field components, A_{nm} , for M (C_{3i}) site of $\text{Na}_3\text{M}_2\text{Li}_3\text{F}_{12}$	78
12.3.2 Theoretical crystal-field parameters, B_{nm} , for Al (C_{3i}) site of $\text{Na}_3\text{Al}_2\text{Li}_3\text{F}_{12}$	79
12.3.3 Theoretical crystal-field parameters, B_{nm} , for Sc (C_{3i}) site of $\text{Na}_3\text{Sc}_2\text{Li}_3\text{F}_{12}$	80
12.3.4 Theoretical crystal-field parameters, B_{nm} , for In (C_{3i}) site of $\text{Na}_3\text{In}_2\text{Li}_3\text{F}_{12}$	81
12.4 Experimental Parameters for Cr^{3+} in $\text{Na}_3\text{M}_2\text{Li}_3\text{F}_{12}$	81
12.5 Bibliography and References	82
13. Cs_2SnBr_6	84
13.1 Crystallographic Data on Cs_2SnBr_6	84
13.2 Crystal-Field Components, A_{nm} , for Sn (O_h) Site	84
13.3 Experimental Parameters	84
13.4 Bibliography and References	84
14. KMgF_3	86
14.1 Crystallographic Data on KMgF_3	86
14.2 Crystal-Field Components, A_{nm} , for Mg (O_h) Site	86
14.3 Experimental Parameters	86
14.4 Bibliography and References	86

CONTENTS (cont'd)

	<u>Page</u>
15. BeAl_2O_4 (Chrysoberyl, Cr: BeAl_2O_4 = Alexandrite)	90
15.1 Crystallographic Data on BeAl_2O_4	90
15.2 X-Ray Data	90
15.3 Crystal-Field Components	91
15.4 Bibliography and References	91
16. ZnAl_2O_4	94
16.1 Crystallographic Data on ZnAl_2O_4	94
16.2 Crystal Fields for Zn (T_d) Site	94
16.2.1 Crystal-field components, A_{nm} , for Zn (T_d) site	94
16.2.2 Crystal-field components, A_{nm} , for Al (D_{3d}) site	94
16.3 Experimental Values of $F^{(2)}$, $F^{(4)}$, α , ζ , and B_{nm}^N for nd^N Ions	94
16.4 Bibliography and References	95
17. LiMgZrO_4	96
17.1 Crystallographic Data on LiMgZrO_4	96
17.2 Crystal-Field Components, A_{nm} , for 4(a) (D_{2d}) Site	96
17.3 Reference	96
18. $\text{La}_3\text{Lu}_2\text{Ga}_3\text{O}_{12}$	97
18.1 Crystallographic Data on $\text{La}_3\text{Lu}_2\text{Ga}_3\text{O}_{12}$	97
18.2 Crystal-Field Components, A_{nm}	97
18.2.1 For Ga ion in 24(d) (S_4) site	97
18.2.2 For Lu ion in 16(a) (C_{3i}) site	97
18.2.3 For La ion in 24(c) (D_2) site	98
18.3 Experimental Parameters	98
18.4 Bibliography and References	98
19. ZnO	100
19.1 Crystallographic Data on ZnO	100
19.2 X-Ray Data	100
19.3 Crystal-Field Components, A_{nm} , for Zn (C_{3v}) Site	100
19.4 Experimental Parameters	101
19.5 Bibliography and References	101

CONTENTS (cont'd)

	<u>Page</u>
20. ZnS	104
20.1 Crystallographic Data on ZnS	104
20.1.1 Cubic T_d^2 ($F\bar{4}3m$), 216, $Z = 4$	104
20.1.2 Hexagonal C_{6v}^4 ($P6_3mc$), 186, $Z = 2$	104
20.2 Crystal Fields	104
20.2.1 Crystal-field components, A_{nm} , for Zn (T_d) site of cubic ZnS	104
20.2.2 Crystal-field components, A_{nm} , for Zn (C_{3v}) site of hexagonal ZnS	104
20.3 Experimental Values of $F^{(2)}$, $F^{(4)}$, ζ , and B_{40} for $3d^N$ Ions	105
20.4 Bibliography and References	105
21. K_2PtCl_6	108
21.1 Crystallographic Data on K_2PtCl_6	108
21.2 Crystal-Field Components, A_{nm} , for Pt (O_h) Site	108
21.3 Experimental Parameters	108
21.4 Bibliography and References	108
22. $Y_3Ga_5O_{12}$ (YGG)	110
22.1 Crystallographic Data on $Y_3Ga_5O_{12}$	110
22.2 Crystal-Field Components, A_{nm}	110
22.2.1 For Ga ion in 24(d) (S_4) site	110
22.2.2 For Ga_1 ion in 16(a) (C_{3i}) site	110
22.3 Experimental Parameters	111
22.4 Bibliography and References	111
23. $La_{2-x}Sr_xCuO_4$	113
23.1 Crystallographic Data on $La_{1.85}Sr_{0.15}CuO_4$	113
23.1.1 Tetragonal, D_{4h}^{17} ($I\bar{4}/mmm$), 139, $Z = 2$; $T = 300$ K	113
23.1.2 Orthorhombic, D_{2h}^{18} ($Cmca$), 64, $Z = 4$; $T = 10$ K and 60 K	113

CONTENTS (cont'd)

	<u>Page</u>
23.2 X-Ray Data	113
23.2.1 Tetragonal, T = 300 K	113
23.2.2 Orthorhombic, T = 10 K and 60 K	113
23.3 Crystal-Field Components, A_{nm}	114
23.3.1 For La (C_{4v}) site in tetragonal $La_{1.85}Sr_{0.15}CuO_4$	114
23.3.2 For L_a (C_s) site orthorhombic $La_{1.85}Sr_{0.15}CuO_4$	114
23.4 References	116
24. Al_2O_3 (Corundum)	117
24.1 Crystallographic Data on Al_2O_3	117
24.2 X-Ray Data	117
24.3 Crystal-Field Components, A_{nm} , for Al (C_3) Site	117
24.4 Experimental Parameters for Transition-Metal Ions	119
24.5 Bibliography and References	120
25. $MgAl_2O_4$	124
25.1 Crystallographic Data on $MgAl_2O_4$	124
25.2 Crystal-Field Components, A_{nm}	124
25.2.1 For Al (D_{3d}) site	124
25.2.2 For Mg (T_d) site	124
25.3 Experimental Parameters for Transition-Metal Ions	124
25.4 Bibliography and References	125
26. $A_3^{+2}B_2^{+3}Ge_3O_{12}$ (Germanium Garnet)	126
26.1 Crystallographic Data on $A_3B_2Ge_3O_{12}$	126
26.2 X-Ray Data on $A_3B_2Ge_3O_{12}$	126
26.3 Crystal-Field Components, A_{nm}	127
26.3.1 For Al ion in 16(a) (C_{3i}) site in $Ca_3Al_2Ge_3O_{12}$	127
26.3.2 For Sc ion in 16(a) (C_{3i}) site in $Ca_3Sc_2Ge_3O_{12}$	127
26.3.3 For Lu ion in 16(a) (C_{3i}) site in $Ca_3Lu_2Ge_3O_{12}$	127
26.3.4 For In ion in 16(a) (C_{3i}) site in $Ca_3In_2Ge_3O_{12}$	128
26.3.5 For Sc ion in 16(a) (C_{3i}) site in $Sr_3Sc_2Ge_3O_{12}$	128
26.3.6 For Sc ion in 16(a) (C_{3i}) site in $Cd_3Sc_2Ge_3O_{12}$	128
26.4 Experimental Values of B_{40} , $F^{(2)}$, and $F^{(4)}$ for nd^N Ions in $Ca_3Ga_2Ge_3O_{12}$	128
26.5 Bibliography and References	129

CONTENTS (cont'd)

	<u>Page</u>
27. $ZnGa_2O_4$	131
27.1 Crystallographic Data on $ZnGa_2O_4$	131
27.2 Crystal-Field Components, A_{nm}	131
27.2.1 For Zn (T_d) site	131
27.2.2 For Ga (D_{3d}) site	131
27.3 Bibliography and References	131
28. Cs_2GeF_6	133
28.1 Crystallographic Data on Cs_2GeF_6	133
28.2 Crystal-Field Components, A_{nm}	133
28.2.1 For Ge (O_h) site	133
28.2.2 For Cs (T_d) site	133
28.3 Experimental Parameters	133
28.4 Index of Refraction	134
28.5 Bibliography and References	134
29. $R_2Ti_2O_7$ (R=Y)	136
29.1 Crystallographic Data on $R_2Ti_2O_7$	136
29.2 X-Ray Data on $R_2Ti_2O_7$ and Polarizabilities, α_R , of Rare-Earth Ions, R^{3+} ($4f^N$)	136
29.3 Crystal-Field Components, A_{nm}	136
29.3.1 A_{20} for R site 16c (D_{3d})	137
29.3.2 A_{40} for R site 16c (D_{3d})	137
29.3.3 A_{43} for R site 16c (D_{3d})	137
29.3.4 A_{60} for R site 16c (D_{3d})	138
29.3.5 A_{63} for R site 16c (D_{3d})	138
29.3.6 A_{66} for R site 16c (D_{3d})	138
29.3.7 A_{20} for Ti site 16c (D_{3d})	139
29.3.8 A_{40} for Ti site 16d (D_{3d})	139
29.3.9 A_{43} for Ti site 16d (D_{3d})	139
29.3.10 A_{60} for Ti site 16d (D_{3d})	140
29.3.11 A_{63} for Ti site 16d (D_{3d})	140
29.3.12 A_{66} for Ti site 16d (D_{3d})	140
29.3.13 A_{32} for vacancy site, X, 8b (T_d)	141
29.3.14 A_{40} for vacancy site, X, 8b (T_d)	141
29.3.15 A_{44} for vacancy site, X, 8b (T_d)	141
29.3.16 A_{60} for vacancy site, X, 8b (T_d)	142
29.3.17 A_{64} for vacancy site, X, 8b (T_d)	142

CONTENTS (cont'd)

	<u>Page</u>
29.3.18 A_{72} for vacancy site, X, 8b (T_d)	142
29.3.19 A_{76} for vacancy site, X, 8b (T_d)	143
29.4 Experimental Parameters	143
29.5 Bibliography and References	143
30. $Y_2Ti_2O_7$	145
30.1 Crystallographic Data on $Y_2Ti_2O_7$ for Two Choices of Ion Sites.....	145
30.1.1 Cubic O_h^7 ($Fd\bar{3}m$), 227 (second setting), Z = 8 (reference 4).....	145
30.1.2 Cubic O_h^7 ($Fd\bar{3}m$), 227 (second setting), Z = 8 (reference 2)	145
30.2 Crystal-Field Components, A_{nm}	145
30.2.1 For Y ion in 16c (D_{3d}) site	145
30.2.2 For Ti ion in 16d (D_{3d}) site	146
30.2.3 For vacancy site, X, 8b (T_d)	146
30.2.4 For Y ion in 16d (D_{3d}) site	146
30.2.5 For Ti ion in 16c (D_{3d}) site	146
30.2.6 For vacancy site, X, 8a (T_d)	147
30.3 Experimental Parameters	147
30.4 Bibliography and References	147
31. K_2ReCl_6	149
31.1 Crystallographic Data on K_2ReCl_6	149
31.2 Crystal-Field Components, A_{nm} , for Re (O_h) Site	149
31.3 Experimental Parameters	149
31.4 Bibliography and References	149
32. A_2BF_6 ($A = K, Rb, Cs; B = Ge, Zr$)	151
32.1 Crystallographic Data on A_2BF_6	151
32.2 X-Ray Data	151
32.3 Crystal-Field Components, A_{nm}	151
32.3.1 For Ge (D_{3d}) site of K_2GeF_6	151
32.3.2 For Ge (D_{3d}) site of Rb_2GeF_6	151

CONTENTS (cont'd)

	<u>Page</u>
32.3.3 For Zr (D_{3d}) site of Cs_2ZrF_6	152
32.3.4 For Zr (D_{3d}) site of Rb_2ZrF_6	152
32.4 Bibliography and References	152
33. Rb_2SnCl_6	153
33.1 Crystallographic Data on Rb_2SnCl_6	153
33.2 Crystal-Field Components, A_{nm} , for Sn (O_h) Site	153
33.3 Experimental Parameters	153
33.4 Bibliography and References	153
34. Cs_2TeCl_6	155
34.1 Crystallographic Data on Cs_2TeCl_6	155
34.2 Crystal-Field Components, A_{nm} , for Te (O_h) Site	155
34.3 Bibliography and References	155
35. K_2ReF_6	157
35.1 Crystallographic Data on K_2ReF_6	157
35.2 Crystal-Field Components, A_{nm} , for Re (D_{3d}) Site	157
35.3 Experimental Parameters	157
35.4 References	157
36. Cs_2ZrCl_6	158
36.1 Crystallographic Data on Cs_2ZrCl_6	158
36.2 Crystal-Field Components, A_{nm} , for Zr (O_h) Site	158
36.3 Experimental Parameters	158
36.4 Bibliography and References	158
ACKNOWLEDGEMENTS	160
DISTRIBUTION	161

TABLES

1. Free-Ion Data: $F^{(2)}$, $F^{(4)}$, ζ , and α for nd^N Ions	14
2. Hartree-Fock Values for $F^{(k)}$, ζ , and $\langle r^k \rangle$ for nd^N Ions	21

1. Introduction

This report contains information on various potential laser host materials for transition-metal ions of the nd^N electronic configuration. The list is an update of a previous report [1] with a number of new materials added. Many of the new host materials have been reported as practical laser systems, employing transition-metal ions as well as rare-earth ions. Frequently the decision for the inclusion of a particular host material was made on the grounds that the material had some particular interesting feature in addition to being a potential laser host.

Extensive data on the free-ion parameters for the $3d^N$ electronic configuration have been reported, and these are given in table 1 for the doubly, triply, and quadruply ionized states. Also included in table 1 are the parameters of the $4d^N$ and $5d^N$ electronic configurations; a considerable number of these latter configurations have not been investigated. Nonrelativistic Hartree-Fock values for $F^{(k)}$, ζ , and $\langle r^k \rangle$ for the doubly, triply, and quadruply ionized states of the $3d^N$, $4d^N$, and $5d^N$ electronic configurations are given in table 2.

A number of host materials were selected because lasers had been reported employing $3d^N$ ions as impurities. These host materials with limited amounts of experimental energy levels were reported during the early 1960's, and some later work has been done in some of these hosts. Unfortunately, much of the reported absorption data have been taken at room temperature (~300 K) and are quite unreliable because of the presence of vibronics and absorption from excited levels. Further complications arise when the data are extracted from the excitation spectra. There is a real need for low-temperature absorption spectra of many of these ions.

TABLE 1. FREE-ION DATA: $F^{(2)}$, $F^{(4)}$, ζ , and α for nd^N ions (cm^{-1})
(A) $3d^N$

nd^N	Ion	$F^{(2)}$	$F^{(4)}$	ζ	α	Reference
$3d^1$	Sc^{2+}	--	--	79.06	--	--
$3d^1$	Ti^{3+}	--	--	152.84	--	--
$3d^1$	V^{4+}	--	--	249.95	--	--
$3d^2$	Sc^{1+}	35,469	19,832	63.18	27	4
$3d^2$	Ti^{2+}	53,061	30,920	126.4	56.4	4
$3d^2$	Ti^{2+}	54,870	32,034	129.4	20.80	5
$3d^2$	Ti^{2+}	53,322 ^a	29,000 ^a	120.4 ^b	--	1
$3d^2$	Ti^{2+}	54,927	32,206	118.0	20.52	9
$3d^2$	V^{3+}	67,200	40,522	219.6	75	4
$3d^2$	V^{3+}	69,547	42,234	206.0	27.54	9
$3d^2$	Cr^{4+}	75,831	47,061	337.9	--	4
$3d^2$	Cr^{4+}	82,406	50,755	319.0	37.64	9
$3d^3$	V^{2+}	55,153	20,954	186.3	199	4
$3d^3$	V^{2+}	59,669	35,882	176.7	24.58	5
$3d^3$	V^{2+}	57,437 ^a	36,363 ^a	167.8 ^b	--	7
$3d^3$	V^{2+}	59,924	36,268	170.0	22.90	9
$3d^3$	Cr^{3+}	75,950	30,076	295.6	437	4
$3d^3$	Cr^{3+}	70,905 ^a	45,986 ^a	296.4 ^b	--	8
$3d^3$	Cr^{3+}	74,201	45,822	275.0	29.87	9
$3d^3$	Mn^{4+}	80,332	47,754	437.0	91	4
$3d^3$	Mn^{4+}	86,939	54,219	405.0	39.01	9
$3d^4$	Cr^{2+}	59,121 ^a	46,179 ^a	234.3 ^b	--	8
$3d^4$	Cr^{2+}	62,300	38,934	263.2	61.0	4
$3d^4$	Cr^{2+}	64,467	39,730	239.4	28.36	5
$3d^4$	Cr^{2+}	64,798	40,288	231.0	25.83	9
$3d^4$	Mn^{3+}	81,970	46,998	387.7	12	4
$3d^4$	Mn^{3+}	71,593 ^a	55,647 ^a	361.8 ^b	--	2
$3d^4$	Mn^{3+}	78,756	49,404	--	32.60	9
$3d^4$	Fe^{4+}	87,269	56,183	564.6	85	4
$3d^4$	Fe^{4+}	91,372	57,696	513.0	40.66	9

TABLE 1 (cont'd). FREE-ION DATA: $F^{(2)}$, $F^{(4)}$, ζ , and α for nd^N ions (cm^{-1})
 (A) $3d^N$ (cont'd)

nd^N	Ion	$F^{(2)}$	$F^{(4)}$	ζ	α	Reference
$3d^5$	Mn^{2+}	67,685	40,698	351.4	74.8	3
$3d^5$	Mn^{2+}	69,266	43,578	317.5	32.14	5
$3d^5$	Mn^{2+}	69,485	44,305	316.0	29.20	9
$3d^5$	Fe^{3+}	83,302	53,070	463.0	35.40	9
$3d^5$	Co^{4+}	95,819	61,152	654.0	42.68	9
$3d^6$	Fe^{2+}	79,149	49,153	440.5	81	4
$3d^6$	Fe^{2+}	74,064	47,426	411.0	35.92	5
$3d^6$	Fe^{2+}	74,282	48,241	422.0	33.21	9
$3d^6$	Co^{3+}	84,377 ^a	60,291 ^a	584.6 ^b	--	6
$3d^6$	Co^{3+}	87,762	56,823	606.0	37.93	9
$3d^6$	Ni^{4+}	100,186	64,788	830.0	44.17	9
$3d^7$	Co^{2+}	77,532	50,123	560.3	65	4
$3d^7$	Co^{2+}	78,906	52,277	536.0	37.48	9
$3d^7$	Co^{2+}	78,863	51,274	519.9	39.70	5
$3d^7$	Ni^{3+}	92,204	60,579	749.0	41.01	9
$3d^7$	Cu^{4+}	104,534	68,395	1008	46.40	9
$3d^8$	Ni^{2+}	86,933	60,871	701.7	42	4
$3d^8$	Ni^{2+}	83,661	55,122	644.2	43.48	5
$3d^8$	Ni^{2+}	83,514	56,164	668.0	42.49	9
$3d^8$	Cu^{3+}	96,631	64,302	911.0	44.79	9
$3d^8$	Zn^{4+}	108,877	71,954	1203.0	49.84	9
$3d^9$	Cu^{2+}	--	--	828.68	--	--
$3d^9$	Zn^{3+}	--	--	--	--	--
$3d^9$	Ga^{4+}	--	--	--	--	--

^aThe Slater parameters are obtained by fitting the centroids of the reported experimental data for a given nd^N configuration.

^bThe ζ values are obtained by fitting the lowest J multiple of the Hund ground state of the nd^N configuration.

References for part A, $3d^N$ ions

- (1) C. Corliss and J. Sugar, Energy Levels of Titanium, Ti I through Ti XXII, *J. Phys. Chem. Ref. Data* 8 (1979), 1.
- (2) C. Corliss and J. Sugar, Energy Levels of Manganese, Mn I through Mn XXV, *J. Phys. Chem. Ref. Data* 6 (1977), 1253.
- (3) T. M. Dunn and W.-K. Li, Magnetic Interactions for the Electronic Configuration d^5 , *J. Chem. Phys.* 46 (1967), 2907.
- (4) W.-K. Li, Magnetic Interactions in Transition Metal Ions: Part I. Electronic Configurations d^2 , d^3 , and d^4 , *Atomic Data* 2 (1970), 45; Part II. Bivalent Cations of the First Transition Series, *Atomic Data* 2 (1970), 58.
- (5) A. Pasternak and Z. B. Goldschmidt, Spin-Dependent Interactions in the $3d^N$ Configurations of the Third Spectra of the Iron Group, *Phys. Rev. A* 6 (1972), 55.

The parameters are given in the form

$$F^{(2)} = 69,266 + 4798.5(N - 5)$$

$$F^{(4)} = 43,578 + 3848(N - 5)$$

$$\alpha = 32.14 + 3.78(N - 5)$$

$$\zeta = 348.3 + 85.8(N - 5) + 7.7[(N - 5)^2 - 4]$$

- (6) J. Sugar and C. Corliss, Energy Levels of Cobalt, Co I through Co XXVII, *J. Phys. Chem. Ref. Data* 10 (1981), 1097.
- (7) J. Sugar and C. Corliss, Energy Levels of Vanadium, V I through V XXIII, *J. Phys. Chem. Ref. Data* 7 (1978), 1191.
- (8) J. Sugar and C. Corliss, Energy Levels of Chromium, Cr I through Cr XXIV, *J. Phys. Chem. Ref. Data* 6 (1977), 317.
- (9) P.H.M. Uylings, A.J.J. Raassen, and J. F. Wyart, Energies of N Equivalent Electrons Expressed in Terms of Two-Electron Energies and Independent Three-Electron Parameters: A New Complete Set of Orthogonal Operators: II. Application of $3d^N$ Configurations, *J. Phys. B* 17 (1984), 4103.

TABLE 1 (cont'd). FREE-ION DATA: $F^{(2)}$, $F^{(4)}$, ζ , and α for ^{4d}N ions (cm^{-1})
(B) ^{4d}N

^{4d}N	Ion	$F^{(2)}$	$F^{(4)}$	ζ	α	Reference
4d ¹	Y^{2+}	--	--	289.92	--	1
4d ¹	Zr^{3+}	--	--	500.24	--	2
4d ¹	Nb^{4+}	--	--	742.16	--	3
4d ²	Zr^{2+}	34,790	23,373	--	--	4
4d ²	Zr^{2+}	38,721	19,498	408.47	89.94	5
4d ²	Zr^{2+}	37,170	20,160	450	25	6
4d ²	Nb^{3+}	47,297	31,781	646.64	--	7
4d ²	Mo^{4+}	54,755	35,818	920.64	44.48	8
4d ³	Nb^{2+}	39,950	26,901	--	--	4
4d ³	Nb^{2+}	41,517	25,427	535	33	6
4d ³	Mo^{3+}	50,411	32,830	810	38	9
4d ³	Te^{4+}	--	--	--	--	--
4d ⁴	Mo^{2+}	45,080	30,429	--	--	4
4d ⁴	Te^{3+}	--	--	--	--	--
4d ⁴	Ru^{4+}	--	--	--	--	--
4d ⁵	Te^{2+}	50,225	33,957	--	--	4
4d ⁵	Ru^{3+}	--	--	--	--	--
4d ⁵	Rh^{4+}	--	--	--	--	--
4d ⁶	Ru^{2+}	55,370	37,485	--	--	4
4d ⁶	Rh^{3+}	--	--	--	--	--
4d ⁶	Pd^{4+}	--	--	--	--	--
4d ⁷	Rh^{2+}	60,515	41,013	--	--	4
4d ⁷	Rh^{2+}	54,117	38,582	1291	29	6
4d ⁷	Pd^{3+}	61,943	43,516	1699.1	31.6	10
4d ⁷	Ag^{4+}	71,497	51,108	2289	32.2	11
4d ⁸	Pd^{2+}	65,660	44,541	--	--	4
4d ⁸	Pd^{2+}	57,302	41,933	1545	28	6
4d ⁸	Pd^{2+}	57,766	42,591	1551	21.9	12
4d ⁸	Ag^{3+}	65,305	46,002	1996.04	45.98	13
4d ⁸	Cd^{4+}	72,155	50,707	2494.91	47.78	14
4d ⁹	Ag^{2+}	--	--	1843.68	--	15
4d ⁹	Ag^{2+}	--	--	1825	--	6
4d ⁹	Cd^{3+}	--	--	2325	--	16
4d ⁹	La^{4+}	--	--	--	--	--

References for part B, $4d^N$ ions

1. C. Moore, Atomic Energy Levels, National Bureau of Standards Circular 467, vol. 2-3, U.S. Government Printing Office, Washington, D.C. (1952-1958); reprinted 1971, NSRDS-NBS 35.
2. N. Aquista and J. Reader, Spectrum and Energy Levels of Triply Ionized Zirconium (Zr IV), *J. Opt. Soc. Am.* 70 (1980), 789.
3. Q. Shujauddin, A. Mushtaq, and M. S. Z. Chagtai, The Fifth Spectrum of Niobium (Nb V), *Phys. Scr.* 25 (1982), 924.
4. L. DiSipio, E. Tondello, G. DeMichelis, and L. Oleari, Slater-Condon Parameters for Atoms and Ions of the Second Transition Metal Series, *Inorg. Chem.* 9 (1970), 927.
5. Z. A. Khan, M. S. Z. Chagtai, and K. Rahimullah, Classified Lines and Energy Levels of Doubly Ionized Zirconium, *Phys. Scr.* 23 (1981), 29.
6. Y. Shadmi, The Configurations $4D^n + 4d^{n-1} 5S$ in Doubly-Ionized Atoms of the Palladium Group, *J. Res. Nat. Bur. Stand. Sect. A.* 70A (1966), 435.
7. E. Meinders, F. G. Meijer, and L. Remijin, The Spectrum of Triply Ionized Niobium, *Phys. Scr.* 25 (1982), 527.
8. J. Sugar and A. Musgrave, Energy Levels of Molybdenum, Mo I Through Mo XLII, *J. Phys. Chem.* 17 (1988), 155.
9. M. T. Fernandez, I. Cabeza, L. Iglesias, O. Garcia-Riquelme, F. R. Rico, and V. Kaufman, Fundamental Configurations in Mo IV Spectrum, *Phys. Scr.* 35 (1987), 819.
10. M. M. Barakat, Th.A.M. Van Kleef, and A.J.J. Raassen, Analysis of the Fourth Spectrum of Palladium: Pd IV 1. $4d^7-4d^6$ 5p Transitions, *Physica* 132C (1985), 240.
11. Th.A.M. Van Kleef and Y. N. Joshi, $4d^7$ 5s- $4d^7$ 5p Transitions in Ag IV, *Can. J. Phys.* 61 (1983), 36.
12. M. M. Barakat, Th.A.M. Van Kleef, and A.J.J. Raassen, Extension of the Analysis of the Three Lowest Configurations in the Third Spectrum of Palladium (PdIII), *Physica* 132C (1985), 111.
13. Th.A.M. Van Kleef and Y. N. Joshi, Analysis of ed^8-4d^7 5p Transitions in Triply Ionized Silver: Ag IV, *Can. J. Phys.* 59 (1981), 1930.
14. Th.A.M. Van Kleef, Y. N. Joshi, and R. P. Srivastava, Analysis of Cd V: $I--4d^8-4d^7$ 5p Transitions, *Physica* 114C (1982), 105.
15. H. Benschop, Y. N. Joshi, and Th.A.M. Van Kleef, The Spectrum of Doubly Ionized Silver: Ag III, *Can. J. Physics* 53 (1975), 498.
16. Y. N. Joshi and Th.A.M. Van Kleef, $4d^9-4d^8$ 5p Transitions in CdIV, Sn VI, and Sb VII and Resonance Lines of Sn V and Sb VI, *Can. J. Phys.* 55 (1977), 714.

TABLE 1 (cont'd). FREE-ION DATA: $F^{(2)}$, $F^{(4)}$, ζ , and α for nd^N ions (cm^{-1})
(C) 5d^N

5d ^N	Ion	F^2	F^4	ζ	α	Reference
5d ¹	Lu ²⁺	---	1,176.08	--	1	--
5d ¹	Hf ³⁺	--	1,876.8	--	2	--
5d ¹	Ta ⁴⁺	--	2,643.32	--	3	--
5d ²	Hf ²⁺	--	--	--	--	--
5d ²	Ta ³⁺	45,551	28,658 22,813	66.22	4	
5d ²	W ⁴⁺	52,112	34,335 3,102	--	9	
5d ³	Ta ²⁺	--	--	--	--	--
5d ³	W ³⁺	47,530	29,988 2,720	25	10	
5d ³	Re ⁴⁺	--	--	--	--	--
5d ⁴	W ²⁺	--	--	--	--	--
5d ⁴	Re ³⁺	--	--	--	--	--
5d ⁴	Os ⁴⁺	--	--	--	--	--
5d ⁵	Re ²⁺	30,870	22,050	--	--	--
5d ⁵	Os ³⁺	--	--	--	--	--
5d ⁵	Ir ⁴⁺	--	--	--	--	--
5d ⁶	Os ²⁺	30,135	18,963	1,900	3200	6
5d ⁶	Ir ³⁺	--	--	--	--	--
5d ⁶	Pt ⁴⁺	--	--	--	--	--
5d ⁷	Ir ²⁺	--	--	--	--	--
5d ⁷	Pt ³⁺	--	--	--	--	--
5d ⁷	Au ⁴⁺	--	--	--	--	--
5d ⁸	Pt ²⁺	--	--	--	--	--
5d ⁸	Au ³⁺	--	--	--	--	--
5d ⁸	Hg ⁴⁺	--	--	--	--	--
5d ⁹	Au ²⁺	--	5,078	--	11	--
5d ⁹	Hg ³⁺	--	6,274	--	11	--
5d ⁹	Tl ⁴⁺	--	--	--	--	--

References for part C, $5d^N$ ions

1. V. Kaufman and J. Sugar, One-Electron Spectrum of Doubly Ionized Lutetium (Lu III) and Nuclear Moment, *J. Opt. Soc. Am.* 61 (1971), 1693.
2. P.F.A. Klinkenberg, Th.A.M. Van Kleef, and P. E. Noorman, Spectral Structure of Doubly and Triply Ionized Hafnium, *Physica* 27 (1961), 1177.
3. F. G. Meijer and P.F.A. Klinkenberg, The Structure of the Spectrum of Ta V, *Physica (Utrecht)* 69 (1973), 111.
4. F. G. Meijer and B. C. Metsch, The Analysis of the Fourth Spectrum of Tantalum, Ta IV, *Physica (Utrecht)* 94C (1978), 259.
5. J. C. Eisenstein, Magnetic Properties and Optical Spectrum of K_2ReCl_6 , *J. Chem. Phys.* 34 (1961), 1628.
6. J. C. Eisenstein, Absorption Spectrum and Magnetic Properties of Osmium Hexafluoride, *J. Chem. Phys.* 34 (1961), 310.
7. J. C. Ehrhardt and S. P. Davis, Precision Wavelengths and Energy Levels of Gold, *J. Opt. Soc. Am.* 61 (1971), 1342.
8. C. Moore, Atomic Energy Levels, National Bureau of Standards circular 467, vol. 3, U.S. Government Printing Office, Washington, D.C. (1952-1958); reprinted 1971, NSRDS-NBS 35.
9. F. G. Meijer, The Fifth Spectrum of Tungsten, W V, *Physica* 141C (1986), 230.
10. L. Iglesias, V. Kaufman, O. Garcia-Requelme, and F. R. Rico, Analysis of the Fourth Spectrum of Tungsten (W IV), *Phys. Scr.* 31 (1985), 173.
11. Y. N. Joshi, A.J.J. Raassen, and B. Arcimowicz, Fourth Spectrum of Mercury: Hg IV, *J. Opt. Soc. Am.* B6 (April 1989), 534-538.

TABLE 2. HARTREE-FOCK VALUES FOR $F^{(k)}$, ζ , AND $\langle r^k \rangle$ FOR nd^N IONS

 (A) $3d^N$

Z	X^{2+}	nd^N	$F^{(2)}$ (cm $^{-1}$)	$F^{(4)}$ (cm $^{-1}$)	ζ_d (cm $^{-1}$)	$\langle r^2 \rangle$ (Å 2)	$\langle r^4 \rangle$ (Å 4)
21	Sc	$3d^1$	--	--	85.95	0.8346	1.4997
22	Ti	$3d^2$	67,932	42,357	131.15	0.6716	0.9808
23	V	$3d^3$	74,062	46,171	187.17	0.5677	0.7112
24	C	$3d^4$	79,790	49,726	256.60	0.4910	0.5401
25	Mn	$3d^5$	85,637	53,368	342.85	0.4277	0.4145
26	Fe	$3d^6$	89,877	55,927	441.38	0.3893	0.3527
27	Co	$3d^7$	94,600	58,817	561.21	0.3525	0.2949
28	Ni	$3d^8$	99,392	61,756	703.19	0.3203	0.2478
29	Cu	$3d^9$	--	--	869.65	0.2923	0.2097

Z	X^{3+}	nd^N	$F^{(2)}$ (cm $^{-1}$)	$F^{(4)}$ (cm $^{-1}$)	ζ_d (cm $^{-1}$)	$\langle r^2 \rangle$ (Å 2)	$\langle r^4 \rangle$ (Å 4)
22	Ti	$3d^1$	--	--	157.75	0.5341	0.5769
23	V	$3d^2$	82,940	52,097	220.47	0.4571	0.4270
24	Cr	$3d^3$	88,514	55,558	296.26	0.4018	0.3344
25	Mn	$3d^4$	93,852	58,861	388.01	0.3578	0.2688
26	Fe	$3d^5$	99,367	62,291	499.53	0.3196	0.2168
27	Co	$3d^6$	103,474	64,758	625.26	0.2947	0.1884
28	Ni	$3d^7$	108,043	67,546	775.62	0.2705	0.1615
29	Cu	$3d^8$	112,696	70,392	951.32	0.2489	0.1389
30	Zn	$3d^9$	--	--	1154.85	0.2297	0.1200

Z	X^{4+}	nd^N	$F^{(2)}$ (cm $^{-1}$)	$F^{(4)}$ (cm $^{-1}$)	ζ_d (cm $^{-1}$)	$\langle r^2 \rangle$ (Å 2)	$\langle r^4 \rangle$ (Å 4)
23	V	$3d^1$	--	--	253.27	0.4398	0.6494
24	Cr	$3d^2$	96,286	60,775	337.03	0.3708	0.4203
25	Mn	$3d^3$	101,615	64,078	436.20	0.3568	0.4097
26	Fe	$3d^4$	106,766	67,260	554.03	0.2914	0.2686
27	Co	$3d^5$	112,112	70,581	694.80	0.2721	0.2271
28	Ni	$3d^6$	116,164	73,011	851.77	0.2497	0.1875
29	Cu	$3d^7$	120,659	75,748	1036.93	0.2283	0.1524
30	Zn	$3d^8$	125,241	78,548	1250.84	0.2100	0.1200
31	Ca	$3d^9$	--	--	1496.12	0.1800	0.0800

TABLE 2 (cont'd.). HARTREE-FOCK VALUES FOR $F^{(k)}$, ζ , AND $\langle r^k \rangle$ FOR nd^N IONS
 (B) $4d^N$

Z	X^{2+}	nd^N	$F^{(2)}$ (cm $^{-1}$)	$F^{(4)}$ (cm $^{-1}$)	ζ (cm $^{-1}$)	$\langle r^2 \rangle$ (Å 2)	$\langle r^4 \rangle$ (Å 4)
39	Y	$4d^1$	--	--	312	1.5737	4.4402
40	Zr	$4d^2$	51,177	33,321	432	1.2734	2.8974
41	Nb	$4d^3$	55,683	36,328	566	1.0769	2.0761
42	Mo	$4d^4$	59,873	39,117	718	0.9316	1.5580
43	Tc	$4d^5$	64,052	41,911	891	0.8145	1.1907
44	Ru	$4d^6$	67,247	43,978	1082	0.7365	0.9869
45	Rh	$4d^7$	70,673	46,224	1299	0.6656	0.8126
46	Pd	$4d^8$	74,108	48,480	1544	0.6045	0.6744
47	Ag	$4d^9$	--	--	1820	0.5516	0.5644
1							
Z	X^{3+}	nd^N	$F^{(2)}$ (cm $^{-1}$)	$F^{(4)}$ (cm $^{-1}$)	ζ (cm $^{-1}$)	$\langle r^2 \rangle$ (Å 2)	$\langle r^4 \rangle$ (Å 4)
40	Zr	$4d^1$	--	--	51.0	1.0840	1.989
41	Nb	$4d^2$	60,253	36,327	655	0.9288	1.461
42	Mo	$4d^3$	64,276	42,326	815	0.8149	1.128
43	Tc	$4d^4$	68,116	44,878	997	0.7244	0.8953
44	Ru	$4d^5$	72,001	47,470	1201	0.6479	0.7175
45	Rh	$4d^6$	75,061	49,443	1426	0.5936	0.6094
46	Pd	$4d^7$	78,342	51,586	1680	0.5435	0.5147
47	Ag	$4d^8$	81,645	53,754	1964	0.4993	0.4372
48	Cd	$4d^9$	--	--	2283	0.4603	0.3736
2							
Z	X^{4+}	nd^N	$F^{(2)}$ (cm $^{-1}$)	$F^{(4)}$ (cm $^{-1}$)	ζ (cm $^{-1}$)	$\langle r^2 \rangle$ (Å 2)	$\langle r^4 \rangle$ (Å 4)
41	Nb	$4d^1$	--	--	742	0.8715	1.559
42	Mo	$4d^2$	68,068	54,102	914	0.7520	1.085
43	Tc	$4d^3$	71,843	47,615	1105	0.7039	0.9993
44	Ru	$4d^4$	75,495	50,038	1319	0.5959	0.6777
45	Rh	$4d^5$	79,206	52,512	1557	0.5522	0.5776
46	Pd	$4d^6$	82,196	54,434	1820	0.5071	0.4823
47	Ag	$4d^7$	85,389	56,519	2114	0.4654	0.4005
48	Cd	$4d^8$	88,615	58,631	2441	0.4200	0.3200
49	In	$4d^9$	--	--	2806	0.3800	0.2400

TABLE 2 (cont'd). HARTREE-FOCK VALUES FOR $F^{(k)}$, ζ , AND $\langle r^k \rangle$ FOR nd^N IONS
(C) $5d^N$

Z	X ²⁺	nd ^N	$F^{(2)}$ (cm ⁻¹)	$F^{(4)}$ (cm ⁻¹)	ζ (cm ⁻¹)	$\langle r^2 \rangle$ (Å ²)	$\langle r^4 \rangle$ (Å ²)
71	Lu	5d ¹	-	-	1391	1.6197	4.6324
72	Hf	5d ²	50,350	33,000	1774	1.3646	3.2437
73	Ta	5d ³	54,008	35,526	2170	1.1926	2.4612
74	W	5d ⁴	57,369	37,840	2594	1.0610	1.9385
75	Re	5d ⁵	60,702	40,149	3053	0.9510	1.5467
76	Os	5d ⁶	63,123	41,766	3531	0.8779	1.3277
77	Ir	5d ⁷	65,755	43,550	4056	0.8087	1.1289
78	Pt	5d ⁸	68,388	45,344	4626	0.7474	0.9649
79	Au	5d ⁹	-	-	5248	0.6930	0.6646

Z	X ³⁺	nd ^N	$F^{(2)}$ (cm ⁻¹)	$F^{(4)}$ (cm ⁻¹)	ζ (cm ⁻¹)	$\langle r^2 \rangle$ (Å ²)	$\langle r^4 \rangle$ (Å ²)
72	Hf	5d ¹	-	-	2072	1.1760	2.2810
73	Ta	5d ²	58,176	38,604	2489	1.0420	1.7780
74	W	5d ³	61,293	40,754	2926	0.9399	1.4440
75	Re	5d ⁴	64,247	42,789	3394	0.8563	1.1960
76	Os	5d ⁵	67,234	44,856	3898	0.7829	0.9968
77	Ir	5d ⁶	69,479	46,349	4430	0.7309	0.8745
78	Pt	5d ⁷	71,922	48,001	5011	0.6809	0.7612
79	Au	5d ⁸	74,389	49,674	5640	0.6356	0.6646
80	Hg	5d ⁹	-	-	6323	0.5948	0.5826

Z	X ⁴⁺	nd ^N	$F^{(2)}$ (cm ⁻¹)	$F^{(4)}$ (cm ⁻¹)	ζ (cm ⁻¹)	$\langle r^2 \rangle$ (Å ²)	$\langle r^4 \rangle$ (Å ²)
73	Ta	5d ¹	-	-	2797	0.9823	1.8522
74	W	5d ²	64,633	43,252	3257	0.8727	1.3654
75	Re	5d ³	67,469	45,208	3741	0.8339	1.2966
76	Os	5d ⁴	70,197	47,082	4259	0.7247	0.9217
77	Ir	5d ⁵	72,980	49,004	4814	0.6841	0.8141
78	Pt	5d ⁶	75,122	50,424	5404	0.6393	0.7024
79	Au	5d ⁷	77,448	51,994	6045	0.5969	0.6030
80	Hg	5d ⁸	79,808	53,587	6736	0.5500	0.5000
81	Tl	5d ⁹	-	-	7486	0.5100	0.4000

S. Fraga, K.M.S. Saxena, and J. Karwowski, Handbook of Atomic Data, Elsevier, New York (1976).

2. Presentation of Data

Each host is described in a series of tables organized as follows.

2.1 Crystallographic Data

The crystallographic data on each host are given in the notation of the International Tables [2]. The crystallographic data are presented in a short table for each host that lists the following information:

- (a) The crystal class: triclinic, orthorhombic, etc.
- (b) The space group symbol and number from the International Tables.
- (c) The number of chemical formula units, Z , per unit cell.
- (d) The setting, if there is more than one for that space group in the International Tables.
- (e) The position (site type in the International Tables), site symmetry (in the Schoenflies notation), and general x , y , and z coordinates (expressed as fractions of the lattice constants) for that site type, for each constituent of the host crystal.
- (f) The lattice constants a , b , and c (in angstroms) and angles α , β , and γ (in degrees and decimal parts).
- (g) The effective charges (usually the valence charge) in units of the electronic charge.
- (h) The electric-dipole polarizabilities, α (in Å^3), for each of the constituent ions.

2.2 Crystal-Field Components, A_{nm} , and Parameters, B_{nm}

For each host, the data described in section 2.1 were used to obtain the point-charge [3,4], point-dipole [5], and self-induced [6] contributions to the crystal-field components, A_{nm} . All the A_{nm} for $1 \leq n \leq 5$ are given and are sufficient for the analysis of the nd^N configuration. The units of A_{nm} are $\text{cm}^{-1}/\text{Å}^n$. The crystal-field parameters for a particular ion are given by $B_{nm} = \langle r^n \rangle A_{nm}$, where $\langle r^n \rangle$ is the radial expectation value [7] of r^n for the ion under consideration. At the bottom of a number of the tables of A_{nm} , the sums $S^{(0)}$, $S^{(2)}$, and $S^{(4)}$ are given.

The $S^{(0)}$ sum yields the interconfiguration shift [8]

$$\Delta E = \Delta E_0 - [\langle r^2 \rangle_{n\ell} - \langle r^2 \rangle_{n\ell}] S^{(0)},$$

and the $S^{(k)}$ sums yield the Slater integral shifts as $\Delta F^{(2)} = -\langle r^2 \rangle^2 S^{(2)}$ and $\Delta F^{(4)} = -\langle r^4 \rangle^2 S^{(4)}$; the units are such that if $\langle r^k \rangle$ is in angstrom units, then each shift is in units of cm^{-1} .

2.3 Experimental Results

For each host we include tables reporting all the experimental data in terms of the Slater integrals, $F^{(k)}$, and the crystal-field parameters, B_{nm} . Since there are a number of different notations we here describe in some detail our conversion from each set of constants to B_{nm} or $F^{(k)}$.

2.3.1 Relation of Dq with B_{40}

McClure [9] in his article gives the electric potential for a sixfold cubic array of charges at a distance R as

$$V = D[x^4 + y^4 + z^4 - \frac{3}{5}r^4], \quad (1)$$

where $D = 35e/4R^5$. The potential energy (in electron-volts) can be written as

$$U = eDr^4(x^4 + y^4 + z^4 - \frac{3}{5}), \quad (2)$$

where $X = x/r$, $Y = y/r$, and $Z = z/r$. For equivalent electrons McClure [9] defines q by $q = 2\langle r^4 \rangle e/105$, so that

$$U = \frac{105}{2} Dq(x^4 + y^4 + z^4 - \frac{3}{5}). \quad (3)$$

In our notation we write the same potential as

$$U = B_{40}[C_{40} + \frac{5}{\sqrt{70}}(C_{44} + C_{4-4})], \quad (4)$$

for sixfold cubic coordination with charges at $(\pm R, 0, 0)$, $(0, \pm R, 0)$, and $(0, 0, \pm R)$. The C_{nm} are given by [8]

$$C_{40} = (35Z^4 - 30Z^2 + 3)/8, \quad (5)$$

$$C_{4\pm 4} = (X \pm iY)^4 (35/128)^{1/2}. \quad (6)$$

Substituting (5) and (6) into (4) gives

$$C_{40} + \frac{5}{\sqrt{70}}(C_{44} + C_{4-4}) = \frac{5}{2}(x^4 + y^4 + z^4 - \frac{3}{5}). \quad (7)$$

Thus, we obtain

$$\frac{5}{2} B_{40} = \frac{105}{2} Dq ,$$

or

$$B_{40} = 21 Dq , \quad (8)$$

$$B_{44} = \sqrt{5/14} |B_{40}| .$$

This relation (8) has been used to convert the Dq reported in the literature to B_{40} .

If, in the cubic group, the principal axis of rotation is the cube diagonal, then the crystal-field interaction is

$$H_{CEF} = B_{40} \sum_{i=1}^N C_{40}(i) + B_{43} \sum_{i=1}^N [C_{43}(i) - C_{4-3}(i)]$$

with $B_{40} = 14 Dq$,

$$B_{43} = \sqrt{10/7} |B_{40}| . \quad (9)$$

If we write the cubic field parameter in equation (9) as $B_{40}^{(3)}$ and the cubic field parameter in equation (8) as $B_{40}^{(4)}$, then for the same crystal field in the two descriptions we have

$$B_{40}^{(3)} = -\frac{2}{3} B_{40}^{(4)} . \quad (10)$$

For a crystal field of low symmetry, the correlation of the various notations used in the analysis of the crystal-field interaction is extremely difficult, and we shall not attempt to be complete here. Instead we shall relate what appears to be the most prevalent. For a crystal field of C_4 and higher symmetry, we write the crystal-field interaction as

$$H_{CEF} = B_{20} \sum_{i=1}^N C_{20}(i) + B_{40} \sum_{i=1}^N C_{40}(i) + B_{44} \sum_{i=1}^N [C_{44}(i) + C_{4-4}(i)] , \quad (11)$$

where

$$C_{kq}(i) = \sqrt{4\pi/(2k+1)} Y_{kq}(\theta_i, \phi_i)$$

and all B_{kq} can be taken real.

The matrix elements of equation (11) for a single electron are given by [11]

$$\begin{aligned}
\langle 20 | H_{\text{CEF}} | 20 \rangle &= \frac{2}{7} B_{20} + \frac{2}{7} B_{40} , \\
\langle 2\pm 1 | H_{\text{CEF}} | 2\pm 1 \rangle &= \frac{1}{7} B_{20} - \frac{4}{21} B_{40} , \\
\langle 2\pm 2 | H_{\text{CEF}} | 2\pm 2 \rangle &= -\frac{2}{7} B_{20} + \frac{1}{21} B_{40} , \\
\langle 2\pm 2 | H_{\text{CEF}} | 2\mp 2 \rangle &= \frac{\sqrt{70}}{21} B_{44} ,
\end{aligned} \tag{12}$$

where $|2m\rangle = Y_{2m}$, $\langle 2m' | C_{kq} | 2m \rangle = \int Y_{2m}^* C_{kq} Y_{2m} d\Omega$, $d\Omega = \sin \theta d\theta d\phi$, and all the arguments of Y_{2m} and C_{kq} are θ and ϕ .

Ballhausen [10] (p 101) gives the corresponding matrix element for tetragonal fields in terms of Dq , Ds , and Dt . Thus, the following relations exist:

$$\begin{aligned}
B_{20} &= -7Ds , \\
B_{40} &= -14Ds - 21Dt , \\
B_{44} &= \frac{3}{2} \sqrt{70} Dq .
\end{aligned} \tag{13}$$

By comparing the matrix elements of Griffith [12] for tetragonal symmetry we obtain

$$\begin{aligned}
B_{20} &= \delta - \mu , \\
B_{40} &= 21Dq - (\delta + \frac{3\mu}{4}) , \\
B_{44} &= (\frac{3\sqrt{70}}{10})Dq + (\delta + \frac{3\mu}{4}) \frac{\sqrt{70}}{10} .
\end{aligned} \tag{14}$$

For C_3 and higher symmetry we write the crystal field for the electronic configuration d^N as

$$H_{\text{CEF}} = B_{20} \sum_{i=1}^N C_{20}(i) + B_{40} \sum_{i=1}^N C_{40}(i) + B_{43} \sum_{i=1}^N [C_{43}(i) - C_{4-3}(i)] . \tag{15}$$

The matrix elements of the first two terms of (15) are the same as in (12) above and

$$\langle 2-2 | H_{\text{CEF}} | 21 \rangle = \frac{\sqrt{35}}{21} B_{43} . \tag{16}$$

By comparing the matrix elements for trigonal symmetry of Ballhausen [10] (p 104) we obtain

$$\begin{aligned}
 B_{20} &= -7D\sigma , \\
 B_{40} &= -14Dq - 21D\tau , \\
 B_{43} &= 2\sqrt{70} Dq .
 \end{aligned} \tag{17}$$

Similarly for the parameters of Pryce and Runciman [13], we obtain

$$\begin{aligned}
 B_{20} &= \frac{7v - 2w}{3} , \\
 B_{40} &= \frac{-7Dq}{5} + \frac{2w}{3} , \\
 B_{43} &= -\sqrt{7/10} (20Dq + \frac{w}{3}) ,
 \end{aligned} \tag{18}$$

where $w = 2v + 3\sqrt{2} v'$.

In obtaining the result given in (18) we use the equations given by Macfarlane [14]. In Macfarlane's convention, the B_{43} is negative; this has no effect on the energy levels, but introduces a phase factor in the wave function. In the tables we simply change the sign of B_{43} after it is computed by using equation (18) using values of Dq , v , and v' reported in the literature.

In all the relations given above (eq (13), (14), (17), and (18)) certain phase conventions are assumed. In order to obtain consistent values for the B_{nm} , we have frequently had to resort to changing the sign of some of the reported parameters. In some cases where theoretical levels are reported, we have resorted to fitting the theoretical results to obtain B_{nm} . Frequently, the point-charge crystal-field components, A_{nm} , indicate the correct phase relations and are used to determine the phases reported in the tables.

2.3.2 Relation between Slater and Racah parameters

For d electrons, Judd [15] gives the following relations

$$\begin{aligned}
 F_0 &= F^{(0)} , \\
 F_2 &= \frac{F^{(2)}}{49} , \\
 F_4 &= \frac{F^{(4)}}{441} ,
 \end{aligned} \tag{19}$$

and

$$\begin{aligned} E^0 &= F_0 - \frac{7F_2}{2} - \frac{63F_4}{2} , \\ E^1 &= \frac{5(F_2 + 9F_4)}{2} , \\ E^2 &= \frac{F_2 - 5F_4}{2} , \end{aligned} \quad (20)$$

and Racah [16] introduces A, B, and C by

$$\begin{aligned} A &= F_0 - 49F_4 , \\ B &= F_2 - 5F_4 , \\ C &= 35F_4 . \end{aligned} \quad (21)$$

All these parameters are used and reported in the literature. We have chosen to put all the reported data in terms of $F^{(k)}$, since Hartree-Fock calculations of $F^{(k)}$ have been reported for a large number of ions [7], and the matrix elements of the Coulomb interaction for d electrons are reported by Nielson and Koster [17] as coefficients of $F^{(k)}$. In terms of A, B, and C, we have

$$\begin{aligned} F^{(0)} &= \frac{5A + 7C}{5} , \\ F^{(2)} &= 7(7B + C) , \\ F^{(4)} &= \frac{63C}{5} ; \end{aligned} \quad (22)$$

in terms of E^k , we have

$$\begin{aligned} F^{(0)} &= E^0 - \frac{49E^1}{10} + \frac{63E^2}{2} , \\ F^{(2)} &= \frac{49(9E^2 - E^1)}{2} , \\ F^{(4)} &= \frac{441(5E^2 - E^1)}{10} , \end{aligned} \quad (23)$$

and the relation between $F^{(k)}$ and F_k is given in equation (19).

2.4 Bibliographies and Reference Lists

The final section on each host material consists of a bibliography of experimental and theoretical work that has been reported. These lists, in most cases, are far from exhaustive and will be continuously updated as new work is reported or older references found. A number of hosts have only x-ray data reported, and we have been unable to find any reference to optical data on transition elements in these hosts. On a number of host materials, references were found which contain important information on that host not contained in the tables. These references have been included.

2.5 References

1. C. A. Morrison, R. P. Leavitt, and A. F. Hansen, Host Materials for Transition-Metal Ions with the nd^N Electronic Configuration, Harry Diamond Laboratories, HDL-DS-85-1 (October 1985).
2. N.F.M. Henry and K. Lonsdale, International Tables for X-Ray Crystallography, vol. I: Symmetry Groups, Kynoch, Birmingham, U.K. (1969).
3. C. A. Morrison and R. P. Leavitt, Spectroscopic Properties of Triply Ionized Lanthanides in Transparent Host Crystals, in Handbook on the Physics and Chemistry of Rare Earths, vol. 5, K. Gschneidner and L. Eyring, eds., North-Holland, New York (1982).
4. N. Karayianis and C. A. Morrison, Rare Earth Ion-Host Interactions: I.--Point Charge Lattice Sum in Scheelites, Harry Diamond Laboratories, TR-1648 (October 1973) (NTIS 011252).
5. C. A. Morrison, Dipolar Contributions to the Crystal Fields in Ionic Solids, Solid State Commun. 18 (1976), 153.
Also, see M. Faucher and D. Garcia, Electrostatic Crystal-Field Contributions in Rare-Earth Compounds with Consistent Multipolar Effects: I.--Contribution to K-Even Parameters, Phys. Rev. B26 (1982), 5451; D. Garcia, M. Faucher, and O. Malta, Electrostatic Crystal-Field Contributions in Rare-Earth Compounds with Consistent Multipolar Effects: II.--Contribution to K-Odd Parameters (Transition Probabilities), Phys. Rev. B27 (1983), 7386; D. Garcia and M. Faucher, Crystal-Field Parameters in Rare-Earth Compounds: Extended Charge Contributions, Phys. Rev. A30 (1984), 1730; M. Faucher and D. Garcia, Crystal-Field Effects on $4f$ Electrons: Theories and Realities, J. Less-Common Metals 93 (1983), 31.
6. C. A. Morrison, G. F. de Sá, and R. P. Leavitt, Self-Induced Multipole Contribution to the Single-Electron Crystal Field, J. Chem. Phys. 76 (1982), 3899.

3.2.2 Theoretical crystal-field parameters, B_{nm} (cm^{-1}), of $\text{Al}_2(\text{S}_4)$ site for transition-metal ions with electronic configuration $3d^N$

(a) For monopole A_{nm}

X^{2+}	N	B_{20}	B_{40}	B_{44}
Sc	1	8719	-101,690	39,942
Ti	2	6819	-62,848	24,687
V	3	5606	-43,103	16,931
Cr	4	4717	-30,960	12,161
Mn	5	3999	-22,512	88,423
Fe	6	3544	-18,154	7,131
Co	7	3125	-14,396	56,545
Ni	8	2766	-11,483	4,511
Cu	9	2460	-9,228	3,625

(b) For total A_{nm}

X^{2+}	N	B_{20}	B_{40}	B_{44}
Sc	1	24,374	-88,055	29,364
Ti	2	19,062	-54,424	18,149
V	3	15,672	-37,325	12,447
Cr	4	13,187	-26,810	8,940
Mn	5	11,180	-19,495	6,501
Fe	6	9,906	-15,721	5,242
Co	7	8,735	-12,466	4,157
Ni	8	7,733	-6,644	3,316
Cu	9	6,877	-7,991	2,665

X^{3+}	N	B_{20}	B_{40}	B_{44}
Ti	1	5057	-32,139	12,624
V	2	4251	-22,944	9,012
Cr	3	3671	-17,339	6,811
Mn	4	3212	-13,455	5,285
Fe	5	2819	-10,480	4,116
Co	6	2555	-8,796	3,455
Ni	7	2305	-7,283	2,861
Cu	8	2084	-6,054	2,378
Zn	9	1892	-50,578	1,987

X^{3+}	N	B_{20}	B_{40}	B_{44}
Ti	1	14,137	-27,831	9281
V	2	11,883	-19,868	6626
Cr	3	10,261	-15,015	5007
Mn	4	8,978	-11,652	3886
Fe	5	7,881	-9,075	3026
Co	6	7,142	-7,617	2540
Ni	7	6,443	-6,307	2103
Cu	8	5,827	-5,243	1748
Zn	9	5,289	-4,380	1461

X^{4+}	N	B_{20}	B_{40}	B_{44}
V	1	3951	-32,566	12,792
Cr	2	3287	-20,515	8,058
Mn	3	3121	-19,472	7,649
Fe	4	2515	-12,432	4,883
Co	5	2318	-10,239	4,022
Ni	6	2100	-8,234	3,234
Cu	7	1895	-6,523	2,562
Zn	8	1721	-5,005	1,966
Ga	9	1456	-3,252	1,277

X^{4+}	N	B_{20}	B_{40}	B_{44}
V	1	11,045	-28,200	9404
Cr	2	9,188	-17,765	5924
Mn	3	8,724	-16,862	5623
Fe	4	7,031	-10,765	3590
Co	5	6,481	-8,866	2957
Ni	6	5,870	-7,131	2378
Cu	7	5,298	-5,649	1884
Zn	8	4,811	-4,334	1445
Ga	9	4,070	-2,816	939

$\text{Y}_3\text{Al}_5\text{O}_12$

3.3 Crystal Fields for 16(a) (C_{3i}) Site

3.3.1 Crystal-field components, A_{nm} ($\text{cm}^{-1}/\text{Å}^n$), for Al_1 (C_{3i}) site (rotated so that z-axis is parallel to (111) crystallographic axis)

A_{nm}	Point charge	Self-induced	Dipole	Total
A_{20}	6,836	-1107	-13,553	-7,823
A_{40}	-20,054	8166	3,273	-8,615
$\text{Re}A_{43}$	2,813	-1422	6,253	7,644
$\text{Im}A_{43}$	-22,370	8639	2,348	-11,383
$ A_{43} $	22,546	--	--	13,711

3.5 Bibliography and References

1. P. A. Arsenev and D. T. Sviridov, Absorption Spectra of Yttrium Aluminum Garnet (YAG) with Contaminant Ions of the Iron Group, Sov. Phys. Crystallogr. 14 (1970), 578.
2. P. A. Arsenev, D. T. Sviridov, and N. P. Fialkovskaya, Sov. Phys. Crystallogr. 15 (1971), 711.
3. Z. T. Azamatov, P. A. Arsenev, T. Yu. Geraskina, and M. V. Chukichev, Properties of Chromium Ions in the Lattice of Yttrium Aluminum Garnet (YAG), Phys. Status Solidi A1 (1970), 801.
4. Kh. S. Bagdasarov, L. V. Bershov, V. O. Martirosyan, and M. L. Meilman, The State of Molybdenum Impurity in Yttrium-Aluminum Garnet, Phys. Status Solidi B46 (1971), 745.
5. W. L. Bond, Measurement of the Refractive Indices of Several Crystals, J. Appl. Phys. 36 (1965), 1674.
6. G. Burns, E. A. Geiss, B. A. Jenkins, and M. I. Nathan, Cr^{3+} Fluorescence in Garnets and Other Crystals, Phys. Rev. A139 (1965), 1687.
7. T. S. Chernaya, L. A. Muradyan, A. A. Rusakov, A. A. Kaminskii, and V. I. Simonov, Refinement and Analysis of Atomic Structures of $Er_3Al_5O_{12}$ and $(Y_{2.80}Er_{0.20})Al_5O_{12}$, Sov. Phys. Crystallogr. 30 (1985), 38.
8. D. P. Devor, R. C. Pastor, and L. G. DeShazer, Hydroxyl Impurity Effects in YAG ($Y_3Al_5O_{12}$), J. Chem. Phys. 81 (1984), 4104.
9. I. N. Douglas, Optical Spectra of Chromium Ions in Crystals of Yttrium Aluminum Garnet, Phys. Status Solidi A9 (1972), 635.
10. F. Euler and J. A. Bruce, Oxygen Coordinates of Compounds with Garnet Structure, Acta Crystallogr. 19 (1965), 971.
11. J. A. Hodges, R. A. Serway, and S. A. Marshall, Electron-Spin Resonance Absorption Spectrum of Platinum in Yttrium Aluminum Garnet, Phys. Rev. 151 (1966), 196.
12. J. P. Hurrell, S.P.S. Porto, I. F. Chang, S. S. Mitra, and R. P. Bauman, Optical Phonons of Yttrium Aluminum Garnet, Phys. Rev. 173 (1968), 851.
13. C. Z. Janusz, W. Jelenski, and A. Niklas, Disclosure of Defects in YAG:Nd Crystals by Thermoluminescence Method, J. Cryst. Growth 57 (1982), 593.

$Y_3Al_5O_{12}$

14. I. I. Karpov, Kh. S. Bagdasarov, B. N. Grechushnikov, E. V. Antonov, and L. S. Garashina, Conditions of Growth of Yttrium-Aluminum Garnet Crystals with Added Titanium, Sov. Phys. Crystallogr. 23, No. 6 (1978), 710.
15. I. I. Karpov, B. N. Grechushnikov, and Kh. S. Bagdasarov, Color Centers in Titanium-Activated Yttrium-Aluminum Garnet Crystals, Sov. Phys. Crystallogr. 23, No. 5 (1978), 609.
16. I. I. Karpov, B. N. Grechushnikov, V. F. Koryagin, A. M. Kevorkov, and P. Z. Ngi, EPR Spectra of V^{2+} Ions in Yttrium-Aluminum Garnet Crystals, Sov. Phys. Dokl. 24, No. 1 (1979), 33.
17. I. I. Karpov, B. N. Grechushnikov, V. F. Koryagin, A. M. Kevorkov, and P. Z. Ngi, Investigation of V^{4+} -Ion Impurity in Crystals of Yttrium-Aluminum Garnet, Sov. Phys. Dokl. 23 (1978), 492.
18. N. A. Kulagin, M. F. Ozerov, and V. O. Rokhmanova, Effect of γ Radiation on the Electron State of Chromium Ions in $Y_3Al_5O_{12}$ Monocrystals, Zh. Prikl. Spektrosk. (trans.), 46 (1987), 393.
19. Landolt-Bornstein, Numerical Data and Functional Relationships in Science and Technology, New Series, Vol. 12, Suppiement and Extension to Vol. 4, Part a, Garnets and Perovskites, Springer-Verlag, New York (1978), 301.
20. R. W. McMillan, Optical Absorption Spectrum of Cr^{3+} in Yttrium Aluminum Garnet, J. Opt. Soc. Am. 67 (1977), 27.
21. M. L. Meilman, M. V. Korzhik, V. V. Kuz'min, M. G. Livshits, Kh. S. Bagdasarov, and A. M. Kevorkov, Sov. Phys. Dokl. 29 (1984), C1.
22. C. A. Morrison and G. A. Turner, Analysis of the Optical Spectra of Triply Ionized Transition Metal Ions in Yttrium Aluminum Garnet (YAG), Harry Diamond Laboratories, HDL-TR-2150 (October 1988).
23. P. C. Schmidt, A. Weiss, and T. P. Das, Effect of Crystal Fields and Self-Consistency on Dipole and Quadrupole Polarizabilities of Closed-Shell Ions, Phys. Rev. B19 (1979), 5525.
24. B. K. Sevast'yanov, D. T. Sviridov, V. P. Orekhovo, L. B. Pasternak, R. K. Sviridova, and T. F. Vermeichik, Optical Absorption Spectra of Excited Cr^{3+} Ions in Yttrium Aluminum Garnet, Sov. J. Electron. 2 (1973), 339.
25. G. A. Slack, D. W. Oliver, R. M. Chrenko, and S. Roberts, Optical Absorption of $Y_3Al_5O_{12}$ from 10^{-} to 55000-cm^{-1} Wave Numbers, Phys. Rev. 177 (1969), 1308.
26. D. T. Sviridov, R. K. Sviridova, N. I. Kulik, and V. B. Glasko, Optical Spectra of the Iso-electronic Ions V^{2+} , Cr^{3+} and Mn^{4+} in an Octahedral Coordination, J. Appl. Spectrosc. 30 (1979), 334.

27. W. F. van der Weg, Th. J. A. Popma, and A. T. Vink, Concentration Dependence of UV and Electron-Excited Tb^{3+} Luminescence in $Y_3Al_5O_{12}$, *J. Appl. Phys.* 57 (1985), 5450.
28. T. F. Veremeichik, B. N. Grechushnikov, T. M. Varina, D. T. Sviridov, and I. N. Kalinkina, Absorption Spectra and Calculation of Energy-level Diagram of Fe^{3+} and Mn^{2+} Ions in Single Crystals of Yttrium Aluminum Garnet, Orthoclase, and Manganese Silicate, *Sov. Phys. Crystallogr.* 19 (1975), 742.
29. Yu. A. Voitukovich, M. V. Korzhik, V. V. Kuz'min, M. G. Livshits, and M. L. Meilman, Energy Structure of Iron (3^+) Impurity Ions in Yttrium Aluminum Garnet ($Y_3Al_5O_{12}$) Crystals, *Opt. Spectrosc.* 63 (1987), 810.
30. R. Wannemacher and J. Heber, Cooperative Emission of Photons by Weakly Coupled Chromium Ions in YAG and $LaAlO_3$, *J. Lumin.* 39 (1987), 49.
31. M. J. Weber and L. A. Rieberg, Optical Spectra of Vanadium Ions in Yttrium Aluminum Garnet, *J. Chem. Phys.* 55 (1971), 2032.
32. M. Wojcik, Estimation of Applicability of the Electrostatic Model to Calculate the Crystal Field Parameters in Garnets, *Physica B (Netherlands)* 121B (1983), 370-388.
33. D. L. Wood, J. Ferguson, K. Knox, and J. F. Dillon, Jr., Crystal-Field Spectra of $d^{3,7}$ Ions: III.--Spectrum of Cr^{3+} in Various Octahedral Crystal Fields, *J. Chem. Phys.* 39 (1963), 890.
34. D. L. Wood and J. P. Remeika, Optical Absorption of Tetrahedral Co^{3+} and Co^{2+} in Garnets, *J. Chem. Phys.* 46 (1967), 3595.

4. K_2NaAlF_6

4.1 Crystallographic Data on Two Forms of K_2NaAlF_6

4.1.1 Cubic T_h^6 (Pa3), 205, $Z = 4$, elpasoite

Ion	Site	Symmetry	x ^a	y	z	q	$\alpha(\text{\AA}^3)$ ^b
Na	4(b)	C_{3i}	1/2	1/2	1/2	1	0.147
K	8(c)	C_3	1/4	1/4	1/4	1	0.827
Al	4(a)	C_{3i}	0	0	0	3	0.0530
F	24(d)	C_1	0.22	0.03	0.01	-1	0.731

^aX-ray data: $a = 8.11 \text{ \AA}$ (reference 7).

^bReference 6.

4.1.2 Cubic O_h^5 (Fm3m), 225, $Z = 4$, elpasolite

Ion	Site	Symmetry	x ^a	y	z	q	$\alpha(\text{\AA}^3)$ ^b
Al	4(a)	O_h	0	0	0	3	0.0530
Na	4(b)	O_h	1/2	1/2	1/2	1	0.147
K	8(c)	T_d	1/4	1/4	1/4	1	0.827
F	24(e)	C_{4v}	0.219	0	0	-1	0.731

^aX-ray data: $a = 8.119 \text{ \AA}$ (reference 5).

^bReference 6.

4.2 Crystal Fields for Pa3 Form

4.2.1 Crystal-field components, A_{nm} ($\text{cm}^{-1}/\text{\AA}$), for Al (C_{3i}) site (rotated so that z-axis is parallel to (111) crystallographic axis)

A_{nm}	Monopole	Self-Induced	Dipole	Total
A_{20}	20,455	-2717	4,145	21,883
A_{40}	-15,791	8018	-10,411	-18,186
ReA_{43}	14,510	-7295	9,008	17,095
ImA_{43}	3,769	-1945	7,546	4,370

4.2.2 Theoretical crystal-field parameters, B_{nm} (cm^{-1}), for monopole A_{nm} for $\text{Al}(\text{C}_{3i})$ site for transition-metal ions with electronic configuration $3d^N$

X^{2+}	N	B_{20}	B_{40}	B_{43}
Sc	1	28,077	-64,001	60,754
Ti	2	21,958	-39,556	37,550
V	3	18,053	-27,129	25,753
Cr	4	15,190	-19,486	18,498
Mn	5	12,878	-1,469	13,451
Fe	6	11,411	-11,426	10,847
Co	7	10,062	-9,061	8,601
Ni	8	8,908	-7,228	6,861
Cu	9	7,922	-5,808	5,513

X^{3+}	N	B_{20}	B_{40}	B_{43}
Ti	1	16,285	-20,228	19,202
V	2	13,688	-14,441	13,708
Cr	3	11,820	-10,913	10,360
Mn	4	10,343	-8,469	8,039
Fe	5	9,078	-6,596	6,261
Co	6	8,227	-5,536	5,256
Ni	7	7,422	-4,584	4,352
Cu	8	6,712	-3,810	3,617
Zn	9	6,092	-3,184	3,022

X^{4+}	N	B_{20}	B_{40}	B_{43}
V	1	12,722	-20,497	19,457
Cr	2	10,584	-12,912	12,257
Mn	3	10,050	-12,255	11,634
Fe	4	8,100	-7,824	7,428
Co	5	7,465	-6,444	6,117
Ni	6	6,761	-5,183	4,920
Cu	7	6,102	-4,106	3,897
Zn	8	5,542	-3,150	2,991
Ga	9	4,688	-2,047	1,943

K_2NaAlF_6

4.3 Crystal Fields for Fm3m Form

4.3.1 Crystal-field components, A_{nm} ($\text{cm}^{-1}/\text{\AA}^n$), for Al (O_h) site

A_{nm}	Monopole	Dipole	Self-induced	Total
A_{40}	23,267	15,593	-12,274	26,586
A_{44}	13,905	9,319	-7,335	15,888

$$S^{(0)} = 16750 \text{ cm}^{-1}/\text{\AA}^2$$

$$S^{(2)} = 15425 \text{ cm}^{-1}/\text{\AA}^4$$

$$S^{(4)} = 2551.3 \text{ cm}^{-1}/\text{\AA}^8$$

3.3.2 Theoretical crystal-field parameters, B_{nm} (cm^{-1}), for $\text{Al}_1(\text{C}_3\text{i})$ site for transition-metal ions with electronic configuration $3d^N$

(a) For monopole A_{nm}

X^{2+}	N	B_{20}	B_{40}	B_{43}
Sc	1	9,379	-81,279	91,379
Ti	2	7,335	-50,235	56,478
V	3	6,031	-34,453	38,734
Cr	4	5,074	-24,747	27,822
Mn	5	4,302	-17,994	20,231
Fe	6	3,812	-14,511	16,314
Co	7	3,361	-11,507	12,937
Ni	8	2,976	-9,179	10,319
Cu	9	2,646	-7,376	8,292

(b) For total A_{nm}

X^{2+}	N	B_{20}	B_{40}	B_{43}
Sc	1	-10,733	-34,917	55,571
Ti	2	-8,394	-21,581	34,346
V	3	-6,902	-14,801	23,555
Cr	4	-5,807	-10,631	16,919
Mn	5	-4,923	-7,730	12,303
Fe	6	-4,362	-6,234	9,921
Co	7	-3,847	-4,943	7,867
Ni	8	-3,405	-3,943	6,276
Cu	9	-3,028	-3,169	5,043

X^{3+}	N	B_{20}	B_{40}	B_{43}
Ti	1	5440	-25,689	28,881
V	2	4573	-18,339	20,618
Cr	3	3949	-13,859	15,582
Mn	4	3455	-10,755	12,091
Fe	5	3032	-8,377	9,418
Co	6	2748	-7,031	7,905
Ni	7	2479	-5,822	6,545
Cu	8	2242	-4,839	5,440
Zn	9	2035	-4,043	4,545

X^{3+}	N	B_{20}	B_{40}	B_{43}
Ti	1	-6226	-11,036	17,564
V	2	-5233	-7,878	12,539
Cr	3	-4519	-5,954	9,476
Mn	4	-3954	-4,620	7,353
Fe	5	-3470	-3,599	5,727
Co	6	-3145	-3,020	4,807
Ni	7	-2837	-2,501	3,980
Cu	8	-2566	-2,079	3,309
Zn	9	-2329	-1,739	2,764

X^{4+}	N	B_{20}	B_{40}	B_{43}
V	1	4250	-26,030	29,265
Cr	2	3536	-16,398	18,436
Mn	3	3357	-15,564	17,498
Fe	4	2706	-9,939	11,172
Co	5	2494	-8,184	9,201
Ni	6	2259	-6,582	7,400
Cu	7	2039	-5,214	5,862
Zn	8	1851	-4,001	4,498
Ga	9	1566	-2,599	2,922

X^{4+}	N	B_{20}	B_{40}	B_{43}
V	1	-4864	-11,182	17,797
Cr	2	-4046	-7,045	11,211
Mn	3	-3842	-6,686	10,641
Fe	4	-3096	-4,269	6,794
Co	5	-2854	-3,516	5,596
Ni	6	-2585	-2,827	4,500
Cu	7	-2333	-2,240	3,565
Zn	8	-2119	-1,719	2,735
Ga	9	-1792	-1,117	1,777

$Y_3Al_5O_{12}$ 3.4 Experimental Values (cm^{-1}) of B_{40} , $F^{(2)}$, and $F^{(4)}$ for nd^N Ions

Ion	B_{40}	$F^{(2)}$	$F^{(4)}$	Temp (K)	Site	Reference	nd^N
Cr^{+3}	-23,730	53,438	34,978	300	C_{3i}	1,3	$3d^3$
Cr^{+3}	-23,072	55,776	36,806	300	C_{3i}	26	$3d^3$
Cr^{+3}	-24,150	53,438	40,320	--	C_{3i}	24	$3d^3$
Cr^{+3}	35,070	--	--	--	C_{3i}	20	$3d^3$
Cr^{+3}	-22,960	54,600	40,950	77	C_{3i}	33	$3d^3$
Mn^{+3}	-27,650	59,500	32,130	300	C_{3i}	1	$3d^4$
Mn^{+4}	-27,874	53,543	43,457	300	C_{3i}	26	$3d^3$
Mn^{+4}	-29,400	--	--	--	C_{3i}	2	$3d^3$
Fe^{+3}	-26,950	39,690	15,876	300	C_{3i}	1	$3d^5$
Fe^{+3}	-17,682	49,224	36,477	--	C_{3i}	19,28	$3d^5$
Fe^{+3}	-21,756	51,023	42,979	--	S_4	19,28	$3d^5$
Fe^{+3}	-16,904	44,821	42,399	--	S_4	21	$3d^5$
Co^{+3}	-25,200	56,630	34,020	300	C_{3i}	1	$3d^6$
Co^{+3}	-17,430	--	--	--	S_4	34	$3d^6$
Co^{+2}	-9,660	--	--	--	S_4	34	$3d^7$
Co^{+2}	-12,880	--	--	--	C_{3i}	34	$3d^7$
Ni^{+3}	-27,580	42,000	22,680	300	C_{3i}	1,24	$3d^7$
Rh^{+3}	-28,840	40,600	21,924	--	C_{3i}	19	$4d^6$
Pd^{+3}	-23,730	39,326	21,218	--	C_{3i}	19	$4d^7$
Pt^{+3}	-23,100	44,520	30,744	--	C_{3i}	19	$5d^7$
V^{+3}	-23,800	--	--	--	C_{3i}	19	$3d^2$
V^{+3}	-17,850	--	--	--	S_4	19	$3d^2$
V^{+4}	-30,800	--	--	--	C_{3i}	19	$3d^1$

7. S. Fraga, K.M.S. Saxena, and J. Karwowski, Physical Science Data: 5. Handbook of Atomic Data, Elsevier, New York (1976). Also, see C. A. Morrison and R. G. Schmalbach, Approximate Values of $\langle r^k \rangle$ for the Divalent, Trivalent, and Quadrivalent Ions with the $3d^N$ Electronic Configuration, Harry Diamond Laboratories, HDL-TL-85-3 (July 1985).
8. C. A. Morrison, Host Dependence of the Rare-Earth Ion Energy Separation $4f^N - 4f^{N-1}nl$, J. Chem. Phys. 72 (1980), 1001. In the expression for the Slater-parameter host-dependent shift, a factor ($k+1$) was omitted. See M. V. Eremin and A. A. Kornienko, Effect of Covalency on Slater Parameters and the Correlation Crystal Field in Transient-Metal Compounds, Opt. Spectrosc. 53 (1982), 45.
9. D. S. McClure, Electronic Spectra of Molecules and Ions in Crystals: II, Solid State Phys. 9 (1959), 420, Academic Press, New York.
10. C. J. Ballhausen, Ligand Field Theory, McGraw Hill, New York (1962), 93.
11. C. A. Morrison and R. P. Leavitt, Crystal Field Splittings of the Hund Ground States of nd^N Ions in S_4 Symmetry: Theory and Applications to the Ga^{3+} Site of $Gd_3Sc_2Ga_3O_{12}$, Harry Diamond Laboratories, HDL-TR-2040 (March 1984).
12. J. S. Griffith, The Theory of Transition-Metal Ions, Cambridge University Press, Cambridge, England (1961), p 226.
13. M.H.L. Pryce and W. A. Runciman, Discuss. Faraday Soc. 26 (1958), 34.
14. R. M. Macfarlane, Analysis of the Spectrum d^3 Ions in Trigonal Crystal Fields, J. Chem. Phys. 39 (1963), 3118.
15. B. R. Judd, Operator Techniques in Atomic Spectroscopy, McGraw-Hill, New York (1963), 221.
16. G. Racah, Theory of Complex Spectra IV, Phys. Rev. 76 (1949), 1352.
17. C. W. Nielson and G. F. Koster, Spectroscopic Coefficients for the p^n , d^n , and f^n Configurations, MIT Press, Cambridge, MA (1963).

3. $\text{Y}_3\text{Al}_5\text{O}_{12}$ (YAG)

3.1 Crystallographic Data on $\text{Y}_3\text{Al}_5\text{O}_{12}$

Cubic O_h^{10} (Ia3d), 230, Z = 8

Ion	Site	Symmetry	x ^a	y	z	q	α (\AA^3) ^b
Al ₁	16(a)	C_{3i}	0	0	0	3	0.0530
Al ₂	24(d)	S_4	0	1/4	3/8	3	0.0530
Y	24(c)	D_2	0	1/4	1/8	3	0.870
O	96(h)	C_1	-0.0306	0.0512	0.1500	-2	1.349

^aX-ray data: a = 12.000 \AA (reference 10).

^bReference 23.

3.2 Crystal Fields for 24(d) (S_4) Site

3.2.1 Crystal-field components, A_{nm} ($\text{cm}^{-1}/\text{A}^n$), for Al₂ (S_4) site

A_{nm}	Point charge	Self-induced	Dipole	Total
A_{20}	6,355	-2,604	14,013	17,765
$\text{Re}A_{32}$	-27,522	8,609	-11,957	-30,870
$\text{Im}A_{32}$	37,839	-11,913	6,332	32,258
A_{40}	-25,089	11,879	-8,516	-21,726
$\text{Re}A_{44}$	-3,763	1,614	1,964	-185.1
$\text{Im}A_{44}$	-9,108	4,740	-2,875	-7,243
$\text{Re}A_{52}$	-2,931	2,287	-3,498	-4,142
$\text{Im}A_{52}$	4,328	-3,207	3,640	4,762
$ A_{44} $	9,855	--	--	7,245

4.3.2 Theoretical crystal-field parameters, B_{nm} (cm^{-1}), for A_{nm} of Al (O_h) site for transition-metal ions with electronic configuration nd^N

(a) For monopole A_{nm}

X^{2+}	N	B_{40}	B_{44}
Sc	1	94,301	56,357
Ti	2	58,284	34,832
V	3	39,973	23,889
Cr	4	28,711	17,159
Mn	5	20,877	12,477
Fe	6	16,836	10,062
Co	7	13,351	7,979
Ni	8	10,649	6,364
Cu	9	8,558	5,114

X^{3+}	N	B_{40}	B_{44}
Ti	1	29,805	17,812
V	2	21,278	12,716
Cr	3	16,080	9,610
Mn	4	12,478	7,457
Fe	5	9,719	5,808
Co	6	8,157	4,875
Ni	7	6,754	4,037
Cu	8	5,614	3,355
Zn	9	4,691	2,803

X^{4+}	N	B_{40}	B_{44}
V	1	30,201	18,049
Cr	2	19,025	11,370
Mn	3	18,058	10,792
Fe	4	11,529	6,890
Co	5	9,495	5,675
Ni	6	7,636	4,564
Cu	7	6,049	3,615
Zn	8	4,642	2,774
Ga	9	3,015	1,802

(b) For total A_{nm}

X^{2+}	N	B_{40}	B_{44}
Sc	1	107,750	64,394
Ti	2	66,598	39,799
V	3	45,675	27,296
Cr	4	32,807	19,606
Mn	5	23,856	14,256
Fe	6	19,238	11,497
Co	7	15,255	9,117
Ni	8	12,168	7,272
Cu	9	9,778	5,844

X^{3+}	N	B_{40}	B_{44}
Ti	1	34,057	20,353
V	2	24,313	14,530
Cr	3	18,374	10,980
Mn	4	14,258	8,521
Fe	5	11,105	6,636
Co	6	9,321	5,570
Ni	7	7,718	4,612
Cu	8	6,415	3,834
Zn	9	5,360	3,203

X^{4+}	N	B_{40}	B_{44}
V	1	34,509	20,623
Cr	2	21,739	12,992
Mn	3	20,633	12,331
Fe	4	13,173	7,873
Co	5	10,850	6,484
Ni	6	87,255	5,214
Cu	7	6,912	4,131
Zn	8	5,304	3,170
Ga	9	3,446	2,059

K_2NaAlF_6

4.4 Bibliography and References

1. C. D. Adam, ENDOR Determination of Covalency in K_2NaAlF_6 , Cr^{3+} , J. Phys. C14 (1981), L105.
2. D. Babel, R. Haegele, G. Pausewang, and F. Wall, Über Kubische und Hexagonale Elpasolithe $A_2^{I}B^{I}M^{III}F_6$, Mater. Res. Bull. 8 (1973), 1371 (in German).
3. P. Greenough and A. G. Paulusz, The $^2E_g \rightarrow ^4A_{2g}$ Phosphorescence Spectrum of the Cr^{3+} Ion in K_2NaAlF_6 , J. Chem. Phys. 70 (1979), 1967.
4. K. Grjotheim, J. G. Holm, and S. A. Mikhaiel, Equilibrium Studies in the Systems $K_3AlF_6-Na_3AlF_6$ and $K_3AlF_6-Rb_3AlF_6$, Acta Chem. Scand. 27 (1973), 1299.
5. L. R. Morss, Crystal Structure of Dipotassium Sodium Fluoroaluminate (Elpasolite), J. Inorg. Nucl. Chem. 36 (1974), 3876.
6. P. C. Schmidt, A. Weiss, and T. P. Das, Effect of Crystal Fields and Self-Consistency on Dipole and Quadrupole Polarizabilities of Closed-Shell Ions, Phys. Rev. B19 (1979), 5525.
7. R.W.G. Wyckoff, Crystal Structures, vol. 3, Interscience, New York (1968), 374.

5. Cs_2TiF_6

5.1 Crystallographic Data on Two Forms of Cs_2TiF_6

5.1.1 Cubic O_h^5 (Fm3m), 225, Z = 4

Ion	Site	Symmetry	x ^a	y	z	q	α (\AA^3) ^b
Ti	4(a)	O_h	0	0	0	+4	0.506
Cs	8(c)	T_d	1/4	1/4	1/4	+1	2.492
F	24(e)	C_{4v}	0.195	0	0	-1	0.731

^aX-ray data: a = 8.96 \AA ; the F position is not reported for Cs_2TiF_6 and is taken from Cs_2MnF_6 (reference 3, p 341).

^bReference 2.

5.1.2 Hexagonal D_{3d}^3 (P3m1), 164, Z = 1

Ion	Site	Symmetry	x ^a	y	z	q	α (\AA^3) ^b
Ti	1(a)	D_{3d}	0	0	0	+4	0.506
Cs	2(d)	C_{3v}	1/3	2/3	0.691	+1	2.492
F	6(i)	C_s	0.167	-0.167	0.206	-1	0.731

^aX-ray data, a = 6.15 \AA , c = 4.96 \AA ; the Cs and F positions are not reported for Cs_2TiF_6 and are taken from Cs_2ZrF_6 (reference 3, p 350).

^bReference 2.

5.2 Crystal Fields for O_h Site

5.2.1 Crystal-field components, A_{nm} ($\text{cm}^{-1}/\text{\AA}^n$), for Ti (O_h) site of cubic form

A_{nm}	Monopole	Dipole	Self-induced	Total
A_{40}	25,400	32,148	-14,102	43,445
A_{44}	15,179	19,212	-8,428	25,963

$$S^{(0)} = 18,682 \text{ cm}^{-1}/\text{\AA}^2$$

$$S^{(2)} = 17,743 \text{ cm}^{-1}/\text{\AA}^4$$

$$S^{(4)} = 3148.1 \text{ cm}^{-1}/\text{\AA}^8$$

Cs₂TiF₆

5.2.2 Theoretical crystal-field parameters, B_{nm} (cm⁻¹), for A_{nm} of Ti (0_h) site for transition-metal ions with electronic configuration nd^N

(a) For monopole A_{nm}

X ²⁺	N	B ₄₀	B ₄₄
Sc	1	102,950	61,520
Ti	2	63,627	38,023
V	3	43,637	26,078
Cr	4	31,344	18,731
Mn	5	22,791	13,620
Fe	6	18,379	10,984
Co	7	14,575	8,710
Ni	8	11,626	6,947
Cu	9	9,342	5,583

X ³⁺	N	B ₄₀	B ₄₄
Ti	1	32,537	19,444
V	2	23,228	13,881
Cr	3	17,554	10,490
Mn	4	13,622	8,141
Fe	5	10,610	6,340
Co	6	8,905	5,322
Ni	7	7,374	4,407
Cu	8	6,129	3,663
Zn	9	5,121	3,060

X ⁴⁺	N	B ₄₀	B ₄₄
V	1	32,969	19,702
Cr	2	20,770	12,412
Mn	3	19,713	11,780
Fe	4	12,586	7,521
Co	5	10,366	6,195
Ni	6	8,366	4,982
Cu	7	6,604	3,947
Zn	8	5,067	3,028
Ga	9	3,292	1,967

(b) For total A_{nm}

X ²⁺	N	B ₄₀	B ₄₄
Sc	1	176,080	105,230
Ti	2	108,830	65,037
V	3	74,639	44,604
Cr	4	53,611	3,2038
Mn	5	38,983	23,297
Fe	6	31,437	18,787
Co	7	24,929	14,898
Ni	8	19,885	11,883
Cu	9	15,979	9,549

X ³⁺	N	B ₄₀	B ₄₄
Ti	1	55,653	33,259
V	2	39,730	23,743
Cr	3	30,025	17,943
Mn	4	23,300	13,924
Fe	5	18,147	10,845
Co	6	15,232	9,103
Ni	7	12,612	7,537
Cu	8	10,483	6,265
Zn	9	8,759	5,234

X ⁴⁺	N	B ₄₀	B ₄₄
V	1	56,392	33,700
Cr	2	35,525	21,230
Mn	3	33,718	20,150
Fe	4	21,527	12,865
Co	5	17,730	10,596
Ni	6	14,259	8,521
Cu	7	11,296	6,750
Zn	8	8,667	5,180
Ga	9	5,631	3,365

5.3 Crystal Fields for D_{3d} Site5.3.1 Crystal-field components, A_{nm} ($\text{cm}^{-1}/\text{\AA}$), for Ti (D_{3d}) site in hexagonal form

A_{nm}	Monopole	Dipole	Self-induced	Total
A_{20}	-5629	-3291	1172	-7748
A_{40}	-5090	-3546	1986	-6651
A_{43}	10051	6316	-3059	13308

$$S^{(0)} = 8919.9 \text{ cm}^{-1}/\text{\AA}^2$$

$$S^{(2)} = 5251.8 \text{ cm}^{-1}/\text{\AA}^4$$

$$S^{(4)} = 460.86 \text{ cm}^{-1}/\text{\AA}^8$$

5.3.2 Theoretical crystal-field parameters, B_{nm} (cm^{-1}), for A_{nm} of Ti (D_{3d}) site for transition-metal ions with electronic configuration nd^N

(a) For monopole A_{nm}

X^{2+}	N	B_{20}	B_{40}	B_{43}
Sc	1	-7723	-20,630	40,737
Ti	2	-6040	-12,750	25,178
V	3	-4966	-8,745	17,268
Cr	4	-4178	-6,281	12,403
Mn	5	-3542	-4,567	9,019
Fe	6	-3139	-3,683	7,273
Co	7	-2768	-2,921	5,767
Ni	8	-2450	-2,330	4,600
Cu	9	-2179	-1,872	3,697

(b) For total A_{nm}

X^{2+}	N	B_{20}	B_{40}	B_{43}
Sc	1	-10,630	-26,957	53,937
Ti	2	-8,314	-16,661	33,337
V	3	-6,835	-11,426	22,863
Cr	4	-5,751	-8,207	16,422
Mn	5	-4,876	-5,968	11,941
Fe	6	-4,320	-4,813	9,630
Co	7	-3,810	-3,816	7,636
Ni	8	-3,373	-3,044	6,091
Cu	9	-2,999	-2,446	4,895

X^{3+}	N	B_{20}	B_{40}	B_{43}
Ti	1	-4480	-6520	12,875
V	2	-3765	-4655	9,192
Cr	3	-3251	-3518	6,946
Mn	4	-2845	-2730	5,390
Fe	5	-2497	-2126	4,198
Co	6	-2263	-1785	3,524
Ni	7	-2042	-1478	2,918
Cu	8	-1846	-1228	2,425
Zn	9	-1676	-1026	2,026

X^{3+}	N	B_{20}	B_{40}	B_{43}
Ti	1	-6166	-8520	17,048
V	2	-5183	-6082	12,170
Cr	3	-4475	-4597	9,197
Mn	4	-3916	-3567	7,137
Fe	5	-3437	-2778	5,559
Co	6	-3115	-2332	4,666
Ni	7	-2810	-1931	3,863
Cu	8	-2541	-1605	3,211
Zn	9	-2307	-1341	2,683

X^{4+}	N	B_{20}	B_{40}	B_{43}
V	1	-3500	-6607	13,046
Cr	2	-2911	-4162	8,219
Mn	3	-2764	-3950	7,801
Fe	4	-2228	-2522	4,980
Co	5	-2054	-2077	4,102
Ni	6	-1860	-1671	3,299
Cu	7	-1679	-1323	2,613
Zn	8	-1524	-1016	2,005
Ga	9	-1290	-660	1,303

X^{4+}	N	B_{20}	B_{40}	B_{43}
V	1	-4817	-8633	17,274
Cr	2	-4007	-5439	10,882
Mn	3	-3805	-5162	10,328
Fe	4	-3067	-3296	6,594
Co	5	-2827	-2714	5,431
Ni	6	-2560	-2183	4,368
Cu	7	-2311	-1729	3,460
Zn	8	-2098	-1327	2,655
Ga	9	-1775	-862	1,725

5.4 Bibliography and References

1. N. B. Manson, G. A. Shah, B. Howes, and C. D. Flint, $^4\text{A}_g \leftrightarrow ^2\text{E}_g$ Transition of Mn^{4+} in $\text{Cs}_2\text{TiF}_6:\text{MnF}_6^{2-}$, *Mol. Phys.* 34 (1977), 1157.
2. P. C. Schmidt, A. Weiss, and T. P. Das, Effect of Crystal Fields and Self-Consistency on Dipole and Quadrupole Polarizabilities of Closed-Shell Ions, *Phys. Rev. B19* (1979), 5525.
3. R.W.G. Wyckoff, *Crystal Structures*, vol. 3, Interscience, New York (1968).

6. $\text{NH}_4\text{Al}(\text{SO}_4)_2$

6.1 Crystallographic Data on $\text{NH}_4\text{Al}(\text{SO}_4)_2$

Trigonal D_3^2 (P321) (hexagonal setting), 150, $Z = 1$

Ion	Site	Symmetry	x ^a	y	z	q	α (\AA^3) ^b
NH_4	1(a)	D_3	0	0	0	1	2.684
Al	1(b)	D_3	0	0	1/2	3	0.0530
S	2(d)	C_3	1/3	2/3	0.222	6	4.893
O_1	2(d)	C_3	1/3	2/3	0.016	-2	1.349
O_2	6(g)	C_2	0.328	0.344	0.317	-2	1.349

^aX-ray data: $a = 4.724 \text{ \AA}$, $c = 8.225 \text{ \AA}$; the positions for S, O_1 , and O_2 in $\text{NH}_4\text{Al}(\text{SO}_4)_2$ are not given. Those listed above are for the same ions in $\text{KAl}(\text{SO}_4)_2$ (reference 3).

^bReference 2.

6.2 Crystal Fields for Al (D_2) Site

6.2.1 Crystal-field components, A_{nm} ($\text{cm}^{-1}/\text{\AA}^n$) for Al (D_2) site

A_{nm}	Monopole	Dipole	Self-induced	Total
A_{20}	13,668	-42,591	-2720.0	-41,994.49
A_{33}	10,708	-17,390	-1961.9	--
A_{40}	-4,089.1	25,994	4005.7	25,293.63
A_{43}	8,105.7	-36,041	840.80	3,661.09
A_{53}	5,996.4	-15,968	-2489.0	--

$$S^{(0)} = 15,593 \text{ cm}^{-1}/\text{\AA}^2$$

$$S^{(2)} = 7176.6 \text{ cm}^{-1}/\text{\AA}^4$$

$$S^{(4)} = 444.17 \text{ cm}^{-1}/\text{\AA}^8$$

6.2.2 Theoretical crystal-field parameters, B_{nm} (cm^{-1}), for A_{nm} of Al (D_2) site for transition-metal ions with electronic configuration nd^N

(a) For monopole A_{nm}

X^{2+}	N	B_{20}	B_{40}	B_{43}	X^{2+}	N	B_{20}	B_{40}	B_{43}
Sc	1	18,752	-16,573	32,852	Sc	1	-57,616	102,520	14,838
Ti	2	14,666	10,243	20,305	Ti	2	-45,060	63,361	9,171
V	3	12,058	-7,025	13,926	V	3	-37,048	43,454	6,290
Cr	4	10,146	-5,046	10,002	Cr	4	-31,173	31,212	4,518
Mn	5	8,601	-3,669	7,273	Mn	5	-26,427	22,696	3,285
Fe	6	7,621	-2,959	5,865	Fe	6	-23,416	18,302	2,649
Co	7	6,721	-2,346	4,651	Co	7	-20,649	14,513	2,101
Ni	8	5,950	-1,872	3,710	Ni	8	-18,280	11,577	1,676
Cu	9	5,291	-1,504	2,981	Cu	9	-16,256	9,303	1,347

X^{3+}	N	B_{20}	B_{40}	B_{43}	X^{3+}	N	B_{20}	B_{40}	B_{43}
Ti	1	10,877	-5238	10,383	Ti	1	-33,419	32,401	4690
V	2	9,143	-3740	7,413	V	2	-28,090	23,131	3348
Cr	3	7,895	-2826	5,602	Cr	3	-24,256	17,480	2530
Mn	4	6,908	-2193	4,347	Mn	4	-21,224	13,565	1963
Fe	5	6,063	-1708	3,386	Fe	5	-18,629	10,565	1529
Co	6	5,495	-1434	2,842	Co	6	-16,882	8,868	1284
Ni	7	4,957	-1187	2,353	Ni	7	-15,231	7,343	1063
Cu	8	4,483	-987	1,956	Cu	8	-13,774	6,103	883
Zn	9	4,069	-824	1,634	Zn	9	-12,502	5,099	738

X^{4+}	N	B_{20}	B_{40}	B_{43}	X^{4+}	N	B_{20}	B_{40}	B_{43}
V	1	8497	-5308	10,521	V	1	-26,108	32,831	4752
Cr	2	7069	-3344	6,628	Cr	2	-21,720	20,683	2994
Mn	3	6712	-3174	6,291	Mn	3	-20,623	19,630	2841
Fe	4	5410	-2026	4,016	Fe	4	-16,621	12,533	1811
Co	5	4986	-1669	3,308	Co	5	-15,320	10,322	1494
Ni	6	4516	-1342	2,660	Ni	6	-13,875	8,301	1202
Cu	7	4076	-1063	2,108	Cu	7	-12,523	6,576	952
Zn	8	3701	-816	1,617	Zn	8	-11,372	5,046	730
Ga	9	3131	-530	1,051	Ga	9	-9,621	3,278	474

6.3 Experimental Parameters (cm^{-1})

Ion	$F^{(2)}$	$F^{(4)}$	ζ	α	B_{40}	Reference
Cr^{3+}	--	--	186	--	-38,156	1

$\text{NH}_4\text{Al}(\text{SO}_4)_2$

6.4 Bibliography and References

1. S.V.J. Lakshaman, B. C. Venkatareddy, and J. Lakshmanarao, Crystal Field, Spin Orbit and Excitation Interactions in the Spectrum of Chromium Doped Ammonium Aluminium Sulphate, *Physica* 98B (1979), 65.
2. P. C. Schmidt, A. Weiss, and T. P. Das, Effect of Crystal Fields and Self-Consistency on Dipole and Quadrupole Polarizabilities of Closed-Shell Ions, *Phys. Rev.* B19 (1979), 5525.
3. R.W.G. Wyckoff, *Crystal Structures*, vol. 3, Interscience, New York (1968), 166.

7. MgF_2

7.1 Crystallographic Data on MgF_2

Tetragonal D_{4h}^{14} ($P4_2/mnm$), 136, $Z = 2$

Ion	Site	Symmetry	x^a	y	z	q	$\alpha (\text{\AA}^3)^b$
Mg	2(a)	D_{2h}	0	0	0	+2	0.0809
F	4(f)	C_{2v}	0.303	0.303	0	-1	0.731

^aX-ray data: $a = 4.623 \text{ \AA}$, $c = 3.052 \text{ \AA}$ (reference 16).

^bReference 12.

7.2 Crystal Fields for Mg (D_{2h}) Site

7.2.1 Crystal-field components, A_{nm} ($\text{cm}^{-1}/\text{\AA}^n$), for Mg (D_{2h}) site

A_{nm}	Monopole	Dipole	Self-induced	Total
A_{20}	-576.3	3745	-592.7	2576
A_{22}	2,447	-1807	-327.8	312.6
A_{40}	-3,020	-381.7	660.3	-2742
A_{42}	-10,015	-212.2	3965	-6262
A_{44}	4,458	-513.4	-2057	1887

$$S^{(0)} = 8871 \text{ cm}^{-1}/\text{\AA}^2$$

$$S^{(2)} = 6315 \text{ cm}^{-1}/\text{\AA}^4$$

$$S^{(4)} = 656.0 \text{ cm}^{-1}/\text{\AA}^8$$

7.2.2 Theoretical crystal-field parameters, B_{nm} (cm^{-1}), for A_{nm} of Mg (D_{2h}) site for transition-metal ions with electronic configuration nd^N

(a) For monopole A_{nm}

X^{2+}	N	B_{20}	B_{22}	B_{40}	B_{42}	B_{44}
Sc	1	-791	3357	-12,240	-40,591	18,068
Ti	2	-618	2626	-7,565	-25,088	11,167
V	3	-508	2159	-5,188	-17,206	76,59
Cr	4	-428	1816	-3,727	-12,359	5,501
Mn	5	-363	1540	-2,710	-8,987	4,000
Fe	6	-321	1364	-2,185	-7,247	3,226
Co	7	-283	1203	-1,733	-5,747	2,558
Ni	8	-251	1065	-1,382	-4,584	2,040
Cu	9	-223	947	-1,111	-3,684	1,640

X^{3+}	N	B_{20}	B_{22}	B_{40}	B_{42}	B_{44}
Ti	1	-459	1947	-3867	-12,829	5711
V	2	-385	1637	-2762	-9,159	4077
Cr	3	-333	1413	-2087	-6,921	3081
Mn	4	-291	1237	-1620	-5,371	2391
Fe	5	-256	1086	-1262	-4,183	1862
Co	6	-232	984	-1059	-3,511	1563
Ni	7	-209	888	-877	2,907	1294
Cu	8	-189	803	-729	-2,417	1076
Zn	9	-172	728	-609	-2,019	899

X^{4+}	N	B_{20}	B_{22}	B_{40}	B_{42}	B_{44}
V	1	-358	1521	-3920	-12,999	5787
Cr	2	-298	1266	-2470	-8,189	3645
Mn	3	-283	1202	-2344	-7,773	3460
Fe	4	-228	969	-1496	-4,962	2209
Co	5	-210	893	-1233	-4,087	1819
Ni	6	-190	808	-991	-3,287	1463
Cu	7	-172	730	-785	-2,604	1159
Zn	8	-156	663	-602	-1,998	889
Ga	9	-132	561	-391	-1,298	578

(b) For total A_{nm}

X ²⁺	N	B ₂₀	B ₂₂	B ₄₀	B ₄₂	B ₄₄
Sc	1	3534	429	-11,113	-25,380	7648
Ti	2	2764	335	-6,869	-15,686	4727
V	3	2273	276	-4,711	-10,758	3242
Cr	4	1912	232	-3,384	-7,727	2329
Mn	5	1621	197	-2,460	-5,619	1693
Fe	6	1436	174	-1,984	-4,531	1365
Co	7	1267	154	-1,573	-3,593	1083
Ni	8	1121	136	-1,255	-2,866	864
Cu	9	997	121	-1,009	-2,303	694

X ³⁺	N	B ₂₀	B ₂₂	B ₄₀	B ₄₂	B ₄₄
Ti	1	2050	249	-3513	-8022	2417
V	2	1723	209	-2508	-5727	1726
Cr	3	1488	181	-1895	-4328	1304
Mn	4	1302	158	-1471	-3358	1012
Fe	5	1143	139	-1145	-2616	788
Co	6	1036	126	-961	-2196	662
Ni	7	934	113	-796	-1818	548
Cu	8	845	103	-662	-1511	455
Zn	9	767	93	-553	-1262	380

X ⁴⁺	N	B ₂₀	B ₂₂	B ₄₀	B ₄₄	B ₄₄
V	1	1602	194	-3559	-8128	2449
Cr	2	1332	162	-2242	-5120	1543
Mn	3	1265	154	-2128	-4860	1465
Fe	4	1020	124	-1359	-3103	935
Co	5	940	114	-1119	-2556	770
Ni	6	851	103	-900	-2055	619
Cu	7	768	93	-713	-1628	491
Zn	8	698	85	-547	-1249	376
Ga	9	590	72	-355	-812	245

7.3 Experimental Parameters (cm⁻¹)

Ion	F ⁽²⁾	F ⁽⁴⁾	α	ξ	B ₄₀ ^a	Reference
V ²⁺	53,362	28,065	79	--	24,150	10
Y ²⁺	49,508	34,871	--	--	21,735	19

^aCubic approximation B₄₄ = $\sqrt{5/14} |B_{40}|$

7.4 Bibliography and References

1. J. Ferguson, H. J. Guggenheim, L. F. Johnson, and H. Kamimura, Magnetic Dipole Characteristics of the $^3A_{2g} \leftrightarrow ^3T_{2g}$ Transition in Octahedral Nickel (II) Compounds, *J. Chem. Phys.* 38 (1963), 2579.
2. L. F. Johnson, R. E. Dietz, and H. J. Guggenheim, Spontaneous and Stimulated Emission from Co^{2+} Ions in MgF_2 and ZnF_2 , *Appl. Phys. Lett.* 5 (1964), 21.
5. L. F. Johnson, R. E. Dietz, and H. J. Guggenheim, Optical Maser Oscillation from Ni^{2+} in MgF_2 Involving Simultaneous Emission of Phonons, *Phys. Rev. Lett.* 11 (1963), 318.
4. L. F. Johnson and H. J. Guggenheim, Phonon-Terminated Coherent Emission from V^{2+} Ions in MgF_2 , *J. Appl. Phys.* 38 (1964), 483.
5. L. F. Johnson, H. J. Guggenheim, and R. A. Thomas, Phonon-Terminated Optical Masers, *Phys. Rev.* 149 (1966), 179.
6. K. Moncorge and T. Benyuattou, Excited-State Absorption of Ni^{2+} in MgF_2 and MgO , *Phys. Rev.* B37 (1988), 9186.
7. K. Moncorge and T. Benyuattou, Excited State Absorption and Laser Parameters of V^{2+} in MgF_2 and $KMgF_3$, *Phys. Rev.* B37 (1988), 9177.
8. P. F. Moulton, Tunable Solid-State Lasers Targeted for a Variety of Applications, *Laser Focus* 23 (1987), 56.
9. P. F. Moulton and A. Mooradian, Continuously Tunable CW $Ni:MgF_2$ Laser, 1979 IEEE/OSA Conference on Laser Engineering and Applications, p 87D.
10. J. L. Rao, R. M. Krishna, and S. V. J. Lakshman, Nearest Neighbor Point Ion Approximation Calculations of Energy Levels for Mn^{2+} Ions Doped in MgF_2 Single Crystals, *Phys. Status Solidi* B143 (1987), K99.
11. S. Remme, G. Lehmanor, R. Recker, and F. Wallasfon, EPR and Luminescence of Mn^{2+} in MgF_2 Single Crystals, *Solid State Commun.* 56 (1985), 73.
12. P. C. Schmidt, A. Weiss, and T. P. Das, Effect of Crystal Fields and Self-Consistency on Dipole and Quadrupole Polarizabilities of Closed-Shell Ions, *Phys. Rev.* B19 (1979), 5525.
13. R. R. Sharma and S. Sundaram, Transition Metal Ions in Crystals: A Refined Treatment and Deduction of Coulomb and Exchange Interaction Constants, *Solid State Commun.* 33 (1979), 381.
14. W. A. Sibley, S. I. Yun, and L. N. Feuerhelin, Radiation Defect and 3d Impurity Absorption in MgF_2 and $KMgF_3$ Crystals, *J. Phys. Paris* 34 (1973), C9-503.

15. M. D. Sturge, F. R. Merritt, L. F. Johnson, H. J. Guggenheim, and J. P. Van der Ziel, Optical and Microwave Studies of Divalent Vanadium in Octahedral Fluoride Coordination, *J. Chem. Phys.* 54 (1971), 405.
16. R.W.G. Wyckoff, *Crystal Structures*, Vol. 1, Interscience, New York (1968), 251.
17. P. S. Yuen, R. M. Murfitt, and R. L. Collin, Interionic Forces and Ionic Polarization in Alkaline Earth Halide Crystals, *J. Chem. Phys.* 61 (1974), 2383.
18. S. I. Yun, L. A. Kappers, and W. A. Sibley, Enhancement of Impurity Ion Absorption due to Radiation-Produced Defects, *Phys. Rev.* B5 (1973), 773.
19. B. Zhanz, J.-K. Zhy, and S.-H. Liu, Crystal Field Energy Levels and Optical Absorption Intensities of $Ni^{2+}:MgF_2$, NBS Meeting on Basic Properties of Optical Materials (7-9 May 1985).

8. MnF_2

8.1 Crystallographic Data on MnF_2

Tetragonal D_{4h}^{14} ($P4_2/mnm$), 136, $Z = 2$

Ion	Site	Symmetry	x ^a	y	z	q	α (\AA^3) ^b
Mn	2(a)	D_{2h}	0	0	0	+2	0.122
F	4(f)	C_{2v}	0.305	0.305	0	-1	0.731

^aX-ray data: $a = 4.8734 \text{ \AA}$, $c = 3.3099 \text{ \AA}$ (reference 18).

^bReference 14.

8.2 Crystal Fields for Mn (D_{2h}) Site

8.2.1 Crystal-field components, A_{nm} ($\text{cm}^{-1}/\text{\AA}^n$), for Mn (D_{2h}) site

A_{nm}	Monopole	Dipole	Self-induced	Total
A_{20}	901.5	1815.67	-459.22	2258
A_{22}	2638	-847.40	-300.87	1490
A_{40}	-1670	-125.49	266.58	-1529
A_{42}	-7263	-61.74	2376.30	-4948
A_{44}	3218	-222.98	-1239.99	1755

$$S^{(0)} = 6,070 \text{ cm}^{-1}/\text{\AA}^2$$

$$S^{(2)} = 3,813 \text{ cm}^{-1}/\text{\AA}^4$$

$$S^{(4)} = 307.3 \text{ cm}^{-1}/\text{\AA}^8$$

8.2.2 Theoretical crystal-field parameters, B_{nm} (cm^{-1}), for A_{nm} of Mn (D_{2h}) site for transition-metal ions with electronic configuration nd^N

(a) For monopole A_{nm}

X^{2+}	N	B_{20}	B_{22}	B_{40}	B_{42}	B_{44}
Sc	1	1237	3619	-6769	-29,437	13,043
Ti	2	967	2831	-4183	-18,194	8,061
V	3	795	2327	-2869	-12,478	5,529
Cr	4	669	1953	-2061	-8,963	3,971
Mn	5	567	1660	-1499	-6,517	2,888
Fe	6	503	1471	-1208	-5,256	2,329
Co	7	443	1297	-958	-4,168	1,847
Ni	8	392	1148	-764	-3,324	1,473
Cu	9	349	1021	-614	-2,671	1,184

X^{3+}	N	B_{20}	B_{22}	B_{40}	B_{42}	B_{44}
Ti	1	717	2099	-2139	-9304	4122
V	2	603	1765	-1527	-6642	2943
Cr	3	521	1524	-1154	-5020	2224
Mn	4	456	1333	-896	-3895	1726
Fe	5	400	1170	-698	-3034	1344
Co	6	362	1061	-586	-2546	1128
Ni	7	327	957	-485	-2108	934
Cu	8	296	865	-403	-1753	777
Zn	9	268	785	-337	-1464	649

X^{4+}	N	B_{20}	B_{22}	B_{40}	B_{42}	B_{44}
V	1	560	1640	-2168	-9427	4177
Cr	2	466	1364	-1366	-5939	2631
Mn	3	443	1296	-1296	-5637	2498
Fe	4	357	1044	-827	-3599	1595
Co	5	329	962	-682	-2964	1313
Ni	6	298	872	-548	-2384	1056
Cu	7	269	787	-434	-1888	837
Zn	8	244	714	-333	-1449	642
Ga	9	207	604	-216	-941	417

(b) For total A_{nm}

X ²⁺	N	B ₂₀	B ₂₂	B ₄₀	B ₄₂	B ₄₄
Sc	1	3098	2044	-6197	-20,054	7113
Ti	2	2423	1599	-3830	-12,395	4396
V	3	1992	1315	-2527	-8,501	3015
Cr	4	1676	1106	-1887	-6,106	2166
Mn	5	1421	938	-1372	-4,440	1575
Fe	6	1259	831	-1106	-3,580	1270
Co	7	1110	733	-877	-2,839	1007
Ni	8	983	649	-700	-2,265	803
Cu	9	874	577	-562	-1,820	645

X ³⁺	N	B ₂₀	B ₂₂	B ₄₀	B ₄₂	B ₄₄
Ti	1	1797	1186	-1959	-6338	2248
V	2	1510	997	-1398	-4525	1605
Cr	3	1304	861	-1057	-3420	1213
Mn	4	1141	753	-820	-2654	941
Fe	5	1002	661	-639	-2067	733
Co	6	908	599	-536	-1735	615
Ni	7	819	540	-444	-1436	509
Cu	8	741	489	-369	-1194	423
Zn	9	672	444	-308	-998	354

X ⁴⁺	N	B ₂₀	B ₂₂	B ₄₀	B ₄₂	B ₄₄
V	1	1404	926	-1985	-6423	2278
Cr	2	1168	771	-1250	-4046	1435
Mn	3	1109	732	-1187	-3840	1362
Fe	4	894	590	-758	-2452	870
Co	5	824	544	-624	-2019	716
Ni	6	746	492	-502	-1624	576
Cu	7	673	444	-398	-1287	456
Zn	8	611	403	-305	-987	350
Ga	9	517	341	-198	-641	227

8.3 Experimental Parameters (cm⁻¹)

Ion	F(2)	F(4)	α	ζ	B_{40}^a	Reference
Co ²⁺	--	--	--	--	17,220	2
Mn ²⁺	62,230	39,690	76	320	15,750	10
Mn ²⁺	61,355	39,791	76	320	15,792	10
Mn ²⁺	58,849	46,746	--	--	17,220	4
Mn ²⁺	67,830	41,215	66.1	--	16,569	15
Mn ²⁺	67,550	41,240	65	--	17,300	19 ^b
Mn ²⁺	69,510	41,328	--	--	16,380	16

^aCubic approximation $B_{44} = \sqrt{5/14} B_{40}$ ^bFit with full D_{2h} symmetry; $B_{20} = -1480$, $B_{22} = 4750$,
 $B_{42} = -1650$, $B_{44} = -10,260$.8.4 References

1. W. H. Baur, Über die Verfeinerung der Kristallstrukturbestimmung einiger Vertreter des Rutiltyps: II.--Die Difluoride von Mn, Fe, Co, Ni und Zn, *Acta Crystallogr.* 11 (1958), 488.
2. L. F. Blunt, Optical Absorption of Cobalt in Manganese Fluoride, *J. Chem. Phys.* 44 (1966), 2317.
3. D. Curie, C. Barthou, and B. Canny, Covalent Bonding of Mn²⁺ Ions in Octahedral and Tetrahedral Coordination, *J. Chem. Phys.* 61 (1974), 3048.
4. D. M. Finlayson, I. S. Robertson, T. Smith, and R.W.H. Stevenson, The Optical Absorption of Manganese Zinc Fluoride Single Crystals Near the Neel Temperature, *Proc. Phys. Soc.* 76 (1960), 355.
5. H. J. Hrostowski and R. H. Kaiser, Absorption Spectra of MnF₂ and KMnF₃, *Bull. Am. Phys. Soc.* 4 (1959), 167.
6. L. F. Johnson, R. E. Dietz, and H. J. Guggenheim, Exchange Splitting of the Ground State of Ni²⁺ Ions in Antiferromagnetic MnF₂, KMnF₃, and RbMnF₃, *Phys. Rev. Lett.* 17 (1966), 13.
7. L. F. Johnson, R. E. Dietz, and H. J. Guggenheim, Optical Maser Oscillation from Ni²⁺ in MgF₂ Involving Simultaneous Emission of Phonons, *Phys. Rev. Lett.* 11 (1963), 318.
8. L. F. Johnson, H. J. Guggenheim, and R. A. Thomas, Phonon-Terminated Optical Masers, *Phys. Rev.* 149 (1966), 179.
9. N. A. Kulagin and D. T. Sviridov, Charge of the Effective Occupation Numbers of 3d-Shells of Mn²⁺ Ions in Manganese Halide Crystals, *Phys. Status Solidi* B112 (1982), K61.

MnF₂

10. W. Low and G. Rosengarten, *J. Mol. Spectrosc.* 12 (1964), 319.
11. D. S. McClure, R. Meltzer, S. A. Reed, P. Russell, and J. W. Stout, Electronic Transitions with Spin Change in Several Antiferromagnetic Crystals; in *Optical Properties of Ions in Crystals*, Interscience, New York (1967), p 257.
12. B. Ng and D. J. Newman, Ab Initio Calculations of Ligand Field Correlations Effects in Mn²⁺-F⁻, *Chem. Phys. Lett.* 1301 (1986), 410.
13. B. Ng and D. J. Newman, A Linear Model of Crystal Field Correlation Effects in Mn²⁺, *J. Chem. Phys.* 84 (1986), 3291.
14. P. C. Schmidt, A. Weiss, and T. P. Das, Effect of Crystal Fields and Self-Consistency on Dipole and Quadrupole Polarizabilities of Closed-Shell Ions, *Phys. Rev.* B19 (1979), 5525.
15. R. Stevenson, Absorption Spectra of MnF₂, KMnF₂, RbMnF₂, and CsMnF₂, *Can. J. Phys.* 43 (1965), 1732.
16. J. W. Stout, Absorption Spectrum of Manganese Fluoride, *J. Chem. Phys.* 31 (1959), 709.
17. J. W. Stout and S. A. Reed, The Crystal Structure of MnF₂, FeF₂, CoF₂, NiF₂, and ZnF₂, *J. Am. Chem. Soc.* 76 (1954), 5279.
18. R.W.G. Wyckoff, *Crystal Structures*, Vol. 1, Interscience, New York (1968), 251. (See also ref 1 above.)
19. W.-L. Yu and M.-G. Zhao, Determination of the MnF₂ and ZnF₂ Crystal Structure from the EPR and Optical Measurement of Mn²⁺, *J. Phys.* C18 (1985), L1087.

9. ZnF_2

9.1 Crystallographic Data on ZnF_2

Tetragonal D_{4h}^{14} ($P4_2/mnm$), 136, $Z = 2$

Ion	Site	Symmetry	x ^a	y	z	q	α (\AA^3) ^b
Zn	2(a)	D_{2h}	0	0	0	+2	0.676
F	4(f)	C_{2v}	0.303	0.303	0	-1	0.731

^aX-ray data: $a = 4.7034 \text{ \AA}$, $c = 3.1335 \text{ \AA}$ (reference 10); a , c same, but $x_F = 0.307$ (reference 8).

^bReference 7.

9.2 Crystal Fields for Zn Site (D_{2h})

9.2.1 Crystal-field components, A_{nm} ($\text{cm}^{-1}/\text{\AA}^n$), for Zn (D_{2h}) site

A_{nm}	Monopole	Dipole	Self-induced	Total
A_{20}	-304.8	2855	-593.0	1957
A_{22}	2659	-1379	-346.0	934.0
A_{40}	-249.1	-268.3	430.1	-2329
A_{42}	-9011	-135.5	3350	-5796
A_{44}	-4046	-383.2	1786	-1876

$$S^{(0)} = 8214.0 \text{ cm}^{-1}/\text{\AA}^2$$

$$S^{(2)} = 5417.7 \text{ cm}^{-1}/\text{\AA}^4$$

$$S^{(4)} = 508.50 \text{ cm}^{-1}/\text{\AA}^8$$

9.2.2 Theoretical crystal-field parameters, B_{nm} (cm^{-1}), for A_{nm} of Zn (D_{2h}) site for transition-metal ions with electronic configuration nd^N

(a) For monopole A_{nm}

X^{2+}	N	B_{20}	B_{22}	B_{40}	B_{42}	B_{44}
Sc	1	-418	3648	-1010	-36,522	-16,398
Ti	2	-327	2853	-624	-22,573	-10,135
V	3	-269	2346	-428	-15,481	-6,951
Cr	4	-226	1974	-307	-11,120	-4,993
Mn	5	-192	1673	-224	-8,086	-3,631
Fe	6	-170	1483	-180	-6,520	-2,928
Co	7	-150	1307	-143	-5,171	-2,322
Ni	8	-133	1158	-114	-4,124	-1,852
Cu	9	-118	1029	-92	-3,314	-1,488

X^{3+}	N	B_{20}	B_{22}	B_{40}	B_{42}	B_{44}
Ti	1	-243	2116	-319	-11,543	-5183
V	2	-204	1779	-228	-8,241	-3700
Cr	3	-176	1536	-172	-6,228	-2796
Mn	4	-154	1344	-134	-4,833	-2170
Fe	5	-135	1180	-104	-3,764	-1690
Co	6	-123	1069	-87	-3,159	-1419
Ni	7	-11	964	-72	-2,616	-1175
Cu	8	-100	872	-60	-2,174	-976
Zn	9	-91	792	-50	-1,817	-816

X^{4+}	N	B_{20}	B_{22}	B_{40}	B_{42}	B_{44}
V	1	-189	1653	-323	-11,696	-5252
Cr	2	-158	1375	-204	-7,368	-3308
Mn	3	-150	1306	-193	-6,993	-3140
Fe	4	-121	1052	-123	-4,465	-2005
Co	5	-111	970	-102	-3,677	-1651
Ni	6	-101	879	-82	-2,957	-1328
Cu	7	-91	793	-65	-2,343	-1052
Zn	8	-83	720	-50	-1,798	-807
Ga	9	-70	609	-32	-1,168	-524

(b) For total A_{mm}

X ²⁺	N	B ₂₀	B ₂₂	B ₄₀	B ₄₂	B ₄₄
Sc	1	2685	1281	-9439	-23,491	-7603
Ti	2	2100	1002	-5834	-14,519	-4699
V	3	1727	824	-4001	-9,958	-3223
Cr	4	1453	693	-2874	-7,152	-2315
Mn	5	1232	588	-2090	-5,201	-1683
Fe	6	1091	521	-1685	-4,194	-1358
Co	7	962	459	-1336	-3,326	-1076
Ni	8	852	407	-1066	-2,653	-859
Cu	9	758	362	-857	-2,132	-690

X ³⁺	N	B ₂₀	B ₂₂	B ₄₀	B ₄₂	B ₄₄
Ti	1	1557	743	-2983	-7425	-2403
V	2	1309	625	-2130	-5300	-1716
Cr	3	1130	539	-1610	-4006	-1297
Mn	4	989	472	-1249	-3108	-1006
Fe	5	868	414	-973	-2421	-784
Co	6	787	375	-817	-2032	-658
Ni	7	710	339	-676	-1683	-545
Cu	8	642	306	-562	-1399	-453
Zn	9	583	278	-470	-1169	-378

X ⁴⁺	N	B ₂₀	B ₂₂	B ₄₀	B ₄₂	B ₄₄
V	1	1217	581	-3023	-7523	-2435
Cr	2	1012	483	-1904	-4739	-1534
Mn	3	961	459	-1808	-4498	-1456
Fe	4	775	370	-1154	-2872	-930
Co	5	714	341	-950	-2365	-766
Ni	6	647	309	-764	-1902	-616
Cu	7	584	279	-606	-1507	-488
Zn	8	530	253	-465	-1156	-374
Ga	9	448	214	-302	-751	-243

9.3 Experimental Parameters (cm⁻¹)

Ion	F ⁽²⁾	F ⁽⁴⁾	α	β	B ₂₀	B ₂₂	B ₄₀	B ₄₂	B ₄₄	Ref
Mn ²⁺	57,550	41,240	65	337	-920	3730	21,180	-1390	-12,660	11

9.4 Bibliography and References

1. D. Curie, C. Barthou, and B. Canny, Covalent Bonding of Mn^{2+} Ions in Octahedral and Tetrahedral Coordination, *J. Chem. Phys.* 61 (1974), 3048.
2. D. M. Finlayson, I. S. Robertson, T. Smith, and R.W.H. Stevenson, The Optical Absorption in Manganese Zinc Fluoride Single Crystals Near the Neél Temperature, *Proc. Phys. Soc.* 76 (1960), 355.
3. L. F. Johnson, R. E. Dietz, and H. J. Guggenheim, Spontaneous and Stimulated Emission from Co^{2+} Ions in MgF_2 and ZnF_2 , *Appl. Phys. Lett.* 5 (1964), 21.
4. L. F. Johnson, H. J. Guggenheim, and R. A. Thomas, Phonon-Terminated Optical Masers, *Phys. Rev.* 149 (1966), 179.
5. D. T. Palumbo and J. J. Brown, Electronic States of Mn^{2+} Activated Phosphors: II.--Orange-to-Red Emitting Phosphors, *J. Electrochem. Soc.* 118 (1971), 1159.
6. M. L. Reynolds and G.F.J. Garlick, The Infrared Emission of Nickel Ion Impurity Centers in Various Solids, *Infrared Phys.* 7 (1967), 151.
7. P. C. Schmidt, A. Weiss, and T. P. Das, Effect of Crystal Fields and Self-Consistency on Dipole and Quadrupole Polarizabilities of Closed-Shell Ions, *Phys. Rev.* B19 (1979), 5525.
8. J. W. Stout and S. A. Reed, The Crystal Structure of MnF_2 , FeF_2 , CoF_2 , NiF_2 , and ZnF_2 , *J. Am. Chem. Soc.* 76 (1954), 5279.
9. M. Tinkham, Paramagnetic Resonance in Dilute Iron Group Fluorides: I.--Fluorine Hyperfine Structure, *Proc. Roy. Soc.* A236 (1956), 535.
10. R.W.G. Wyckoff, Crystal Structures, vol. 1, Interscience, New York, (1968), 251.
11. W.-L. Yu and M.-G. Zhao, Determination of the MnF_2 and ZnF_2 Crystal Structure from the EPR and Optical Measurements of Mn^{2+} , *J. Phys.* C18 (1985), L1087.

10. MgO

10.1 Crystallographic Data on MgO

Cubic O_h^5 (Fm3m), 225, Z = 4

Ion	Site	Symmetry	x ^a	y	z	q	α (Å ³) ^b
Mg	4(a)	O_h	0	0	0	+2	0.0809
O	4(b)	O_h	1/2	1/2	1/2	-2	1.349

^aX-ray data, a = 4.2112 (reference 54).

^bReference 45.

10.2 Crystal Fields for Mg (O_h) Site

10.2.1 Crystal-field components, A_{nm} (cm⁻¹/Åⁿ), for Mg (O_h) site

A_{nm}	Monopole	Self-induced	Total
A_{40}	20,084	-5,812	14,271
A_{44}	12,002	-3,474	8,528.8

$$S^{(0)} = 11,851 \text{ cm}^{-1}/\text{\AA}^2$$

$$S^{(2)} = 7523.7 \text{ cm}^{-1}/\text{\AA}^4$$

$$S^{(4)} = 621.35 \text{ cm}^{-1}/\text{\AA}^8$$

10.2.2 Theoretical crystal-field parameters, B_{nm} (cm^{-1}), for A_{nm} of Mg (O_h) site for transition-metal ions with electronic configuration nd^N

(a) For monopole A_{nm}

X^{2+}	N	B_{40}	B_{44}
Sc	1	81,400	48,644
Ti	2	50,310	30,065
V	3	34,504	20,619
Cr	4	24,784	14,810
Mn	5	18,021	10,769
Fe	6	14,533	8,685
Co	7	11,724	6,887
Ni	8	9,192	5,493
Cu	9	7,387	4,414

(b) For total A_{nm}

X^{2+}	N	B_{40}	B_{44}
Sc	1	57,840	34,567
Ti	2	35,749	21,365
V	3	24,518	14,652
Cr	4	17,610	10,525
Mn	5	12,805	7,653
Fe	6	10,326	6,171
Co	7	8,188	4,894
Ni	8	6,532	3,904
Cu	9	5,249	3,137

X^{3+}	N	B_{40}	B_{44}
Ti	1	25,728	15,375
V	2	18,367	10,976
Cr	3	13,880	8,295
Mn	4	10,771	6,437
Fe	5	8,389	5,013
Co	6	7,042	4,208
Ni	7	5,830	3,484
Cu	8	4,846	2,896
Zn	9	4,049	2,420

X^{3+}	N	B_{40}	B_{44}
Ti	1	18,281	10,925
V	2	13,051	7,800
Cr	3	9,863	5,894
Mn	4	7,654	4,574
Fe	5	5,961	3,563
Co	6	5,003	2,990
Ni	7	4,143	2,476
Cu	8	3,444	2,058
Zn	9	2,877	1,719

X^{4+}	N	B_{40}	B_{44}
V	1	26,069	15,579
Cr	2	16,423	9,814
Mn	3	15,587	9,315
Fe	4	9,952	5,947
Co	5	8,196	4,898
Ni	6	6,592	3,939
Cu	7	5,222	3,121
Zn	8	4,007	2,394
Ga	9	2,603	1,556

X^{4+}	N	B_{40}	B_{44}
V	1	18,524	11,070
Cr2	2	11,669	6,974
Mn	3	11,076	6,619
Fe4	4	7,071	4,226
Co	5	5,824	3,481
Ni6	6	4,684	2,799
Cu	7	3,711	2,218
Zn	8	2,847	1,702
Ga	9	1,850	1,105

10.3 Experimental Parameters (cm⁻¹)

Ion	F ⁽²⁾	F ⁽⁴⁾	α	B ₄₀	Ref.
Cr ³⁺	50,906	37,825	70	33,579	52
V ²⁺	42,429	30,239	60	30,429	52
V ²⁺	47,625	25,455	79	29,400	48
Cr ³⁺	52,780	36,792	70	33,390	7 ^a
Cr ³⁺	54,600	40,950	--	34,020	25 ^b
Cr ³⁺	54,250	40,320	--	34,860	32 ^c
Cr ²⁺	--	--	--	14,000	12
Ni ²⁺	--	--	--	18,060	27 ^d
Ni ²⁺	--	--	--	17,115	40
Ni ²⁺	66,343	44,447	--	17.451	37 ^e

^aζ = 270^bζ = 135^cζ = 210^dRefers to experimental optical data by A. G. Shenstone (reference 46).^eζ = 64510.4 Bibliography and References

1. B. R. Anderson, L. J. Challis, J.H.M. Stoelinga, and P. Wuder, Far Infrared Studies of Cr²⁺ in MgO, *J. Phys. C1* (1974), 2234.
2. K. W. Blazey, Optical Absorption of MgO:F₃, *J. Phys. Chem. Solids*, 38 (1977), 671.
3. A. Boyrivent, E. Duval, M. Montagra, G. Villiani, and O. Pilla, New Experimental Results for the Interpretation of the ⁴A_{2g} → ⁴T_{2g} Spectra of Cr³⁺ and V²⁺ in MgO, *J. Phys. C12* (1979), 1803.
4. L. L. Chase, Electron Spin Resonance of the Excited ²E(3d³) Level of Cr³⁺ and V²⁺ in MgO, *Phys. Rev. 168* (1968), 341.
5. J. J. Davies and J. E. Wertz, Trivalent Titanium in Tetragonal Symmetry in MgO and CaO, *J. Magn. Reson. 1* (1969), 500.

MgO

6. G.G.C.M. Dekort, Millimetre and Submillimetre Wave Spectroscopy of Solids, Doctoral thesis (1979), De Katholieke Universiteit Te Nijmegen, Chapter III, IV.
7. W. M. Fairbanks, Jr., and G. K. Klauminzer, Tetragonal-Field Splittings of Levels in $MgO:Cr^{3+}$, Phys. Rev. B7 (1973), 500.
8. E. R. Feher, Effect of Uniaxial Stresses on the Paramagnetic Spectra of Mn^{3+} and Fe^{3+} in MgO , Phys. Rev. 136 (1964), A145.
9. J. Ferguson, K. Knox, and D. L. Wood, Effect of Next Nearest Neighbor Ions on the Crystal Field Splitting of Transition Metal Ions in Crystals, J. Chem. Phys. 35 (1961), 2236.
10. J. R. Fletcher and K.W.H. Stevens, The Jahn-Teller Effect of Octahedrally Co-ordinated $3d^4$ Ions, J. Phys. C2 (1969), 444.
11. J. R. Gabriel, D. F. Johnston, and M.J.D. Powell, A Calculation of the Ground State Splitting for Mn^{2+} Ions in a Cubic field, Proc. Roy. Soc. (1961), 503.
12. C. Greskovich and V. S. Stubican, Divalent Chromium in Magnesium-Chromium Spinels, J. Phys. Chem. Solids 27 (1966), 1379.
13. F. Hagan, P. S. King, D. J. Monk, D. T. Murphy, V. W. Rampton, and P. C. Wiscombe, Phonon Spectroscopy of Mn^{3+} in MgO , in Phonon Scattering in Condensed Matter, Ed. H. J. Marris, Third International Conference on Phonon Scattering in Condensed Matter, Brown University (1979).
14. F. S. Ham, Acoustic Paramagnetic Resonance Spectrum of Cr^{2+} in MgO , Phys. Rev. B4 (1971), 3854.
15. F. S. Ham, W. M. Schwartz, and M.C.M. O'Brien, Jahn-Teller Effects in the Far-Infrared, EPR, and Mossbauer Spectra of $MgO:Fe^{2+}$, Phys. Rev. 185 (1969), 548.
16. U. Hochli, K. A. Muller, and P. Wysling, Paramagnetic Resonance and Relaxation of Cu^{2+} and Ni^{3+} in MgO and CaO : The Determination of Jahn-Teller Energy Splittings, Phys. Lett. 15 (1965), 5.
17. C. Y. Huang, R. S. Kent, and S. A. Marshall, Temperature Dependence of the Hyperfine-Structure Splitting of Divalent Manganese in Single-Crystal Magnesium Oxide, Phys. Rev. B7 (1973), 552.
18. J. L. Janson and Z. A. Rachko, Nature of Impurity-Induced UV Luminescence of MgO crystals, Phys. Status Solidi A53 (1979), 121.
19. L. F. Johnson, R. E. Dietz, and H. J. Guggenheim, Optical Maser Oscillation from Ni^{2+} in MgF_2 Involving Simultaneous Emission of Phonons, Phys. Rev. Lett. 11 (1963), 318.

20. L. F. Johnson, H. J. Guggenheim, and R. A. Thomas, Phonon-Terminated Optical Masers, *Phys. Rev.* 149 (1966), 179.
21. X.-Y. Kuang, Stark Levels $^4T_1(G)$ in $MgO:Mn^{2+}$, *Phys. Rev.* B37 (1988), 9719.
22. R. Lacroix, J. Weber, E. Duval, and A. Boyrivent, Structure of the $^4A_{2g}$ \rightarrow $^4T_{2g}$ Zero-Phonon Spectrum in $MgO:Cr^{3+}$: Spin-Orbit and Vibronic Coupling, *J. Phys.* C13 (1980), L781.
23. J. Lange, Dynamic Jahn-Teller Effect for Cr^{2+} in MgO: Acoustic Paramagnetic Resonance, *Phys. Rev.* B14 (1976), 4791.
24. J. P. Larkin and G. F. Imbusch, Optical Absorption in $MgO:Cr^{3+}$, *Phys. Rev.* B7 (1973), 495.
25. A. D. Liehr, The Three Electron (or Hole) Cubic Ligand Field Spectrum, *J. Phys. Chem.* 67 (1963), 1314.
26. W. Low, Paramagnetic Resonance in Solids, *Solid State Phys. Suppl.* 2 (1960), 104.
27. W. Low, Paramagnetic and Optical Spectra of Divalent Nickel in Cubic Crystalline Fields, *Phys. Rev.* 109 (1958), 247.
28. W. Low and M. Weger, Paramagnetic Resonance and Optical Spectra of Divalent Iron in Cubic Fields: I.--Theory, *Phys. Rev.* 118 (1960), 1119.
29. W. Low and M. Weger, Paramagnetic Resonance and Optical Spectra of Divalent Iron in Cubic Fields: II.--Experimental Results, *Phys. Rev.* 118 (1960), 1130.
30. Z. Luz, A. Raizman, and J. T. Suss, Oxygen-17 Superfine Structure of Rh^{2+} Jahn-Teller Ions in MgO, *Solid State Commun.* 21 (1977), 849.
31. W. C. Mackrodt, R. F. Stewart, J. C. Campbell, and I. H. Hillier, The Calculated Defect Structure of ZnO, *J. Phys. Paris* 41 (Suppl. to No. 7) (1980), C6-64.
32. R. M. Macfarlane, Perturbation Methods in the Calculation of Zeeman Interactions and Magnetic Dipole Line Strengths for d^3 Trigonal-Crystal Spectra, *Phys. Rev.* 131 (1970), 989. Errata, *Phys. Rev.* B3 (1971), 1054.
33. N. B. Marison and M. D. Sturge, Absence of a Strong Jahn-Teller Effect in the $^4T_{2g}$ Excited State of V^{2+} in MgO, *Phys. Rev.* B22 (1980), 2861.
34. A. J. Mann and P. J. Stephens, Magnetic Circular dichroism of Impurities in Solids: $HgO:Co$, *Phys. Rev.* B9 (1974), B63.

MgO

35. F. G. Marshall and V. W. Rampton, The Acoustic Paramagnetic Resonance Spectrum of Chromous Ions in Magnesium Oxide, *J. Phys. C1* (1968), 594.
36. D. Meyer, M. Regis, and Y. Farge, Far Infrared Absorption of Fe^{2+} Ions in MgO Crystals, *Phys. Lett. 48A* (1974), 41.
37. K. Moncorgé and T. Benyattou, Excited-State Absorption of Ni^{2+} in MgF_2 and MgO, *Phys. Rev. B37* (1988), 9186.
38. M.C.M. O'Brien, The Jahn-Teller Coupling of $3d^6$ Ions in a Cubic Crystal, *Proc. Phys. Soc. 86* (1965), 847.
39. M. Okada, T. K. Awakubo, T. Seiyama, and M. Naka-Gawa, Enhancement of $3d$ -Electron Transitions in Neutron-Irradiated $MgO:Mn^{2+}$ Crystals, *Phys. Status Solidi B144* (1987), 903.
40. R. Pappalardo, D. L. Wood, and R. C. Linares, Jr., Optical Absorption Spectra of Ni-Doped Oxide Systems: I, *J. Chem. Phys. 35* (1961), 1460.
41. J. L. Patel and J. K. Wigmore, Jahn-Teller Parameters of $MgO:Cr^{2+}$ Determined Using Heat Pulses, *J. Phys. C10* (1977), 1829.
42. J. E. Ralph and M. G. Townsend, Fluorescence and Absorption Spectra of Ni^{2+} in MgO (1969), 8.
43. J. E. Ralph and M. G. Townsend, Near-Infrared Fluorescence and Absorption Spectra of Co^{2+} and Ni^{2+} in MgO, *J. Chem. Phys. 48* (1968), 149.
44. M. Régis, Y. Farge, and M. Fontana, Etude des Transitions Optiques dans $MgO:Ni^{2+}$ par Dichroïsme Circulaire Magnétique, *Phys. Status Solidi B57* (1973), 307.
45. P. C. Schmidt, A. Weiss, and T. P. Das, Effect of Crystal Fields and Self-Consistency on Dipole and Quadrupole Polarizabilities of Closed-Shell Ions, *Phys. Rev. B19* (1979), 5525.
46. A. G. Shenstone, *J. Opt. Soc. Am.* (1954), 749.
47. G. Smith, Evidence for Optical Absorption by Fe^{2+} - Fe^{3+} Interactions in $MgO:Fe$, *Phys. Status Solidi A61* (1980), K191.
48. M. D. Sturge, Jahn-Teller Effect in the $^4T_{2g}$ Excited State of V^{2+} in MgO, *Phys. Rev. A140* (1965), 880.
49. M. D. Sturge, Optical Spectrum of Divalent Vanadium in Octahedral Coordination, *Phys. Rev. 130* (1963), 639.
50. M. D. Sturge, Strain-Induced Splitting of the 2E State of V^{2+} in MgO, *Phys. Rev. 131* (1963), 1456.

51. M. D. Sturge, F. R. Merritt, L. F. Johnson, H. J. Guggenheim, and J. P. van der Ziel, Optical and Microwave Studies of Divalent Vanadium in Octahedral Fluoride Coordination, *J. Chem. Phys.* 54 (1971), 405.
52. D. T. Sviridov, R. K. Sviridova, N. I. Kulik, and V. B. Glasko, Optical Spectra of the Isoelectronic Ions V^{2+} , Cr^{3+} , and Mn^{4+} in an Octahedral Coordination, *J. Appl. Spectrosc.* 30 (1979), 334.
53. G. Viliani, M. Montagna, O. Pilla, A. Fontana, M. Bacci, and A. Ranfagni, Magnetic Circular Dichroism in Split Zero-Phonon Line of $MgO:V^{2+}$, *J. Phys.* C11 (1979), L439.
54. J. Y. Wong, Far-Infrared Spectra of Iron-Doped MgO, *Phys. Rev.* 168 (1968), 337.
55. R. W. G. Wyckoff, *Crystal Structures*, vol. 1, Interscience, New York (1964), 88.
56. P. Wysling, K. A. Muller, and U. Hochli, Paramagnetic Resonance and Relaxation of Ag^{2+} and Pd^{3+} in MgO and CaO, *Helv. Phys. Acta* 38 (1965), 358.
57. W. M. Yen, L. R. Elias, and D. L. Huber, Utilization of Near- and Vacuum-Ultra-Violet Synchrotron Radiation for the Excitation of Visible Fluorescences in Ruby and $MgO:Cr^{3+}$, *Phys. Rev. Lett.* 24 (1970), 1011.

11. $\text{Be}_3\text{Al}_2(\text{SiO}_3)_6$ (Beryl, Emerald)

11.1 Crystallographic and X-Ray Data on $\text{Be}_3\text{Al}_2(\text{SiO}_3)_6$

Hexagonal D_{6h}^2 (P6/mcc), 192, $Z = 2$

Ion	Site	Symmetry	x^a	y	z	q	$\alpha(\text{\AA})^{3b}$
Al	4(c)	D_3	1/3	2/3	1/4	+3	0.0530
Be	6(f)	D_2	1/4	0	1/4	+2	0.0125
Si	12(l)	C_s	0.382	0.118	0	+4	0.0165
O ₁	12(l)	C_s	0.294	0.242	0	-2	1.349
O ₂	24(m)	C_1	0.499	0.143	0.138	-2	1.349

^aX-ray data: $a = 9.206 \text{\AA}$, $c = 9.205 \text{\AA}$ (reference 14).

^bReference 9.

11.2 Crystal Fields for Al (D_3) Site

11.2.1 Crystal-field components, A_{nm} ($\text{cm}^{-1}/\text{\AA}^n$), for Al (D_3) site

A_{nm}	Monopole	Dipole	Self-induced	Total
A_{20}	-16,578	13,630	1289	-1659
A_{33}	-i4,113	-i2,941	i2339	-i4716
A_{40}	-16,436	-23,937	6117	-34257
A_{43}	20,357	29,273	-8341	41288
A_{53}	-i4,004	-i3,056	i1543	-i5516

$$S^{(0)} = 18,026 \text{ cm}^{-1}/\text{\AA}^2$$

$$S^{(2)} = 13,560 \text{ cm}^{-1}/\text{\AA}^4$$

$$S^{(4)} = 1,535.7 \text{ cm}^{-1}/\text{\AA}^8$$

11.2.2 Theoretical crystal-field parameters, B_{nm} (cm^{-1}), for A_{nm} of Al (D_3) site for transition-metal ions with electronic configuration nd^N

(a) For monopole A_{nm}

X^{2+}	N	B_{20}	B_{40}	B_{43}
Sc	1	-22,745	-66,615	82,507
Ti	2	-17,788	-41,172	50,994
V	3	-14,625	-28,237	34,973
Cr	4	-12,306	-20,282	25,121
Mn	5	-10,433	-14,748	18,266
Fe	6	-9,244	-11,893	14,730
Co	7	-8,151	-9,431	11,681
Ni	8	-7,216	-7,523	9,317
Cu	9	-6,417	-6,045	7,487

(b) For total A_{nm}

X^{2+}	N	B_{20}	B_{40}	B_{43}
Sc	1	-2276	-138,840	167,340
Ti	2	-1780	-85,814	103,430
V	3	-1464	-58,854	70,933
Cr	4	-1232	-42,273	50,949
Mn	5	-1044	-30,739	37,048
Fe	6	-925	-24,788	29,876
Co	7	-816	-19,657	23,691
Ni	8	-722	-15,679	18,898
Cu	9	-642	-12,600	15,186

X^{3+}	N	B_{20}	B_{40}	B_{43}
Ti	1	-13,193	-21,055	26,077
V	5	-11,089	-15,031	18,616
Cr	3	-9,576	-11,359	14,069
Mn	4	-8,379	-8,815	10,917
Fe	5	-7,354	-6,865	8,503
Co	6	-6,664	-5,763	7,137
Ni	7	-6,013	-4,771	5,910
Cu	8	-5,438	-3,966	4,912
Zn	9	-4,935	-3,314	4,104

X^{3+}	N	B_{20}	B_{40}	B_{43}
Ti	1	-1320	-43,883	52,890
V	2	-1110	-31,328	37,758
Cr	3	-958	-23,675	28,534
Mn	4	-838	-18,372	22,143
Fe	5	-736	-14,309	17,246
Co	6	-667	-12,011	14,476
Ni	7	-602	-9,945	11,986
Cu	8	-544	-8,266	9,963
Zn	9	-494	-6,906	8,324

X^{4+}	N	B_{20}	B_{40}	B_{43}
V	1	-10,307	-21,334	26,423
Cr	2	-8,574	-13,440	16,646
Mn	3	-8,142	-12,756	15,799
Fe	4	-6,562	-8,144	10,087
Co	5	-6,048	-6,708	8,308
Ni	6	-5,477	-5,394	6,681
Cu	7	-4,944	-4,273	5,293
Zn	8	-4,489	-3,279	4,061
Ga	9	-3,798	-2,130	2,638

X^{4+}	N	B_{20}	B_{40}	B_{43}
V	1	-1031	-44,466	53,592
Cr	2	-858	-28,012	33,761
Mn	3	-815	-26,587	32,044
Fe	4	-657	-16,974	20,458
Co	5	-605	-13,980	16,850
Ni	6	-548	-11,243	13,551
Cu	7	-495	-8,907	10,735
Zn	8	-449	-6,834	8,237
Ga	9	-380	-4,440	5,351

11.3 Experimental Parameters (cm^{-1})

Ion	$F^{(2)}$	$F^{(4)}$	α	ζ	B_{20}	B_{40}	B_{43}	Ref
Cr^{3+}	58,940	37,296	--	--	--	-2,280	2,725.12	5
V^{3+}	49,560	37,170	--	--	-2742	-24,652	27,187	3

$\text{Be}_3\text{Al}_2(\text{SiO}_3)_6$

11.4 Bibliography

1. A. A. Akhunyan, Zh. A. Arakelyan, G. V. Bukin, R. M. Martirosyan, and V. K. Ogneva, Quantum Parametric Amplifier Utilizing Synthetic Emerald Crystals, Sov. J. Quantum Electron. 9 (1979), 61.
2. A. A. Akhunyan, R. M. Martirosyan, and N. G. Pogosyan, Quantum Amplification of Millimeter Waves by Synthetic Emerald Crystals, Sov. Tech. Phys. Lett. 7 (1981), 371.
3. P. J. Beckwith and E. J. Troup, The Optical and Infrared Absorption of V^{3+} in Beryl ($\text{Be}_3\text{Al}_2\text{Si}_6\text{O}_{18}$), Phys. Status Solidi A16 (1973), 181.
4. J. Buchert and R. R. Alfano, Emerald--A New Gem Laser Material, Laser Focus (September 1983), 117.
5. J. E. Geusic, M. Peter, and E. O. Schultz-Dubois, Bell Syst. Tech. J. 38 (1959), 291.
6. R. M. Martirosyan, M. O. Manvelyan, G. A. Mnatsakanyan, and V. S. Sevastyanov, Spin-Lattice Relaxation of Cr^{3+} Ions in Emerald, Sov. Phys. Solid State 22 (1980), 563.
7. L. V. Nikol'skaya, and M. I. Samoilovich, Optical Absorption Spectra of Beryls in the Near Infrared (900-2500 nm), Sov. Phys. Crystallogr. 24 (1979), 604.
8. K. Schmetzer and H. H. Eysel, Absorption and Emission Spectra of $\text{V}^{2+}/\text{V}^{3+}$ Doped Beryls, Z. Naturforsch. Teil A 29 (1974), 1458.
9. P. C. Schmidt, A. Weiss, and T. P. Das, Effect of Crystal Fields and Self-Consistency on Dipole and Quadrupole Polarizabilities of Closed-Shell Ions, Phys. Rev. B19 (1979), 5525.
10. B. V. Shul'gin, M. V. Vasilenko, V. P. Palvanov, and A. V. Kruzhakov, Electronic Spectra and Structure of Beryl and Chrysoberyl, Zh. Prikl. Spektrosk. 34 (1981), 116.
11. V. P. Solntsev, A. S. Lebedev, V. S. Pavlyuchenko, and V. A. Klyakhin, Copper Centers in Synthetic Beryl, Sov. Phys. Solid State 18 (1976), 805.
12. M. V. Vasilenko, A. V. Kruzhakov, and G. V. Bukin, Excitation Spectra of Synthetic Emerald in the Vacuum Ultraviolet Region, in Proceedings of the All-Union Conference on Physics of Dielectrics and New Areas for Their Use [in Russian], Karaganda (1978), 97.
13. D. L. Wood and K. Nassau, Infrared Spectra of Foreign Molecules in Beryl, J. Chem. Phys. 47 (1967), 2220.
14. R. W. G. Wyckoff, Crystal Structures, vol. 4, Interscience, New York (1968), 277.

12. $\text{Na}_3\text{M}_2\text{Li}_3\text{F}_{12}$ (Fluoride Garnets)

12.1 Crystallographic Data on $\text{Na}_3\text{M}_2\text{Li}_3\text{F}_{12}$

Cubic O_h^{10} (Ia3d), 230, Z = 8

Ion	Site	Symmetry	x	y	z	q	α (\AA^3)
M	16(a)	C_{3i}	0	0	0	3	α_x
Na	24(e)	D_2	0	1/4	1/8	1	0.147 ^a
Li	24(d)	S_4	0	1/4	3/8	1	0.0321 ^a
F	96(f)	C_1	x	y	z	-1	0.731 ^a

^aReference 18.

12.2 X-Ray Data on $\text{Na}_3\text{M}_2\text{Li}_3\text{F}_{12}$

M	a (\AA)	x	y	z	α_x (\AA^3)	Ref.
Al	12.122	-0.02888	0.04268	0.13989	0.0530	21
Sc	12.607	-0.0343	0.0499	0.1407	0.0540	14
In	12.693	-0.0349	0.0507	0.1422	0.574	14
Ti	12.498	-0.035	0.050	0.140	0.33 ^a	13
V	12.409	-0.035	0.050	0.140	0.31 ^a	13
Cr	12.328	-0.035	0.050	0.140	0.29 ^a	13
Mn	12.141	--	--	--	0.27 ^a	--
Fe	12.393	-0.035	0.050	0.140	0.24 ^a	13
Fe	12.387	-0.02954	0.04737	0.14538	0.24 ^a	10
Co	12.326	-0.035	0.050	0.140	0.23 ^a	13
Ni	12.446	--	--	--	0.22 ^a	--
Rh	12.415	-0.035	0.050	0.140	0.71 ^a	13

^aReference 6.

$\text{Na}_3\text{M}_2\text{Li}_3\text{F}_{12}$

12.3 Crystal-Field Data

12.3.1 Crystal-field components, A_{nm} (cm⁻¹ / Åⁿ), for M (C_{3i}) site in $\text{Na}_3\text{M}_2\text{Li}_3\text{F}_{12}$ (rotated so that z-axis is along (111) crystallographic axis)

M	Monopole			Total		
	A_{20}	A_{40}	A_{43}	A_{20}	A_{40}	A_{43}
Al	-2051	-14,470	16,491	732.8	-15,454	18,471
Sc	107.7	-10,058	11,840	-307.3	-11,064	13,385
In	-123.3	-9,150	10,803	-482.5	-10,065	12,202
Ti	-466.9	-10,590	12,596	-841.2	-11,667	14,241
V	-477.0	-10,975	13,054	-881.1	-12,090	14,770
Cr	-486.5	-11,340	13,489	-919.6	-12,492	15,273
Fe	-478.8	-11,046	13,139	-888.6	-12,168	14,868
Fe	-3026	-10,404	11,650	1966.2	-11,351	13,247
Co	-486.7	-11,349	13,500	-920.6	-12,502	15,285
Rh	-476.3	-10,948	13,023	-878.4	-12,062	14,734

12.3.2 Theoretical crystal-field parameters, B_{nm} (cm^{-1}), for Al (C_{3i}) site of $\text{Na}_3\text{Al}_2\text{Li}_3\text{F}_{12}$ for transition-metal ions with electronic configuration $3d^N$

(a) For monopole A_{nm}

X^{2+}	N	B_{20}	B_{40}	B_{43}
Sc	1	-2814	-58,646	66,838
Ti	2	-2201	-36,247	41,310
V	3	-1809	-24,859	28,332
Cr	4	-1522	-17,856	20,350
Mn	5	-1291	-12,984	14,797
Fe	6	-1144	-10,470	11,933
Co	7	-1008	-8,303	9,463
Ni	8	-893	-6,623	7,548
Cu	9	-794	-5,322	6,065

(b) For total A_{nm}

X^{2+}	N	B_{20}	B_{40}	B_{43}
Sc	1	1006	-62,636	74,865
Ti	2	786	-38,713	46,271
V	3	647	-26,551	31,734
Cr	4	544	-19,071	22,794
Mn	5	461	-13,867	16,575
Fe	6	409	-11,183	13,366
Co	7	360	-8,868	10,599
Ni	8	319	-7,073	8,455
Cu	9	284	-5,684	6,794

X^{3+}	N	B_{20}	B_{40}	B_{43}
Ti	1	-1632	-18,536	21,125
V	2	-1372	-13,233	15,081
Cr	3	-1185	-10,000	11,397
Mn	4	-1037	-7,760	8,844
Fe	5	-910	-6,044	6,888
Co	6	-824	-5,073	5,782
Ni	7	-744	-4,201	4,787
Cu	8	-673	-3,492	3,979
Zn	9	-611	-2,917	3,325

X^{3+}	N	B_{20}	B_{40}	B_{43}
Ti	1	583	-19,797	23,662
V	2	490	-14,133	16,892
Cr	3	423	-10,680	12,766
Mn	4	370	-8,288	9,906
Fe	5	325	-6,455	7,716
Co	6	295	-5,418	6,476
Ni	7	266	-4,486	5,362
Cu	8	240	-3,729	4,457
Zn	9	218	-3,116	3,724

X^{4+}	N	B_{20}	B_{40}	B_{43}
V	1	-1275	-18,782	21,405
Cr	2	-1061	-11,832	13,485
Mn	3	-1007	-11,230	12,799
Fe	4	-812	-7,170	8,171
Co	5	-748	-5,905	6,730
Ni	6	-678	-4,749	5,412
Cu	7	-612	-3,762	4,288
Zn	8	-555	-2,887	3,290
Ga	9	-470	-1,875	2,137

X^{4+}	N	B_{20}	B_{40}	B_{43}
V	1	456	-20,060	23,976
Cr	2	379	-12,637	15,104
Mn	3	360	-11,994	14,336
Fe	4	290	-7,658	9,153
Co	5	267	-6,307	7,538
Ni	6	242	-5,072	6,062
Cu	7	219	-4,018	4,803
Zn	8	198	-3,083	3,685
Ca	9	168	-2,003	2,394

Na₃M₂Li₃F₁₂

12.3.3 Theoretical crystal-field parameters, B_{nm} (cm^{-1}), for Sc (C_{3i}) site of $\text{Na}_3\text{Sc}_2\text{Li}_3\text{F}_{12}$ for transition-metal ions with electronic configuration $3d^N$

(a) For monopole A_{nm}

X^{2+}	N	B_{20}	B_{40}	B_{43}
Sc	1	-148	41,243	-48,020
Ti	2	-116	25,491	-29,679
V	3	-95	17,482	-20,355
Cr	4	-80	12,557	-14,620
Mn	5	-68	9,131	-10,631
Fe	6	-60	7,363	-8,573
Co	7	-53	5,839	-6,798
Ni	8	-47	4,658	-5,423
Cu	9	-42	3,743	-4,358

(b) For total A_{nm}

X^{2+}	N	B_{20}	B_{40}	B_{43}
Sc	1	-422	-44,842	54,249
Ti	2	-330	-27,715	33,529
V	3	-271	-19,008	22,995
Cr	4	-228	-13,653	16,517
Mn	5	-193	-9,928	12,010
Fe	6	-171	-8,006	9,685
Co	7	-151	-6,349	7,680
Ni	8	-134	-5,064	6,126
Cu	9	-119	-4,069	4,923

X^{3+}	N	B_{20}	B_{40}	B_{43}
Ti	1	-86	13,035	-15,177
V	2	-72	9,306	-10,835
Cr	3	-62	7,033	-8,188
Mn	4	-54	5,457	-6,354
Fe	5	-48	4,251	-4,949
Co	6	-43	3,568	-4,154
Ni	7	-39	2,954	-3,440
Cu	8	-35	2,456	-2,859
Zn	9	-32	2,052	-2,389

X^{3+}	N	B_{20}	B_{40}	B_{43}
Ti	1	-245	-14,173	17,146
V	2	-206	-10,118	12,241
Cr	3	-177	-7,646	9,250
Mn	4	-155	-5,934	7,178
Fe	5	-136	-4,621	5,591
Co	6	-124	-3,879	4,693
Ni	7	-111	-3,212	3,886
Cu	8	-101	-2,670	3,230
Zn	9	-91	-2,231	2,698

X^{4+}	N	B_{20}	B_{40}	B_{43}
V	1	-67	13,208	-15,379
Cr	2	-56	8,321	-9,688
Mn	3	-53	7,898	-9,195
Fe	4	-43	5,042	-5,871
Co	5	-39	4,153	-4,835
Ni	6	-36	3,340	-3,889
Cu	7	-32	2,646	-3,081
Zn	8	-29	2,030	-2,364
Ga	9	-25	1,319	-1,536

X^{4+}	N	B_{20}	B_{40}	B_{43}
V	1	-191	-14,361	17,374
Cr	2	-159	-9,047	10,945
Mn	3	-151	-8,587	10,388
Fe	4	-122	-5,482	6,632
Co	5	-112	-4,515	5,462
Ni	6	-102	-3,631	4,393
Cu	7	-92	-2,877	3,480
Zn	8	-83	-2,207	2,670
Ga	9	-70	-1,434	1,735

$\text{Na}_3\text{M}_2\text{Li}_3\text{F}_{12}$

12.3.4 Theoretical crystal-field parameters, B_{nm} (cm^{-1}), for In (C_{3i}) site of $\text{Na}_3\text{In}_2\text{Li}_3\text{F}_{12}$ for transition-metal ions with electronic configuration $3d^N$

(a) For monopole A_{nm}

X^{2+}	N	B_{20}	B_{40}	B_{43}
Sc	1	-169	-37,086	43,785
Ti	2	-132	-22,922	27,062
V	3	-109	-15,720	18,560
Cr	4	-92	-11,291	13,331
Mn	5	-78	-8,211	9,694
Fe	6	-69	-6,621	7,817
Co	7	-61	-5,250	6,199
Ni	8	-54	-4,188	4,945
Cu	9	-48	-3,366	3,973

(b) For total A_{nm}

X^{2+}	N	B_{20}	B_{40}	B_{43}
Sc	1	-562	-40,793	49,455
Ti	2	-518	-25,213	30,566
V	3	-426	-17,292	20,963
Cr	4	-358	-12,420	15,057
Mn	5	-304	-9,031	10,949
Fe	6	-269	-7,283	8,829
Co	7	-237	-5,775	7,002
Ni	8	-210	-4,607	5,585
Cu	9	-187	-3,702	4,488

X^{3+}	N	B_{20}	B_{40}	B_{43}
Ti	1	-98	-11,722	13,839
V	2	-82	-8,368	9,879
Cr	3	-71	-6,324	7,466
Mn	4	-62	-4,907	5,794
Fe	5	-55	-3,822	4,512
Co	6	-50	-3,208	3,788
Ni	7	-45	-2,656	3,136
Cu	8	-40	-2,208	2,607
Zn	9	-37	-1,845	2,178

X^{3+}	N	B_{20}	B_{40}	B_{43}
Ti	1	-384	-12,893	15,631
V	2	-323	-9,204	11,159
Cr	3	-279	-6,956	8,433
Mn	4	-244	-5,398	6,544
Fe	5	-214	-4,204	5,097
Co	6	-194	-3,529	4,278
Ni	7	-175	-2,922	3,542
Cu	8	-158	-2,429	2,944
Zn	9	-144	-2,029	2,460

X^{4+}	N	B_{20}	B_{40}	B_{43}
V	1	-77	-11,877	14,022
Cr	2	-64	-7,482	8,834
Mn	3	-61	-7,102	8,384
Fe	4	-49	-4,534	5,353
Co	5	-45	-3,734	4,409
Ni	6	-41	-3,003	3,546
Cu	7	-37	-2,379	2,809
Zn	8	-33	-1,826	2,155
Ga	9	-28	-1,186	1,400

X^{4+}	N	B_{20}	B_{40}	B_{43}
V	1	-300	-13,064	15,838
Cr	2	-250	-8,230	9,978
Mn	3	-237	-7,811	9,470
Fe	4	191	-4,987	6,046
Co	5	-176	-4,108	4,980
Ni	6	-159	-3,303	4,005
Cu	7	-144	-2,617	3,173
Zn	8	-131	-2,008	2,434
Ga	9	-111	-1,304	1,581

12.4 Experimental Parameters (cm^{-1}) for Cr^{3+} in $\text{Na}_3\text{M}_2\text{Li}_3\text{F}_{12}$

M	$F^{(2)}$	$F^{(4)}$	B_{20}	B_{40}	B_{43}	Ref
In	59,696	42,714	0	-22,218 ^a	--	5
Ga	59,973	42,242	0	-22,988 ^a	--	1

^aCubic approx. $B_{43} = \sqrt{10/7} |B_{40}|$

$\text{Na}_3\text{M}_2\text{Li}_3\text{F}_{12}$

12.5 Bibliography and References

1. J. A. Caird, S. A. Payne, P. R. Staver, A. J. Ramponi, L. L. Chase, and W. F. Krupke, Quantum Electronic Properties of the $\text{Na}_3\text{Ga}_2\text{Li}_3\text{F}_{12}:\text{Cr}^{3+}$ Laser, *IEEE J. Quantum Electron.* QE-24 (1988), 1077.
2. J. A. Caird, P. R. Staver, M. D. Shinn, H. J. Guggenheim, and D. Bahnck, Single Crystal $\text{Na}_3\text{Ga}_2\text{Li}_3\text{F}_{12}:\text{Cr}^{3+}$ Laser Pumped Laser Experiments, in *Advances in Laser Science--II*, M. Lapp, W. C. Stwalley, and G. A. Kenny-Wallace, Eds., New York: AIP (1987), pp 120-123.
3. J. Chenavas, J. C. Joubert, M. Marezio, and B. Ferrand, On the Crystal Symmetry of the Garnet Structure, *J. Less-Common Metals* 62 (1978), 373.
4. J. C. Cretenet, Composés Définis et Solutions Solides dans des Systèmes $\text{M}_3\text{VF}_6-\text{M}_3^1\text{VF}_6$, *C. R. Acad. Sci. C268* (1969), 2092.
5. D. De Viry, J. P. Denis, B. Blanzat, and J. Grannec, Spectroscopic Properties of Trivalent Chromium in the Fluoride Garnet $\text{Na}_3\text{In}_2\text{Li}_3\text{F}_{12}$, *J. Solid State Chem.* 71 (1987), 109.
6. S. Fraga, K.M.S. Saxena, and J. Karwowski, *Handbook of Atomic Data*, Elsevier, New York (1976).
7. N. M. Javoronkov, J. A. Buslaev, and V. P. Tarasov, Une Etude par Résonance Magnétique Nucléaire Grenat Fluoré D'Aluminium, *Bull. Soc. Chim. Fr.* 7 (1969), 2333.
8. R. H. Langley and G. D. Sturgeon, Infrared Spectra of Fluoride Garnets, *Spectrochim. Acta* 35A (1979), 209.
9. R. H. Langley and G. D. Sturgeon, Synthesis of Transition Metal Fluoride Garnets, *J. Fluorine Chem.* 14 (1979), 1.
10. W. Massa, B. Post, and Babel, Verfeinrung der Granatstruktur des Natrium-Lithium-Eisen (III) Fluorids $\text{Na}_3\text{Li}_3\text{Fe}_2\text{F}_{12}$, *Z. Kristallogr.* 158 (1982), 299.
11. S. Naka, Y. Takeda, K. Kawada, and M. Inagaki, Growth of Single Crystals of $\text{Na}_3\text{Al}_2\text{Li}_3\text{F}_{12}$ Garnet Under Hydrothermal Conditions, *J. Crystal Growth* 46 (1979), 461.
12. S. Naka, Y. Takeda, M. Sone, and Y. Suwa, Synthesis of the Fluoride Garnet $\{\text{Na}_3\}[\text{M}_2^{3+}](\text{Li}_3)\text{F}_{12}$ ($\text{M} = \text{Al, Cr, Fe}$), private communication.

$\text{Na}_3\text{M}_2\text{Li}_3\text{F}_{12}$

13. R. de Pape, J. Portier, G. Gauthier, P. Hagenmuller, and P. Pascal, Les Grenats Fluorés des éléments de Transition $\text{Na}_3\text{Li}_3\text{M}_2\text{F}_{12}$ (M = Ti, V, Cr, Fe ou Co), C. R. Acad. Sci. C265 (1967), 1244.
14. R. de Pape, J. Portier, J. Granne, G. Gauthier, P. Hagenmuller, and H. Mourieu, Sur Quelques Nouveaux Grenats Fluorés, C. R. Acad. Sci. C269 (1969), 1120.
15. H. Pauly, Gladstone-Dale Calculations Applied to Fluorides, Can. Mineral. 20 (1982), 593.
16. H. Pauly, Cryolite, Chiolite, and Cryolithionite: Optical Data Redetermined, Bull. Geol. Soc. Den. 26 (1977), 95.
17. J. Sawicki and S. S. Hafner, Sign of Electric Field Gradient at ^{57}Fe Nuclei in Garnets, Phys. Lett. 68A (1978), 80.
18. P. C. Schmidt, A. Weiss, and T. P. Das, Effect of Crystal Fields and Self-Consistency on Dipole and Quadrupole Polarizabilities of Closed-Shell Ions, Phys. Rev. B19 (1979), 5525.
19. Y. Takeda, M. Inagaki, and S. Naka, High Pressure Form of Fluoride Garnets $\text{Na}_3\text{M}_2\text{Li}_3\text{F}_{12}$ (M = Al & Fe), Mater. Res. Bull. 12 (1977), 689.
20. Y. Takeda, M. Sone, Y. Suma, M. Inagaki, and S. Naka, Synthesis of Fluoride Garnets $\{\text{Na}_3\}[\text{M}_2^{3+}](\text{Li}_3)\text{F}_{12}$ (M = Al, Cr, and Fe) from Aqueous Solution and Their Properties, J. Solid State Chem. 20 (1977), 261.
21. R.W.G. Wyckoff, Crystal Structures, vol. 3, Interscience, New York (1968), 222.

13. Cs_2SnBr_6

13.1 Crystallographic Data on Cs_2SnBr_6

Cubic O_h^5 (Fm3m), 225, $Z = 4$

Ion	Site	Symmetry	x^a	y	z	q	$\alpha(\text{\AA}^3)$
Sn	4(a)	O_h	0	0	0	4	0.37 ^b
Cs	8(c)	T_d	1/4	1/4	1/4	1	2.492 ^c
Br	24(e)	C_{4v}	x	0	0	-1	3.263 ^c

^aX-ray data: $a = 10.81 \text{ \AA}$, $x = 0.245$ (reference 7).

^bReference 5.

^cReference 6.

13.2 Crystal-Field Components, A_{nm} ($\text{cm}^{-1}/\text{\AA}^n$), for Sn (O_h) Site

A_{nm}	Monopole	Self-induced	Dipole	Total
A_{40}	3325.2	-2255.7	5087.6	6157.0
A_{44}	1987.2	-1348.0	3040.4	3679.5

13.3 Experimental Parameters (cm^{-1})

:

Ion	nd^N	$F^{(2)}$	$F^{(4)}$	ζ	B_{40}	Ref
Os^{4+}	$5d^4$	88,308	34,676	3212	10,096	4

13.4 Bibliography and References

1. J. C. Collingwood, P. N. Schatz, and P. J. McCarthy, Absorption and Magnetic Circular Dichroism Spectra of Ru^{4+} in Cs_2ZrCl_6 and Cs_2SnBr_6 , *Mol. Phys.* 30 (1975), 269.
2. P. B. Dorain, Magnetic and Optical Properties of Transition Metal Ions in Single Crystals, Aerospace Laboratories Report, ARL-73-0139 (October 1973), NTIS AD 769870.
3. C. D. Flint, Luminescence Spectra and Relaxation Process of ReCl_6^{2-} in Cubic Crystals, *J. Chem. Soc. Faraday Trans. 2* 74 (1978), 767.
4. C. D. Flint and A. G. Paulusz, High Resolution Infrared and Visible Luminescence Spectra of ReCl_6^{2-} and ReBr_6^{2-} in Cubic Crystals, *Mol. Phys.* 43 (1981), 321.
5. S. Fraga, K.M.S. Saxena, and J. Karwowski, Handbook of Atomic Data, Elsevier, New York (1976).

Cs_2SnBr_6

6. P. C. Schmidt, A. Weiss, and T. P. Das, Effect of Crystal Fields and Self-Consistency on Dipole and Quadrupole Polarizabilities of Closed-Shell Ions, *Phys. Rev. B19* (1979), 5525.
7. R.W.G. Wyckoff, *Crystal Structures*, vol. 3, Interscience, New York (1968), 339.

14. KMgF_3

14.1 Crystallographic Data on KMgF_3

Cubic O_h^1 (Pm3m), 221, $Z = 1$

Ion	Site	Symmetry	x ^a	y	z	q	α (\AA^3) ^b
K	1(a)	O_h	0	0	0	1	0.827
Mg	1(b)	O_h	1/2	1/2	1/2	2	0.0809
F	3(d)	D_{4h}	1/2	1/2	0	-1	0.731

^aX-ray data: $a = 3.973 \text{ \AA}$ (reference 33).

^bReference 25.

14.2 Crystal-Field Components, A_{nm} ($\text{cm}^{-1}/\text{\AA}^n$), for Mg (O_h) (1b) Site

A_{nm}	Point charge	Self-induced	Dipole	Total
A_{40}	13,281	-5022	0	8260
A_{44}	7,937	-3001	0	4936

14.3 Experimental Parameters (cm^{-1})

Ion	$F^{(2)}$	$F^{(4)}$	ζ	α	B_{40} ^a	Ref.
V^{2+}	53,362	28,065	--	79	25,515	29
Co^{2+}	70,224	48,787	500	--	16,800	6
Ni^{2+}	74,480	50,274	620	--	14,658	4
Mn^{2+}	64,099	38,983	0	0	18,659	29
Ni^{2+}	76,405	53,298	--	--	15,225	13
Ni^{2+}	74,270	49,322	--	--	15,909	(b)

^a $B_{44} = \sqrt{5/14} B_{40}$

^bBest fit to the data (reference 31) with $F^{(2)}$, $F^{(4)}$, and B_{40} varied.

14.4 Bibliography and References

1. M. T. Barriuso and M. Moreno, Determination of the Mn^{2+} -F⁻ Distance from the Isotropic Superhyperfine Constant for $[\text{MnF}_6]^{4-}$ in Ionic Lattices, Phys. Rev. B29 (1984), 3623.
2. J. Brynestad, H. L. Yakel, and G. P. Smith, Temperature Dependence of the Absorption Spectrum of Nickel (II)-Doped KMgCl_3 and the Crystal Structure of KMgCl_3 , J. Chem. Phys. 45 (1966), 4652.

3. J. Ferguson, H. J. Guggenheim, L. F. Johnson, and H. Kamimura, Magnetic Dipole Character of $^3A_{2g} \leftrightarrow ^3T_{2g}$ Transition in Octahedral Nickel (II) Compounds, *J. Chem. Phys.* 38 (1963), 2579.
4. J. Ferguson, H. J. Guggenheim, and D. L. Wood, Electronic Absorption Spectrum of Ni II in Cubic Perovskite Fluorides: I, *J. Chem. Phys.* 40 (1964), 822.
5. J. Ferguson and H. Masui, Optical Spectra of Nearest Neighbour Nickel Pairs in $KMgF_3$ and $KZnF_3$ Crystals, *Mol. Phys.* 37 (1979), 737.
6. J. Ferguson, D. L. Wood, and K. Knox, Crystal-Field Spectra of d^3, d^7 Ions: II.-- $KCoF_3$, $CoCl_2$, $CoBr_2$ and $CoWO_4$, *J. Chem. Phys.* 39 (1963), 881.
7. J. C. Gacon, A. Gros, H. Bill, and J. P. Wicky, New Measurements of the Emission Spectra of Sm^{2+} in $KMgF_3$ and $NaMgF_3$ Crystals, *J. Phys. Chem. Solids* 42 (1981), 587.
8. T.P.P. Hall, W. Hayes, K.W.H. Stevenson, and J. Wilkens, Investigation of the Bonding of Iron-Group Ions in Fluoride Crystals: II, *J. Chem. Phys.* 39 (1963), 35.
9. T.P.P. Hall, W. Hayes, K.W.H. Stevenson, and J. Wilkens, Investigation of the Bonding of Iron-Group Ions in Fluoride Crystals: I, *J. Chem. Phys.* 38 (1963), 1977.
10. L. F. Johnson, H. J. Guggenheim, and D. Bahnek, Phonon-Terminated Laser Emission from Ni^{2+} Ions in $KMgF_3$, *Opt. Lett.* 8 (1983), 371.
11. L. F. Johnson, H. J. Guggenheim, and R. A. Thomas, Phonon-Terminated Optical Masers, *Phys. Rev.* 149 (1966).
12. P. J. King and J. Monk, Anomalous Acoustic Relaxation Absorption and Acoustic Paramagnetic Resonance in $KMgF_3$ Containing Fe^{2+} , *Acta Phys. Slovaca* 30 (1980), 11.
13. K. Knox, R. G. Shulman, and S. Sugano, Covalency Effects in $KNiF_3$: II.--Optical Studies, *Phys. Rev.* 130 (1963), 512.
14. B. B. Krichevtskov, P. A. Marokvin, S. V. Petrov, and R. V. Pisarev, Isotropic and Anisotropic Magnetic Refraction of Light in the Antiferromagnets $KNiF_3$ and $RbMnF_3$, *Sov. Phys. JETP* 59 (1984), 1316.
15. A. L. Larionov, Calculation of Electric Field Constants for Tetragonal Cr^{3+} Centres in $KMeF_3$ ($Me = Mg, Zn$), *Magn. Reson. Relat. Phenom., Proc. Congr.* (Eds. E. Kundla, E. Lippmaa, and T. Saluvere) (1979), 204.
16. K. H. Lee and W. A. Sibley, Exchange Enhancement of Co^{2+} and Mn^{2+} Transitions Due to Radiation Defects, *Phys. Rev.* B12 (1975), 3392.

KMgF₃

17. W.L.W. Ludekens and A.J.E. Welch, Reaction Between Metal Oxides and Flourides: Some New Double-Fluoride Structures of Type ABF₃, *Acta Crystallogr.* 5 (1952), 841.
18. K. Moncorge and T. Benyattou, Excited-State Absorption of Ni²⁺ in MgF₂ and MgO, *Phys. Rev.* B37 (1988), 9186.
19. S. Muramatsu, Intensity of the Zero-Phonon Lines for the $^4T_1 \rightarrow ^4T_2$ Transition of Co²⁺ in KMgF₃, *Phys. Status Solidi* B98 (1980), K167.
20. D. E. Onopko, N. V. Starostin, and S. A. Titov, Interpretation of High-Energy Absorption Spectra of 3d Transition Elements in KMgF₃ Crystal, *Sov. Phys. Solid State* 19 (1977), 340.
21. H. Onuki, F. Sugawara, M. Hirano, and Y. Yamaguchi, Ultraviolet Photoemission Study of Pervskite Fluorides KMgF₃ (M:Mn, Fe, Co, Ni, Cu, Zn) in the Valence Band Region, *J. Phys. Soc. Jpn.* 49 (1980), 2314.
22. A. Poirer and D. Walsh, Photoluminescence of Iron-Doped KMgF₃, *J. Phys.* C16 (1983), 2619.
23. M. L. Reynolds and G.F.J. Garlick, The Infrared Emission of Nickel Ion Impurity Centres in Various Solids, *Infrared Phys.* 7 (1967), 151.
24. D. K. Sardar, W. A. Sibley, and R. Alcala, Optical Absorption and Emission from Irradiated RbMgF₃:Eu²⁺ and KMgF₃:Eu²⁺, *J. Lumin.* 27 (1982), 401.
25. P. C. Schmidt, A. Weiss, and T. P. Das, Effect of Crystal Fields and Self-Consistency on Dipole and Quadrupole Polarizabilities of Closed-Shell Ions, *Phys. Rev.* B19 (1979), 5525.
26. W. A. Sibley, S. I. Yun, and L. N. Feuerhelm, Radiation Object and 3d Impurity Absorption in MgF₂ and KMgF₃ Crystals, *J. Phys. Paris* 34 (1973), C9-503.
27. W. A. Sibley, S. I. Yun, and W. E. Vehse, Colour Centre Luminescence in KMgF₃:Mn Crystals, *J. Phys.* C6 (1973), 1105.
28. M. D. Sturge, Dynamic Jahn-Teller Effect in the $^4T_2^-$ Excited States of d_{3,7} Ions in Cubic Crystals: I.-V²⁺ in KMgF₃, *Phys. Rev.* B1 (1970), 1005.
29. M. D. Sturge, F. R. Merritt, L. F. Johnson, H. J. Guggenheim, and J. P. van der Ziel, Optical and Microwave Studies of Divalent Vanadium in Octahedral Fluoride Coordination, *J. Chem. Phys.* 54 (1971), 405.
30. E. G. Valashko, S. N. Bodrug, A. V. Krutikov, V. N. Mednikova, and V. A. Smirnov, Absorption Spectra of Sm²⁺ in the Double Fluoroperovskites KMgF₃ and NaMgF₃, *Opt. Spectrosc. (USSR)* 44 (1978), 425.

31. P. J. Walker and H. G. Tang, Growth of $KMg_{1-x}M_xF_3$ ($M = V^{2+}, Co^{2+}, Ni^{2+}$) Mixed Crystals by the Czochralski Method, *J. Crystal Growth* 55 (1981), 539.
32. D. Walsh and J. Lange, Dynamic Jahn-Teller Effects in the Photoluminescence of Fe^{2+} in $KMgF_3$, *Phys. Rev.* B23 (1981), 8.
33. R.W.G. Wyckoff, *Crystal Structures*, Vol. 2 (1964), 392.
34. S. J. Yun, L. A. Kappers, and W. A. Sibley, Enhancement of Impurity-Ion Absorption Due to Radiation-Produced Defects, *Phys. Rev.* B8 (1973), 773.
35. S. J. Yun, K. H. Lee, W. A. Sibley, and W. E. Vehse, Use of 3d-Impurity-Ion Absorption to Study the Distribution of Radiation Damage in Crystals, *Phys. Rev.* B10 (1974), 1665.

15. BeAl_2O_4 (Chrysoberyl, Cr:BeAl₂O₄ = Alexandrite)

15.1 Crystallographic Data on BeAl₂O₄

Orthorhombic D_{2h}^{16} (Pnma), 62, $Z = 4$

Ion	Site	Symmetry	x	y	z	q	α (\AA^3) ^a
Al ₁	4(a)	C_i	0	0	0	3	0.0530
Al ₂	4(c)	C_s	x	1/4	z	3	0.0530
Be	4(c)	C_s	x	1/4	z	2	0.0125
O ₁	4(c)	C_s	x	1/4	z	-2	1.349
O ₂	4(c)	C_s	x	1/4	z	-2	1.349
O ₃	8(d)	C_1	x	y	z	-2	1.349

^aReference 15.

15.2 X-Ray Data

Cell size			Al ₂		Be	
a	b	c	x	z	x	z
9.4041	5.4756	4.4267	0.27319	-0.00595	0.09294	0.43347
9.407	5.4781	4.4285	0.27283	-0.00506	0.09276	0.43402

O ₁		O ₂		O ₃		Ref.
x	z	x	z	x	y	z
0.09051	0.79016	0.43343	0.24097	0.16318	0.01718	0.25850
0.09031	0.78779	0.43302	0.24137	0.16330	0.01529	0.25687

15.3 Crystal-Field Components

A_{nm} ($\text{cm}^{-1}/\text{\AA}^n$) for Al₂ (C_S) site (rotated so that z-axis is perpendicular to mirror plane)

Calculated using data from reference 28

Calculated using data from reference 3

A_{nm}	Monopole	Total	A_{nm}	Monopole	Total
ReA ₁₁	-1,474	-2533	ReA ₁₁	-1,247	-2303
ImA ₁₁	-5,753	-1586	ImA ₁₁	6,656	-1410
A ₂₀	4,776	-658.4	A ₂₀	4,828	-471.4
A ₂₂	5,573	6129	A ₂₂	5,584	5661
ReA ₃₁	6,459	3852	ReA ₃₁	6,754	3340
ImA ₃₁	-7,028	3936	ImA ₃₁	-6,192	3415
ReA ₃₃	-4,503	-346.7	ReA ₃₃	-4,408	-79.97
ImA ₃₃	-1,662	46.55	ImA ₃₃	-2,256	-50.58
A ₄₀	-4,588	-1744	A ₄₀	-4,872	-1994
ReA ₄₂	-18,247	-2571	ReA ₄₂	-17,366	-2231
ImA ₄₂	-12,176	8657	ImA ₄₂	-13,550	8786
ReA ₄₄	4,922	-3188	ReA ₄₄	3,246	-3544
ImA ₄₄	11,144	-4138	ImA ₄₄	11,736	-3798
ReA ₅₁	180.6	322.5	ReA ₅₁	153.9	378.6
ImA ₅₁	-2,189	1879	ImA ₅₁	-1,991	1914
ReA ₅₃	-1,037	1287	ReA ₅₃	-969.5	1295
ImA ₅₃	-1,271	-687.8	ImA ₅₃	-1,395	-849.1
ReA ₅₅	-1,674	812.1	ReA ₅₅	-1,566	984.6
ImA ₅₅	360.7	1159	ImA ₅₅	42.10	994.5

15.4 Bibliography and References

1. G. V. Bukin, S. Yu Volkov, V. N. Matrosov, B. K. Sevast'yanov, and M. I. Timosheshkin, Stimulated Emission from Alexandrite (BeAl₂O₄:Cr³⁺) Sov. J. Quantum Electron. 8 (1978), 671.
2. C. F. Cline, R. C. Morris, M. Dutoit, and P. J. Harget, Physical Properties of BeAl₂O₃ Single Crystals, J. Mater. Sci. 14 (1979), 941.
3. A. P. Dudka, B. K. Sevast'yanov, and V. I. Simonov, Refinement of Atomic Structure of Alexandrite, Sov. Phys. Crystallogr. 30 (1985), 277.

BeAl_2O_4

4. C. E. Forbes, Analysis of the Spin-Hamiltonian Parameters for Cr^{3+} in Mirror and Inversion Symmetry Sites of Alexandrite ($\text{Al}_{2-x}\text{Cr}_x\text{BeO}_4$): Determination of the Relative Site Occupancy by EPR, *J. Chem. Phys.* 79 (1983), 2590.
5. S. K. Gayen, W. B. Wang, V. Petricević and R. R. Alfano, Picosecond Time Resolved Studies of Nonradiative Relaxation in Ruby and Alexandrite, *A.I.P. Conference Proceedings* 146 (1986), 206.
6. A. M. Ghazzawi, J. K. Tyminski, R. C. Powell, and J. C. Walling, Four-Wave Mixing in Alexandrite Crystals, *Phys. Rev.* B30 (1984), 7182.
7. Xiang-an Guo, Bang-xing Zhang, Lu-Sheng Wu, and Mei-Ling Cherc, Czochralski Growth and Laser Performance of Alexandrite Crystals, *A.I.P. Conference Proceedings* 146, New York (1986), 249.
8. D. F. Heller and J. C. Walling, High-Power Performance of Alexandrite Lasers, *Cleo '84* (20 June 1984), 101.
9. P. T. Kenyon, L. Andrews, B. McCollum, and A. Lempicki, Tunable Infrared Solid-State Laser Materials Based on Cr^{3+} in Low Ligand Fields, *IEEE J. Quantum Electron.* QE-18 (1982), 1189.
10. T. Kottke and F. Williams, Pressure Dependence of the Alexandrite Emission Spectrum, *Phys. Rev.* B28 (1983), 1923.
11. R. C. Powell, Lin Xi, Xu Garg, G. J. Quarles, and J. C. Walling, Spectroscopic Properties of Alexandrite Crystals, *Phys. Rev.* B32 (1985), 2788.
12. R. C. Sam, W. R. Rapport, and S. Matthews, New Developments in High-Power High Repetition Rate Injection-Locked Alexandrite Lasers, *Cleo '84* (20 June 1984), 101.
13. H. Samelson and D. J. Harter, High-Pressure Arc Lamp Excited cw Alexandrite Lasers, *Cleo '84* (20 June 1984), 101.
14. K. L. Schepler, Fluorescence of Inversion Site Cr^{3+} Ions in Alexandrite, *J. Appl. Phys.* 56 (1984), 1314.
15. P. Schmidt, A. Weiss, and T. P. Das, Effect of Crystal Fields and Self-Consistency on Dipole and Quadrupole Polarizabilities of Closed-Shell Ions, *Phys. Rev.* B19 (1979), 5525.
16. Y. Segawa, A. Sugimoto, P. H. Kim, S. Namba, K. Yamagishi, Y. Anzai, and Y. Yamaguchi, Optical Properties and Lasing of Ti^{3+} Doped BeAl_2O_4 , *Topical Meeting on Tunable Solid State Lasers*, vol. 26-28 (October 1987), 154.

17. B. K. Sevast'yanov, Y. L. Remigailo, V. P. Orekhova, V. P. Matrosov, E. G. Tsvetkov, and G. V. Bukin, Spectroscopic and Lasing Characteristics of an Alexandrite (Chromium +3) Doped Beryllium Aluminum Oxide Laser, Dokl. Akad. Nauk SSSR 256 (1981), 373-376; Sov. Phys.-Doklady 26, No. 1 (January 1981) 62-64.
18. M. L. Shand and H. P. Jenssen, Energy Kinetics in Alexandrite, Proc. Int. Conf. Lasers (1983), 559.
19. M. L. Shand, J. C. Walling, and R. C. Morris, Excited State Absorption in the Pump Region of Alexandrite, J. Appl. Phys. 52 (1981), 953.
20. M. A. Shiaoshan, Lu Jiajin, Qian Zhenying, Hou Yinchun, Wang Siting, Shen Yajang, and Jing Zonru, The Growth Habits of Alexandrite Crystals, Chin. J. Physics Peking Engl. Transl. 4 (1984), 771.
21. G. J. Troup, A. Edgar, D. R. Hutton, and P. P. Phakey, 8mm Wavelength EPR Spectrum of Cr^{3+} in Laser-Quality Alexandrite, Phys. Status Solidi A71 (1982), K29.
22. J. C. Walling, H. P. Jenssen, R. C. Morris, E. W. O'Dell, and O. G. Peterson, Tunable-Laser Performance in $\text{BeAl}_2\text{O}_4:\text{Cr}^{3+}$, Opt. Lett. 4 (1979), 182.
23. J. C. Walling and O. G. Peterson, High Gain Laser Performance in Alexandrite, IEEE J. Quantum Electron. QE-16 (1980), 119.
24. J. C. Walling and O. G. Peterson, High Gain Laser Performance in Alexandrite, IEEE OSA Conf. on Laser Engineering and Applications (1979), p 86D.
25. J. C. Walling, O. G. Peterson, H. P. Jenssen, R. C. Morris, and E. W. Q'Dell, Tunable Alexandrite Lasers, IEEE J. Quantum Electron. QE16 (1980), 1302.
26. J. C. Walling, O. G. Peterson, and R. C. Morris, Tunable cw Alexandrite Laser, IEEE J. Quantum Electron. QE-16 (1980), 120.
27. Wu Guang-Zhao and Zang Xiu-rong, Crystal-Field Energy Levels of $\text{BeAl}_2\text{O}_4:\text{Cr}^{3+}$, Acta Phys. Sin. 32 (1983), 64-70 (translation, Chin. J. Phys. Peking Engl. Transl. 3 (1983), 570).
28. R.W.G. Wyckoff, Crystal Structures, Vol. 3 (1965), 91; and Vol. 4 (1968), 159.
29. Zhang Shondu and Zhang Kemin, Experiment on Laser Performance of Alexandrite Crystals, Chin. J. Lasers 11 (1984), 44-46 (translation, Chin. J. Phys. Peking Engl. Transl. 4 (1984), 667).

16. ZnAl_2O_4

16.1 Crystallographic Data on ZnAl_2O_4

Cubic O_h^7 ($\text{Fd}\bar{3}\text{m}$), 227, $Z = 8$

Ion	Site	Symmetry	x^a	y	z	q	$\alpha (\text{\AA}^3)^b$
Zn	8(a)	T_d	0	0	0	2	0.676
Al	16(d)	D_{3d}	5/8	5/8	5/8	3	0.0530
O	32(e)	C_{3v}	x	x	x	-2	1.349

^aX-ray data: $a = 8.0883 \text{ \AA}$, $x = 0.390$ (reference 13).

^bReference 10.

16.2 Crystal Fields for Zn (T_d) Site

16.2.1 Crystal-field components, A_{nm} ($\text{cm}^{-1}/\text{\AA}^n$), for Zn (T_d) site

A_{nm}	Monopole	Dipole	Self-induced	Total
A_{32}	-127,467	17189	16951	-11,327
A_{40}	-12,005	4187	4544	-3,274
A_{44}	-7,174	2502	2716	-1,956

$$i = \sqrt{-1}$$

16.2.2 Crystal-field components, A_{nm} ($\text{cm}^{-1}/\text{\AA}^n$), for Al (D_{3d}) site (rotated so that z-axis is parallel to (111) crystallographic axis)

A_{nm}	Monopole	Dipole	Self-induced	Total
A_{20}	5,004	22,132	-2576	24,559
A_{40}	-21,556	-3,990	9380	-16,162
A_{43}	24,259	1,899	-9322	16,830

16.3 Experimental Values (cm^{-1}) of $F^{(2)}$, $F^{(4)}$, α , ζ , and B_{nm} for nd^N Ions

Ion	d^N	$F^{(2)}$	$F^{(4)}$	α	ζ	B_{20}	B_{40}	B_{44}	B_{43}	Ref.
Co^{2+}	$3d^7$	59,367	42,210	86	420	--	-8,640	5145.46	--	9
Cr^{3+}	$3d^3$	56,700	40,320	--	250	4608	-30,625	--	28,415	3,7,12

16.4 Bibliography and References

1. G. Burns, E. A. Geiss, B. A. Jenkins, and M. I. Nathan, Cr^{3+} Fluorescence in Garnets and Other Crystals, Phys. Rev. A139 (1965), 1687.
2. J. Ferguson and D. L. Wood, Crystal Field Spectra of $d^{3,7}$ Ions: VI.-- The Weak Field Journalism and Covalency, Aust. J. Chem. 23 (1970), 861.
3. J. Ferguson, D. L. Wood, and L. G. van Uittert, Crystal Field Spectra of $d^{3,7}$ Ions: V.--Tetrahedral Co^{2+} in $ZnAl_2O_4$ Spinel, J. Chem. Phys. 51 (1969), 2904.
4. R. D. Gillen and R. E. Salomon, Optical Spectra of Chromium (III), Cobalt (II), and Nickel (II) Ions in Mixed Spinels, Phys. Chem. 74 (1970), 4252.
5. P. P. Kisliuk, D. L. Wood, R. M. Macfarlane, G. F. Imbusch, and D. M. Larkin, Optical Spectrum of Cr^{3+} Ions in Spinels, Air Force Report No. TR-0158 (9230-02)-3 (March 1968), NTIS AD 668446.
6. R. M. Macfarlane, Perturbation Methods in the Calculation of Zeeman Interaction and Magnetic Dipole Line Strengths for d^3 Trigonal-Crystal Spectra, Phys. Rev. B1 (1970), 989.
7. W. Mikenda, N-Lines in the Luminescence Spectra of Cr^{3+} -Doped Spinels: III.--Partial Spectra, J. Lumin. 26 (1981), 85-98.
8. W. Mikenda and A. Preisinger, N-Lines in the Luminescence Spectra of Cr^{3+} -Doped Spinels: I.--Identification of N-Lines, J. Lumin. 26 (1981), 53-66.
9. W. Mikenda and A. Preisinger, N-Lines in the Luminescence Spectra of Cr^{3+} -Doped Spinels: II.--Origins of N-Lines, J. Lumin. 26 (1981), 67-83.
10. P. C. Schmidt, A. Weiss, and T. P. Das, Effect of Crystal Fields and Self-Consistency on Dipole and Quadrupole Polarizabilities of Closed-Shell Ions, Phys. Rev. B19 (1979), 5525.
11. D. L. Wood, W. E. Burke, and L. G. van Uittert, Zeeman Effect of Cr^{3+} in $ZnAl_2O_4$, J. Chem. Phys. 51 (1969), 1966.
12. D. L. Wood, G. F. Imbusch, R. M. Macfarlane, P. Kisliuk, and D. M. Larkin, Optical Spectrum of Cr^{3+} Ions in Spinels, J. Chem. Phys. 48 (1968), 5255.
13. R.W.G. Wyckoff, Crystal Structures, vol. 3, Interscience, New York (1968), 75.

17. LiMgZrO_4

17.1 Crystallographic Data on LiMgZrO_4

Tetragonal ($I4_1/\text{amd}$), 141 (second setting), $Z = 2$

Ion	Site	Symmetry	x^a	y	z	q	$\alpha (\text{\AA}^3)$
O	8(e)	C_{2v}	0	1/4	0.108	-2	1.349
Zr, Mg	4(a)	D_{2d}	0	3/4	1/8	4,2	0.280
Li	4(b)	D_{2d}	0	1/4	3/8	1	0.0321

^aX-ray data: $a = 4.209 \text{ \AA}$, $c = 9.145 \text{ \AA}$ (reference 1).

17.2 Crystal-Field Components, A_{nm} ($\text{cm}^{-1}/\text{\AA}^n$) for 4a (D_{2d}) Site

Assuming that average charge on site 4(a) is +3

A_{nm}

A_{nm}	Monopole	Self-induced	Dipole	Total
A_{20}	-4,837	99.2	13,303	8,564
A_{32}	618.0	-854.3	4,448	4,212
A_{40}	19,053	-5338	2,835	16,550
A_{44}	11,142	-3404	-430.3	7,308
A_{52}	-1,763	599.6	-1,229	-2,393

17.3 Reference

1. M. Castellanos, A. R. West, and W. B. Reid, Dilithium Magnesium Zirconium Tetraoxide with an $\alpha\text{-LiFeO}_2$ Structure, *Acta Crystallogr. C41* (1985), 1707.

18. $\text{La}_3\text{Lu}_2\text{Ga}_3\text{O}_{12}$

18.1 Crystallographic Data on $\text{La}_3\text{Lu}_2\text{Ga}_3\text{O}_{12}$

Cubic O_h^{10} (Ia3d), 230, $Z = 8$

Ion	Site	Symmetry	x ^a	y	z	q	α (\AA^3) ^b
La	24(c)	D_2	0	1/4	1/8	3	1.41
Lu	16(a)	C_{3i}	0	0	0	3	0.77
Ga	24(d)	S_4	0	1/4	3/8	3	0.458
O	96(h)	C_1	-0.02976	0.05819	0.15699	-2	1.349

^aX-ray data: $a = 12.93$ (reference 1).

^bValues for α are from reference 6, and for values not given there, the α values are from reference 2.

18.2 Crystal-Field Components, A_{nm} ($\text{cm}^{-1}/\text{\AA}^n$)

18.2.1 For Ga ion in 24(d) (S_4) site

A_{nm}	Point charge	Self-induced	Dipole	Total
A_{20}	10,298	-2189	8197	16,306
$\text{Re}A_{32}$	-14,919	4063	-7814	-18,670
$\text{Im}A_{32}$	32,502	-8342	6011	30,171
A_{40}	-18,159	7076	-5524	-16,607
$\text{Re}A_{44}$	-4,696	1758	4006	-2,538
$\text{Im}A_{44}$	-5,156	2214	-2319	-5,260
$\text{Re}A_{52}$	-1,758	1130	-1683	-2,311
$\text{Im}A_{52}$	3,807	-2351	2290	3,475

18.2.2 For Lu ion in 16(a) (C_{3i}) site (rotated so that z-axis is parallel to (111) crystallographic axis)

A_{nm}	Point charge	Self-induced	Dipole	Total
A_{20}	8,619	-839	-9970	-2190
A_{40}	-10,698	3041	8056	-6852
$\text{Re}A_{43}$	600	-316	2583	2867
$\text{Im}A_{43}$	-11,521	3056	-13	-8478

$\text{La}_3\text{Lu}_2\text{Ga}_3\text{O}_{12}$

18.2.3 For La ion in 24(c) (D_2) site^a

A_{nm}	Point charge	Self-induced	Dipole	Total
A_{20}	-1196	-369	11,910	10,345
A_{22}	1305	-155	-107	43
A_{32}	-i1029	-i34	i1,453	i390
A_{40}	-663	-70	-20	-753
A_{42}	5073	-990	-323	3,760
A_{44}	-2522	530	971	-1,021
A_{52}	i1783	-i477	i106	i1,414
A_{54}	1967	-i253	-i87	i627
A_{60}	-1203	336	4	-863
A_{62}	549	-213	200	536
A_{64}	567	-193	-235	139
A_{66}	-474	166	202	106
A_{72}	-i73	i32	i124	i83
A_{74}	i106	-i60	i68	i114
A_{76}	i159	-i54	-i43	i62

$$a_i = \sqrt{-1}$$

18.3 Experimental Parameters (cm^{-1})

Ion	Symmetry	$F^{(2)}$	$F^{(4)}$	B_{40}	T	Ref.
Cr^{3+}	C_{3i}	49,830	35,097	-20,720	4 K	7

18.4 Bibliography and References

1. T. H. Allik, S. A. Stewart, D. K. Sardar, G. J. Quarles, R. C. Powell, C. A. Morrison, G. A. Turner, M. R. Kokta, W. W. Hovis, and A. A. Pinto, Preparation, Structure, and Spectroscopic Properties of $\text{Nd}^{3+} : \{\text{La}_{1-x} \text{Lu}_x\}_3[\text{Lu}_{1-y} \text{Ga}_y]_2\text{Ga}_3\text{O}_{12}$ Crystals, *Phys. Rev.* 37 (1988), 9129.
2. S. Fraga, J. Karwowski, and K.M.S. Saxena, *Handbook of Atomic Data* (1976), 319.
3. M. Kokta and M. Grasso, New Substituted Gallium Garnets Containing Trivalent Lanthanum on Dodecahedral Crystallographic Sites, *J. Solid State Chem.* 8 (1973), 357.
4. K. Petermann and G. Huber, Broad Band Fluorescence of Transition Metal Doped Garnets and Tungstates, *J. Lumin.* 31,32 (1984), 71.
5. D. K. Sardar, G. J. Quarles, R. C. Powell, and M. R. Kokta, Spectroscopic Properties of $\text{La}_3\text{Lu}_2\text{Ga}_3\text{O}_{12}:\text{Nd}^{3+}$ Crystals, *A.I.P. Proceedings* 146, New York (1986).

6. P. C. Schmidt, A. Weiss, and T. P. Das, Effect of Crystal Fields and Self-Consistency on Dipole and Quadrupole Polarizabilities of Closed-Shell Ions, *Phys. Rev. B19* (1979), 5525.
7. B. Struve and G. Huber, The Effect of the Crystal Field Strength on the Optical Spectra of Cr^{3+} in Gallium Garnet Laser Crystals, *Appl. Phys. B36* (1985), 195.
8. E. V. Zharikov, A. S. Zolot'ko, V. F. Kitaeva, V. V. Laptev, V. V. Osiko, N. N. Sobolev, and I. A. Sychev, Measurement of Elastic and Photoelastic Constants of the Garnet $\{\text{La}_2\text{Nd}_{0.3}\text{Lu}_{0.7}\} \text{Lu}_2\text{Ga}_3\text{O}_{12}$, *Sov. Phys. Solid State 25* (1983), 568.

19. ZnO

19.1 Crystallographic Data on ZnO

Hexagonal C_{6v}^4 ($P6_3mc$), 186, $Z = 2$

Ion	Site	Symmetry	x	y	z	q	α (Å^3) ^a
Zn	2(b)	C_{3v}	1/3	2/3	0	2	0.676
O	2(b)	C_{3v}	1/3	2/3	z	-2	1.349

^aReference 24.

19.2 X-Ray Data

a	c	z	Ref.
3.24950	5.2069	0.345	30
3.24270	5.1948	0.3826	23
3.24968	5.20662	0.3825	1

19.3 Crystal-Field Components, A_{nm} ($\text{cm}^{-1}/\text{Å}^n$), for Zn (C_{3v}) Site

Calculated using data from reference 30

A_{nm}	Point charge	Self-induced	Dipole	Total
A_{10}	31,224	0	7,662	38,886
A_{20}	17,809	-2,962	22,891	37,738
A_{30}	36,957	-9,440	8,892	36,409
A_{33}	15,279	-3,287	-4,742	7,249
A_{40}	10,043	-5,353	4,269	8,959
A_{43}	-8,681	2,903	1,141	-4,637
A_{50}	4,136	-3,662	6,358	6,831
A_{53}	39.7	-578.3	1,254	1,415

Calculated using data from reference 23

A_{nm}	Point charge	Self-induced	Dipole	Total
A_{10}	28,160	0	-311.5	27,849
A_{20}	-1,685	254.0	14,628	13,197
A_{30}	29,882	-6,758	6,088	29,211
A_{33}	20,084	-4,709	-3,930	11,446
A_{40}	8,622	-3,384	-449.8	-5,885
A_{43}	-9,102	3,384	-167.6	-5,885
A_{50}	-551.3	269.1	2,694	2,411
A_{53}	-886.2	250.6	1,696	1,060

Calculated using data from reference 1

A_{nm}	Point charge	Self-induced	Dipole	Total
A_{10}	28,033	0	-293.4	27,740
A_{20}	-1,631	244.7	14,444	13,058
A_{30}	29,635	-6658	5,992	28,968
A_{33}	19,895	-4633	-3,870	11,392
A_{40}	8,522	-3148	-435.8	4,938
A_{43}	-9,003	3325	-161.1	-5,840
A_{50}	-536.4	258.1	2,646	2,368
A_{53}	-868.7	242.5	1,661	1,035

19.4 Experimental Parameters (cm⁻¹)

Ion	nd ^N	F(2)	F(4)	α	β	ζ	B_{20}	B_{40}	B_{43}	Ref.
Ni ²⁺	3d ⁸	63,630	46,620	--	--	500	95.69	7072	6529	2
Ni ²⁺	3d ⁸	63,602	46,570	--	--	500	--	5880	7028	29a
Ni ²⁺	3d ⁸	63,218	43,674	--	--	630	--	5670	6777	20a
Co ²⁺	3d ⁷	62,388	43,943	--	--	630	--	5460	6526	29a
Co ²⁺	3d ⁷	61,250	44,100	--	--	450	-590	4077	7331	16
Co ²⁺	3d ⁷	56,350	39,690	--	--	540	--	5460	6526	11a
Cu ³⁺	3d ⁹	--	--	--	--	--	--	7000	8367	29a

^aCubic, $B_{20} = 0$, $B_{43} = \sqrt{10/7} |B_{40}|$

19.5 Bibliography and References

1. S. C. Abrahams and J. L. Bernstein, Remeasurement of the Structure of Hexagonal ZnO, *Acta Crystallogr.* B25 (1969), 1233.
2. R. S. Anderson, Lattice-Vibration Effects in the Spectra of ZnO:Ni and ZnO:Co, *Phys. Rev.* 164 (1967), 398.
3. G. D. Archard, Anomalous Lattice Constants of Zinc Oxide, *Acta Crystallogr.* 6 (1953), 657.
4. W. Bond, Measurement of Refractive Indexes of Several Crystals, *J. Appl. Phys.* 36 (1965), 1674.
5. I. J. Broser, R.K.F. Germer, H.-Joachin, E. Shultz, and K. P. Wisznewski, Fine Structure and Zeeman Effects of the Excited State of the Green Emitting Copper Centre in Zinc Oxide, *Solid-State Electron.* 21 (1978), 1597.
6. H. E. Brown, Zinc Oxide Properties and Applications, International Lead Zinc Research Organization, New York, NY (1981). (This reference contains a very extensive bibliography.)

ZnO

7. R. Collins and D. Kleinman, Infrared Reflectivity of ZnO, *Phys. Chem. Solids* 11 (1959), 190.
8. R. Dingle, Luminescent Transitions Associated with Divalent Impurities and the Green Emission from Semiconductivity ZnO, *Phys. Rev. Lett.* 23 (1969), 579.
9. I. T. Drapak, Growing Zinc Oxide Single Crystals and Films, *Neorg. Mater.* 16 (1980), 362.
10. K. Fischer and E. Sinn, On the Preparation of ZnO Single Crystals, *Cryst. Res. Tech.* 16 (1981), 689.
11. G. Heiland, E. Moilwo, and F. Stockmann, Electronic Processes in Zinc Oxide, *Solid State Phys.* 8 (1959), 193.
12. W. Johnston, Characteristics of Optically Pumped Platelet Lasers of ZnO, CdS, CdSe, and CdS-Se Between 300° and 80°K, *J. Appl. Phys.* 42 (1971), 2731.
13. S. A. Kazandzhiev, M. M. Malov, V. D. Chernyi, M. N. Mendakov, A. N. Lobachev, and I. P. Kuzmina, Effect of Growth Conditions on Optical Properties of Zinc Oxide Single Crystals Grown by Hydrothermal Synthesis, *Opticheskie Issledovaniya Polysrovodnikov* (1980), p 99.
14. A. D. Liehr, The Three Electron (or Hole) Cubic Ligand Field Spectrum, *J. Phys. Chem.* 67 (1963), 1314. (This reference contains a multitude of references to earlier work.)
15. D. Louer, J. P. Auffredic, J. I. Langford, D. Ciosmak, and J. C. Niepce, A Precise Determination of the Shape, Size and Distribution of Size of Crystallites in Zinc Oxide by Oxides by X-Ray Line-Broadening Analysis, *J. Appl. Crystallogr.* 16 (1983), 183.
16. R. M. Macfarlane, Perturbation Methods in the Calculation of Zeeman Interactions and Magnetic Dipole Line Strengths for d^3 Trigonal-Crystal Spectra, *Phys. Rev. B1* (1970), 989.
17. W. C. Mackrodt, R. F. Stewart, J. C. Campbell, and I. H. Hillier, The Calculated Defect Structure of ZnO, *J. Phys. Paris* 41 (Suppl. to No. 7), (1980), C6-64.
18. G. Muller, Optical and Electrical Spectroscopy of Zinc Oxide Crystals Simultaneously Doped with Copper and Donors, *Phys. Status Solidi B* 76 (1976), 525.
19. R. Pappalardo, D. L. Wood, and R. C. Linares, Jr., Optical Absorption Study of Co-Doped Oxide Systems: II, *J. Chem. Phys.* 35 (1961), 2041.
20. R. Pappalardo, D. L. Wood, and R. C. Linares, Jr., Optical Absorption Spectra of Ni-Doped Oxide Systems: I, *J. Chem. Phys.* 35 (1961), 1460.

21. R. Purlis, A. Jakimavicius, and A. Sirvaitis, Temperature Dependence of Root-Mean-Square Dynamic Displacement and X-Ray Diffraction Characteristics of ZnS and ZnO, *Izv. Vyssh. Ucheln. Zaved. Fiz.* 24 (1981), 115.
22. M. L. Reynolds and G.F.J. Garlick, The Infrared Emission of Nickel Ion Impurity Centres in Various Solids, *Infrared Phys.* 7 (1967), 151.
23. T. M. Sabine and S. Hogg, The Wurtzite Z Parameter for Beryllium Oxide and Zinc Oxide, *Acta Crystallogr.* B25 (1969), 2254.
24. P. C. Schmidt, A. Weiss, and T. P. Das, Effect of Crystal Fields and Self-Consistency on Dipole and Quadrupole Polarizabilities of Closed-Shell Ions, *Phys. Rev.* B19 (1979), 5525.
25. H.-J. Schultz and M. Thiede, Optical Spectroscopy of $3d^7$ and $3d^8$ Impurity Configurations in a Wide-Gap Semiconductor (ZnO:Co, Ni, Cu), *Phys. Rev.* B35 (1987), 18.
26. T. Shiraishi, The Crystal Structure of Zinc Oxide-Chromium (IV) Oxide System Catalysts for Methanol Synthesis, *Nihama Kogyo Kuto Semmon Gakko Kiyo* 17 (1981), 45.
27. A. E. Tsurkan, L. V. Buzhor, B. I. Kidyarov, and P. G. Pas'kov, Electrical Properties of Zinc Oxide Single Crystals Prepared by Different Methods, *Poluchenie I Issled. Nov. Materialov Poluprovodn. Tekhn.* (1980), 161.
28. V. P. Vlasov, G. I. Distler, V. M. Kanevskii, and G. D. Shnyrev, Effects of Impurity Structures on Brittle Fracture in ZnS and ZnO Crystals, *Izv. Akad. Nauk SSSR Ser. Fiz.* 44 (1980), 1302.
29. H. A. Weakliem, Optical Spectra of Ni^{2+} , Co^{2+} , and Cu^{2+} in Tetrahedral Sites in Crystals, *J. Chem. Phys.* 36 (1962), 2117.
30. R.W.G. Wyckoff, *Crystal Structures*, vol. 1, Interscience, New York (1968), 111.
31. E. Ziegler, A. Heinrich, H. Oppermann, and G. Stover, Electrical Properties of Non-stoichiometry on ZnO Single Crystals, *Phys. Status Solidi A* 66 (1981), 635.

20. ZnS

20.1 Crystallographic Data on ZnS

20.1.1 Cubic T_d^2 ($F\bar{4}3m$), 216, Z = 4

Ion	Site	Symmetry	x ^a	y	z	q	α (\AA^3) ^b
Zn	4a	T_d	0	0	0	2	0.676
S	4c	T_d	1/4	1/4	1/4	-2	4.893

^aX-ray data: a = 5.4093 \AA (reference 32, p 110).

^bReference 20.

20.1.2 Hexagonal C_{6v}^4 ($P6_3mc$), 186, Z = 2

Ion	Site	Symmetry	x ^a	y	z	q	α (\AA^3)
Zn	2(b)	C_{3v}	1/3	2/3	0	2	0.676
S	2(b)	C_{3v}	1/3	2/3	z	-2	4.893

^aX-ray data: a = 3.811 \AA , c = 6.234 \AA (reference 32, p 112).

20.2 Crystal Fields

20.2.1 Crystal-field components, A_{nm} ($\text{cm}^{-1}/\text{A}^n$), for Zn (T_d) site of cubic ZnS

A_{nm}	Monopole	Self-induced	Total
A_{32}	15,219	-7349	7869
A_{40}	-4,610	4035	-574.8
A_{44}	2,755	-2411	343.5

20.2.2 Crystal-field components, A_{nm} ($\text{cm}^{-1}/\text{A}^n$), for Zn (C_{3v}) site of hexagonal ZnS

A_{nm}	Monopole	Self-induced	Dipole	Total
A_{10}	20,496	0	9,537	30,033
A_{20}	10,188	-3,463	26,174	32,899
A_{30}	18,608	-10,166	7,716	16,158
A_{33}	7,926	-3,754	-4,809	-636.8
A_{40}	3,800	-4,417	3,128	2,511
A_{43}	-3,877	2,887	952.3	-37.21
A_{50}	1,334	-2,505	4,341	3,171
A_{53}	339.5	-518.3	874.1	695.3

20.3 Experimental Values (cm⁻¹) of F⁽²⁾, F⁽⁴⁾, ζ , and B₄₀^N for 3d^N Ions

Ion	3d ^N	F ⁽²⁾	F ⁽⁴⁾	ζ	B ₄₀ ^a	Ref
Y ²⁺	3d ³	--	--	--	-10,326	8
Cr ²⁺	3d ⁴	81,148	31,529	--	-10,924	6
Mn ²⁺	3d ⁵	44,280	43,981	--	-10,351	7
Mn ²⁺	3d ⁵	56,454	32,925	--	-11,603	22
Fe ²⁺	3d ⁶	51,433	36,195	--	-7,486	24,10
Co ²⁺	3d ⁷	49,516	35,438	583	-7,897	31
Co ²⁺	3d ⁷	53,851	40,619	--	-7,509	15
Ni ²⁺	3d ⁸	46,449	32,211	477	-9,321	31
Ni ²⁺	3d ⁸	50,119	29,445	--	-10,701	19

$$^a B_{44} = \sqrt{5/14} |B_{40}|, Dq = 21 |B_{40}|$$

20.4 Bibliography and References

1. S. W. Biernacki, Parametrization of Crystal Field Spectra of Mn²⁺ in ZnSe and ZnS, Phys. Status Solidi B132 (1985), 557.
2. F. J. Bryant and A. Krier, Low-Voltage Direct Current Electroluminescence in ZnS:Re Thin Films, IEE Proc. 130 (1983), 160.
3. D. Curie, C. Barthou, and B. Canny, Covalent Bonding of Mn²⁺ Ions in Octahedral and Tetrahedral Coordinates, J. Chem. Phys. 61 (1974), 3048.
4. B. Clerjaud, A. Gelineau, G. Gendron, C. Porte, J. M. Baranowski, and Z. Liro, Optical Properties of Ni⁺ (d⁹) in ZnS, Physica 116B (1983), 500-502.
5. A. Fazzio, M. J. Caldas, and A. Zunger, Many Electron Multiplet Effects in the Spectra of 3d Impurities in Heteropolar Semiconductors, Phys. Rev. B30 (1984), 3430.
6. G. Grebe and H. J. Schultz, Phys. Status Solidi B54 (1972), K 69.
7. H. E. Gumlich, R. L. Pfrogner, J. C. Schaffer, and F. E. Williams, J. Chem. Phys. 44 (1966), 3929.
8. Le. M. Hoang and J. M. Baranowski, Phys. Status Solidi B84 (1977), 361.
9. G. L. House and H. G. Drickamer, High Pressure Luminescence Studies of Localized Excitations in ZnS Doped with Pb²⁺ and Mn²⁺, J. Chem. Phys. 67 (1977), 3230.
10. F. F. Kodzhespirov, M. Bulanyi, and J. A. Tereb, Sov. Phys. Solid State 16 (1975), 2052.

ZnS

11. W. Low and M. Weger, Paramagnetic Resonance and Optical Spectra of Divalent Iron in Cubic Fields: I.--Theory, *Phys. Rev.* 118 (1960), 1119.
12. W. Low and M. Weger, Paramagnetic Resonance and Optical Spectra of Divalent Iron in Cubic Fields: II.--Experimental Results, *Phys. Rev.* 118 (1960), 1130.
13. D. Langer and S. Ibuki, Zero-Phonon Lines and Phonon Coupling in ZnS:Mn, *Phys. Rev.* A138 (1965), 809.
14. D. S. McClure, Optical Spectra of Exchange Coupled Mn⁺⁺ Ion Pairs in ZnS:MnS, *J. Chem. Phys.* 39 (1963), 2850.
15. J. M. Noras, H. R. Szawelska, and J. W. Allen, *J. Phys.* C14 (1981), 3255.
16. D. T. Palumbo and J. J. Brown, Electronic States of Mn²⁺ Activated Phosphors: II.--Orange-to-Red Emitting Phosphors, *J. Electrochem. Soc.* 118 (1971), 1159.
17. M. L. Reynolds and G.F.J. Garlick, The Infrared Envision of Nickel Ion Impurity Centers in Various Solids, *Infrared Phys.* 7 (1967), 151.
18. G. Roussos, J. Nagel, and H.-J. Schultz, Luminescent Ni⁺ Centers and Changes of the Charge State of Nickel Ions in ZnS and ZnSe, *Z. Phys.* B53 (1983), 96.
19. G. Roussos and H.-J. Schultz, *Phys. Status Solidi* B100 (1980), 577.
20. P. C. Schmidt, A. Weiss, and T. P. Das, Effect of Crystal Fields and Self-Consistency on Dipole and Quadrupole Polarizabilities of Closed-Shell Ions, *Phys. Rev.* B19 (1979).
21. J. Schneider and A. Rauber, Electron Spin Resonance of Ti²⁺ in ZnS, *Phys. Lett.* 21 (1966), 380.
22. H.-J. Schultz and M. Thiede, Optical Spectroscopy of 3d⁷ and 3d⁸ Impurity Configurations in a Wide-Gap Semiconductor (ZnO: Co, Ni, Cu), *Phys. Rev.* B35 (1987), 18.
23. M. Skowronski, M. Godlewski, and Z. Liro, The Fe²⁺ Ion Energy Scheme in ZnS Crystals, *Proc. Conf. Phys.*, vol 2 (1981), 112.
24. M. Skowronski and Z. Liro, *J. Phys.* C15 (1982), 137.
25. G. A. Slack, F. S. Ham, and R. M. Chrenko, Optical Absorption of Tetrahedral Fe²⁺ (3d⁶) in Cubic ZnS, CdTe, and MgAl₂O₄, *Phys. Rev.* 152 (1966), 376-402.
26. G. A. Slack and B. M. O'Meara, Infrared Luminescence of Fe²⁺ in ZnS, *Phys. Rev.* 163 (1967), 335.

27. G. A. Slack, S. Roberts, and F. S. Ham, Far-Infrared Optical Absorption of Fe^{2+} in ZnS, Phys. Rev. 155 (1967), 170.
28. V. J. Sokolov, A. N. Mamedov, T. P. Surkova, M. V. Chukichev, and M. P. Kulakov, Energy States of Cobalt in Zinc Selenide and Zinc Sulphide, Opt. Spectrosc. 62 (1987), 480.
29. J. T. Valliu, G. A. Slack, S. Roberts, and A. E. Hughes, Infrared Absorption in Some II-IV Compounds Doped with Cr, Phys. Rev. B2 (1970), 4313.
30. V. P. Vlasov, G. I. Distler, V. M. Kanevskii, and G. D. Shnyrev, Effects of Impurity Structures on Brittle Fracture in ZnS and ZnO Crystals, Izv. Akad. Nauk SSSR Ser. Fiz. 44 (1980), 1302.
31. H. A. Weakliem, Optical Spectra of Ni^{2+} , Co^{2+} and Cu^{2+} in Tetrahedral Sites in Crystals, J. Chem. Phys. 36 (1962), 2117-2140.
32. R.W.G. Wyckoff, Crystal Structures, vol. 1, Interscience, New York (1968).

21. K_2PtCl_6 21.1 Crystallographic Data on K_2PtCl_6 Cubic O_h^5 (Fm $\bar{3}m$) 225, $Z = 4$

Ion	Site	Symmetry	x^a	y	z	q	α (\AA^3)
Pt	4(a)	O_h	0	0	0	4	0.67 ^b
K	8(c)	T_d	1/4	1/4	1/4	1	0.827 ^c
Cl	24(e)	C_{4v}	x	0	0	-1	2.694 ^c

^aX-ray data: $a = 9.755 \text{ \AA}$, $x = 0.240$ (reference 12).^bReference 5.^cReference 10.21.2 Crystal-Field Components, A_{nm} ($\text{cm}^{-1}/\text{\AA}^n$), for Pt (O_h) Site

A_{nm}	Monopole	Self-induced	Dipole	Total
A_{40}	6115.0	-5016.9	10,480	11,578
A_{44}	3654.4	-2998.2	6,262.7	6,919.0

21.3: Experimental Parameters (cm^{-1})

Ion	nd^N	$F^{(2)}$	$F^{(4)}$	ζ	B_{40}	Ref.
Ru ⁴⁺	4d ⁴	48,888	17,174	1044	39,732	9
Re ⁴⁺	5d ³	28,749	22,907	2392	63,729	4
Os ⁴⁺	5d ⁴	45,381	16,330	2416	47,229	3
Re ⁴⁺	5d ³	28,843	22,582	2360	63,477	6
Re ⁴⁺	5d ³	29,963	22,907	2392	63,729	14

21.4 Bibliography and References

1. P. B. Dorain, Magnetic and Optical Properties of Transition Metal Ions in Single Crystals, Aerospace Laboratories Report, ARL-73-0139 (October 1973), NTIS AD 769870.
2. P. B. Dorain, The Spectrum of Re⁴⁺ in Cubic Crystal Fields, in Transition Metal Chemistry, ed. R. L. Carlin, vol. 4 (1968), Marcel Dekker, New York, pp 1-31.
3. P. B. Dorain, H. H. Patterson, and P. C. Jordan, Optical Spectra of Os⁴⁺ in Single Cubic Crystals at 4.2°K, J. Chem. Phys. 49 (1968), 3845.

4. P. B. Dorain and R. G. Wheeler, Optical Spectrum of Re^{4+} in Single Crystals of K_2PtCl_6 and Cs_2ZrCl_6 at $4.2^\circ K$, *J. Chem. Phys.* 45 (1966), 1172.
5. S. Fraga, K.M.S. Saxena, and J. Karwowski, *Handbook of Atomic Data*, Elsevier, New York (1976).
6. C. D. Flint and A. G. Pauley, High Resolution Infrared and Visible Luminescence Spectra of $ReCl_6^{2-}$ and $ReBr_6^{2-}$ in Cubic Crystals, *Mol. Phys.* 43 (1981), 321.
7. S. M. Khan and H. H. Patterson, Multiple State Luminescence for the d^4 $OsCl_6^{2-}$ Impurity Ion in K_2PtCl_6 and Cs_2ZrCl_6 Cubic Crystals, *Mol. Phys.* 35 (1978), 1623.
8. S. Maniv, J. Bronstein, and W. Low, Electron-Paramagnetic-Resonance Spectrum of Tc^{4+} in Single Crystals of K_2PtCl_6 , *Phys. Rev.* 187 (1969), 403.
9. H. Patterson and P. Dorain, Optical Spectra of Ru^{4+} in Single Crystals of K_2PtCl_6 and Cs_2ZrCl_6 at $4.2^\circ K$, *J. Chem. Phys.* 52 (1970), 849.
10. P. C. Schmidt, A. Weiss, and T. P. Das, Effect of Crystal Fields and Self-Consistency on Dipole and Quadrupole Polarizabilities of Closed-Shell Ions, *Phys. Rev.* B19 (1979), 5525.
11. H.-H. Schmidtke and D. Strand, The Emission Spectrums of $OsCl_6^{2-}$ Doped in Various Cubic Host Lattices, *Inorg. Chim. Acta* 62 (1982), 153.
12. R.W.G. Wyckoff, *Crystal Structures*, vol. 3, Interscience, New York, (1968), 339.
13. Li Xuequi and Cheng Yu, A Program for the Calculation of Ligand Field Theory, *Chem. J. Chinese Univ.* 5 (1984), 725.
14. Han Yande, Li Baifu, Zhu Yukui, and Sun Chia-Chung, The Analysis of the Ligand Field Theory of Crystal Spectrum of d^3 (Re^{4+}) and d^4 (Os^{+4}) Configuration, *Chem. J. Chinese Univ.* 3 (1982), 97.

22. $\text{Y}_3\text{Ga}_5\text{O}_{12}$ (YGG)

22.1 Crystallographic Data on $\text{Y}_3\text{Ga}_5\text{O}_{12}$

Cubic O (Ia3d), 230, Z = 8

Ion	Site	Symmetry	x ^a	y	z	q	α (\AA^3) ^b
Y	24(c)	D_2	0	1/4	1/8	3	0.870
Ga ₁	16(a)	C_{3i}	0	0	0	3	0.458
Ga ₂	24(d)	S_{4i}	0	1/4	3/8	3	0.458
O	96(h)	C_1	-0.0272	0.05580	0.1501	-2	1.349

^aX-ray data: a = 12.28 (reference 5).

^bReference 10.

22.2 Crystal-Field Components, A_{nm} ($\text{cm}^{-1}/\text{\AA}^n$)

22.2.1 For Ga ion in 24(d) (S_{4i}) site

A_{nm}	Monopole	Self-induced	Dipole	Total
A_{20}	7,529.074	-2139.311	9280.060	14,669.823
$\text{Re}A_{32}$	-19,875.040	5487.624	-9440.532	-23,827.948
$\text{Im}A_{32}$	32,745.166	-8848.915	5910.520	29,806.771
A_{40}	-19,871.204	8061.824	-6493.768	-18,303.148
$\text{Re}A_{44}$	-3,959.054	1499.466	1011.514	-1,448.074
$\text{Im}A_{44}$	-6,410.529	2934.927	-2624.400	-6,100.002
$\text{Re}A_{52}$	-2,135.999	1448.737	-2204.848	-2,892.110
$\text{Im}A_{52}$	3,718.967	-2388.618	2509.017	3,839.366
$ A_{44} $	7,534.52	--	--	6,269.525

22.2.2 For Ga₁ ion in 16(a) (C_{3i}) site (rotated so that z-axis is parallel to (111) crystallographic axis)

A_{nm}	Monopole	Self-induced	Dipole	Total
A_{20}	15,183.2	-1576.3	-14,849	-1,242.3
A_{40}	-17,783.6	6625.2	1,754.4	-9,403.4
$\text{Re}A_{43}$	1,294.6	-745.1	4,955.7	5,505.3
$\text{Im}A_{43}$	-18,677.5	6650.8	530.7	-11,496
$ A_{44} $	18,722	--	--	12,746

22.3 Experimental Parameters (cm⁻¹)

F ⁽²⁾	F ⁽⁴⁾	B ₂₀	B ₄₀	B ₄₃	Ref.
53,994	40,735	--	-22,820 ^a	--	11 ^b
54,638	40,456	--	-21,140 ^a	--	11 ^c

^aCubic approximation $B_{43} = \sqrt{10/7} |B_{40}|$.^bFit to E₀ data of reference 11.^cFit to E_a data of reference 11.22.4 Bibliography and References

1. M. Kh. Ashurov, Yu. K. Voronko, V. V. Osiko, A. A. Sobol, B. P. Starikov, M. I. Timoshchekin, and A. Ya. Yablonskii, Inequivalent Luminescence Centers of Er³⁺ in Gallium Garnet Single Crystals, *Phys. Status Solidi A35* (1976), 645.
2. G. Burns, E. A. Geiss, B. A. Jenkins, and M. I. Nathan, Cr³⁺ Fluorescence in Garnets and Other Crystals, *Phys. Rev. A139* (1965), 1687.
3. J. W. Carson and R. L. White, Zero-Field Splitting of the Cr³⁺ Ground State in YGa and YAl Garnet, *J. Appl. Phys. 32* (1961), 1787.
4. J. R. Chamberlain and R. W. Cooper, Paramagnetic Resonance in Yttrium Gallium Garnet: Co²⁺ and Mn²⁺, *Proc. Phys. Soc. 87* (1966), 967.
5. F. Euler and J. A. Bruce, Oxygen Coordinates of Compounds with Garnet Structures, *Acta Crystallogr. 19* (1965), 971.
6. J. Ferguson and D. L. Wood, Crystal Field Spectra of d^{3,7} Ions: VI.-- The Weak Field Formalism and Covalency, *Aust. J. Chem. 23* (1970), 861.
7. S. Geschwind, Paramagnetic Resonance of Fe³⁺ in Octahedral and Tetrahedral Sites in Yttrium Gallium Garnet (YGaG) and Anisotropy of Yttrium Iron Garnet (YIG), *Phys. Rev. 121* (1961), 363.
8. R. Pappalardo, D. L. Wood, and R. C. Linares, Jr., Optical Absorption Study of Co-Doped Oxide Systems: II, *J. Chem. Phys. 35* (1961), 2041.
9. R. Pappalardo, D. L. Wood, and R. C. Linares, Jr., Optical Absorption Spectra of Ni-Doped Oxide Systems: I, *J. Chem. Phys. 35* (1961), 1460.
10. P. C. Schmidt, A. Weiss, and T. P. Das, Effect of Crystal Fields and Self-Consistency on Dipole and Quadrupole Polarizabilities of Closed-Shell Ions, *Phys. Rev. B19* (1979), 5525.
11. B. Struve and G. Huber, The Effect of the Crystal Field Strength on the Optical Spectra of Cr³⁺ in Gallium Garnet Laser Crystals, *Appl. Phys. B36* (1985), 195.

$\text{Y}_3\text{Ga}_5\text{O}_{12}$

12. M. D. Sturge, F. R. Merritt, J. C. Hensel, and J. P. Remeika, Magnetic Behavior of Cobalt in Garnets: I.--Spin Resonance in Cobalt-Doped Yttrium Gallium Garnet, *Phys. Rev.* 180 (1969), 402.
13. D. L. Wood, J. Ferguson, K. Knox, and J. F. Dillon, Jr., Crystal-Field Spectra of $d^3,7$ Ions: III.--Spectrum of Cr^{3+} in Various Octahedral Crystal Fields, *J. Chem. Phys.* 39 (1967), 3595.
14. D. L. Wood and J. P. Remeika, Optical Absorption of Tetrahedral Co^{3+} and Co^{2+} in Garnets, *J. Chem. Phys.* 46 (1967), 3595.

23. $\text{La}_{2-x}\text{Sr}_x\text{CuO}_4$

23.1 Crystallographic Data on $\text{La}_{1.85}\text{Sr}_{0.15}\text{CuO}_4$

23.1.1 Tetragonal, D_{4h}^{17} (I4/mmm), 139, Z = 2; T = 300 K

Ion	Site	Symmetry	x	y	z	q ^a	q ^b
La/Sr	4(e)	C_{4v}	0	0	z	2.775	2.925
Cu	2(a)	D_{4h}	0	0	0	2.45	2.15
O ₁	4(e)	C_{4v}	0	0	z	-2	-2
O ₂	4(c)	D_{2h}	0	1/2	0	-2	-2

^aThe effective charges on the Cu ions are chosen as 55% Cu²⁺ + 45% Cu³⁺, and the total charge in the unit cell vanishes.

^bThe charge on La is taken as 3 and the charge on Sr is taken as 2, so that the average charge on the La/Sr site is [3(1.85) + 2(0.15)]/2. The charge on the Cu ion is then chosen so that the total charge in a unit cell is zero.

23.1.2 Orthorhombic D_{2h}^{18} (Cmca), 64, Z = 4; T = 10 K and 60 K

Ion	Site	Symmetry	x	y	z	q ^a	q ^b
La/Sr	8(f)	C_s	0	y	z	2.775	2.925
Cu	4(a)	C_{2h}	0	0	0	2.450	2.15
O ₁	8(f)	C_s	0	y	z	-2	-2
O ₂	8(e)	C_2	1/4	y	1/4	-2	-2

^{a,b}See notes to 23.1.1

23.2 X-Ray Data

23.2.1 Tetragonal, T = 300 K

a	c	z_{La}	z_{O_1}	Ref
3.7793	13.226	0.36046	0.1824	1
3.7749	13.2231	0.3606	0.1826	3

23.2.2 Orthorhombic, T = 10 K and 60 K

Temp	a	b	c	y_{La}	z_{La}	y_{O_1}	z_{O_2}	y_{O_2}
10 K	5.3240	13.1832	5.3547	-0.36077	-0.00496	-0.18260	0.0255	-0.00573
60 K	5.3252	13.1844	5.3546	-0.36072	-0.00495	-0.18257	0.0256	-0.00560

Reference 1 (transformed to the standard in the International Tables).

$\text{La}_{2-x}\text{Sr}_x\text{CuO}_4$

23.3 Crystal-Field Components, A_{nm} ($\text{cm}^{-1}/\text{Å}^n$)

23.3.1 For La (C_{4v}) site in tetragonal $\text{La}_{1.85}\text{Sr}_{0.15}\text{CuO}_4$

A_{nm}	300 K (ref 1)	300 K (ref 2)
A_{10}	-6369	4915
A_{20}	8888	9248
A_{30}	-4634	-5675
A_{40}	1954	1451
A_{44}	-1773	-1818
A_{50}	-3188	-3127
A_{54}	1691	1590
A_{60}	364.2	358.4
A_{64}	745.9	720.3
A_{70}	136.4	-123.5
A_{74}	76.61	77.69

23.3.2 For La (C_s) site of orthorhombic $\text{La}_{1.85}\text{Sr}_{0.15}\text{CuO}_4$ rotated so that z-axis of A_{nm} is parallel to b-axis and A_{22} is real and positive

A_{nm}	60 K	10 K
$\text{Re}A_{11}$	3904	3919
$\text{Im}A_{11}$	6897	6952
A_{20}	-4544	-4534
A_{22}	5272	5284
$\text{Re}A_{31}$	-2027	-2023
$\text{Im}A_{31}$	-30.36	-26.08
$\text{Re}A_{33}$	2759	2760
$\text{Im}A_{33}$	-187.2	-149.7
A_{40}	2573	2567
$\text{Re}A_{42}$	496.0	499.0
$\text{Im}A_{42}$	-184.5	-189.9
$\text{Re}A_{44}$	1444	1439
$\text{Im}A_{44}$	-260.8	-245.5

For La (C_s) site (cont'd)

A_{nm}	60 K	10 K
ReA ₅₁	2070	1992
ImA ₅₁	366.8	359.0
ReA ₅₃	48.29	-104.4
ImA ₅₃	466.5	407.40
ReA ₅₅	1657	1711
ImA ₅₅	1010	1084
A ₆₀	404.8	405.6
ReA ₆₂	-46.89	-47.26
ImA ₆₂	81.61	82.61
ReA ₆₄	-688.5	-685.5
ImA ₆₄	-305.5	-314.3
ReA ₆₆	-22.47	-22.21
ImA ₆₆	-32.74	-32.38
ReA ₇₁	-83.33	-83.31
ImA ₇₁	-2.75	-2.87
ReA ₇₃	38.85	39.08
ImA ₇₃	-27.77	-27.61
ReA ₇₅	9.35	9.67
ImA ₇₅	20.60	20.67
ReA ₇₇	85.19	84.98
ImA ₇₇	13.54	15.27

$\text{La}_{2-x}\text{Sr}_x\text{CuO}_4$

23.4 References

1. R. J. Cava, A. Santoro, D. W. Johnson, and W. W. Rhodes, Crystal Structure of the High-Temperature Superconductor $\text{La}_{1.85}\text{Sr}_{0.15}\text{CuO}_4$ Above and Below T_c , *Phys. Rev. B35* (1987), 6716.
2. V. Geiser, M. A. Bens, A. J. Schultz, H. H. Wang, T. J. Allen, M. R. Monaghan, and J. M. Williams, Structure Instability in Single Crystals of the High- T_c Superconductor $\text{La}_{2-x}\text{Sr}_x\text{CuO}_4$, *Phys. Rev. B35* (1987), 6721.
3. T. Kajitani, T. Onozuka, Y. Yamaguchi, M. Hirabayashi, and Y. Syono, Displacement Waves in $\text{La}_2\text{CuO}_{4-w}$ and $\text{La}_{1.85}\text{Sr}_{0.15}\text{CuO}_{4-w}$, *Jpn. J. Appl. Phys. 26* (1987), L1877.

24. Al_2O_3 (Corundum)

24.1 Crystallographic Data on Al_2O_3

Hexagonal D_{3d}^6 (R3c) (second setting), 167, $Z = 6$

Ion	Site	Symmetry	x	y	z	q	α (\AA^3)
Al	12(c)	C_3	0	0	z	3	0.053
O	18(e)	C_2	x	0	1/4	-2	1.349

24.2 X-Ray Data

a	c	z_{Al}	x_0	Ref	Set
4.7628	13.0032	0.352	0.306	37	1
4.7586	12.9897	0.3518	0.6918	51	2
4.75855	12.9906	0.35200	0.6936	51	3
4.75999	12.99481	0.35219	0.69367	51	4
4.7640	13.0091	0.35221	0.30636	12	5

24.3 Crystal-Field Components, A_{nm} ($\text{cm}^{-1}/\text{\AA}^n$), for Al (C_3) Site

Set 1

A_{nm}	Monopole	Self-induced	Dipole	Total
A_{10}	6,472	--	-6424	48.41
A_{20}	-4,896	778.2	1933	-2,185
A_{30}	-9,718	4215	620.4	-4,883
Re A_{33}	-639.7	-1220	1126	-733.6
Im A_{33}	-10,955	3434	1253	-6,268
A_{40}	-18,418	6479	-66.36	-12,005
Re A_{43}	4,371	-1322	629.3	3,678
Im A_{43}	-23,006	9736	417.6	-12,853
A_{50}	8,476	-4130	458.8	4,804
Re A_{53}	1,581	-486.9	107.8	1,201
Im A_{53}	1,766	-592.6	798.9	1,973

Al₂O₃

Set 2

A _{nm}	Monopole	Self-induced	Dipole	Total
A ₁₀	8,456	--	-6841	615
A ₂₀	-5,475	852.5	2003	-2,619
A ₃₀	-9,692	4327	695.7	-4,669
Re A ₃₃	-1,050	-1147	1241	-955.1
Im A ₃₃	11,217	-3561	-1337	6,319
A ₄₀	-18,612	6555	-65.65	-12,123
Re A ₄₃	4,167	-1252	706.9	3,622
Im A ₄₃	23,259	-9890	-440.6	12,928
A ₅₀	8,352	-4057	487.9	4,783
Re A ₅₃	1,564	-470.9	128.8	1,222
Im A ₅₃	-1,543	413.5	-861.5	-1,991

Set 3

A _{nm}	Monopole	Self-induced	Dipole	Total
A ₁₀	6,840	--	-6447	393.1
A ₂₀	-5,026	799.8	1933	-2,293
A ₃₀	-9,783	4267	629.7	-4,886
Re A ₃₃	-704.1	-1214	1140	-778.5
Im A ₃₃	11,064	-3485	-1261	6,318
A ₄₀	-18,498	6524	-64.96	-12,039
Re A ₄₃	4,355	-1319	639.6	3,676
Im A ₄₃	23,136	-9822	-420.9	12,893
A ₅₀	8,497	-4150	460.7	4,808
Re A ₅₃	1,583	-487.1	110.6	1,206
Im A ₅₃	-1,733	561.8	-805.5	-1,976

Set 4

A _{rim}	Monopole	Self-induced	Dipole	Total
A ₁₀	6,774	--	-6442	331.9
A ₂₀	-5,000	795.2	1933	-2,272
A ₃₀	-9,766	4253	627.7	-4,885
Re A ₃₃	-692.5	-1214	1137	-769.6
Im A ₃₃	11,039	-3473	-1259	6,307
A ₄₀	-18,471	6509	-65.14	-12,027
Re A ₄₃	4,355	-1318	637.4	3,675
Im A ₄₃	23,096	-9795	-420.1	12,880
A ₅₀	8,486	-4141	460.0	4,805
Re A ₅₃	1,581	-486.5	110.1	1,205
Im A ₅₃	-1,737	566.4	-803.7	-1,974

Set 5

A _{nm}	Monopole	Self-induced	Dipole	Total
A ₁₀	6,778	--	-5821	957.6
A ₂₀	-5,003	813.0	1753	-2,437
A ₃₀	-10,007	4292	564.1	-5,151
Re A ₃₃	-634.0	-1213	1033	-813.9
Im A ₃₃	-11,173	3512	1140	-6,521
A ₄₀	-18,251	6420	-51.53	-11,882
Re A ₄₃	4,361	-1314	577.4	3,625
Im A ₄₃	-22,971	9724	387.6	-12,860
A ₅₀	8,469	-4134	408.8	4,744
Re A ₅₃	1,563	-481.0	98.52	1,180
Im A ₅₃	1,709	-539.5	720.8	1,891

24.4 Experimental Parameters (cm⁻¹) for Transition-Metal Ions

Ion	nd ^N	Site	F ⁽²⁾	F ⁽⁴⁾	α	ξ	B ₂₀	B ₄₀	B ₄₃	Ref
V ³⁺	3d ²	A1	47,390	31,500	--	155	234	-23,564	30,803	25
Cr ³⁺	3d ³	A1	53,690	39,312	--	170	-1123	-22,350	31,538	26

Al_2O_3

24.5 Bibliography and References

1. R. L. Aggarwal, A. Sanchez, M. M. Stuppi, R. E. Fahey, A. J. Strauss, W. R. Rapoport, and C. P. Khattak, Residual Infrared Absorption in As-Grown and Annealed Crystals of $\text{Ti:Al}_2\text{O}_3$, *IEEE J. Quantum Electron.* QE-24 (1988), 1003.
2. J. O. Artman and J. C. Murphy, Lattice Sum Evaluations of Ruby Spectral Parameters (preprint copy, no date).
3. C. H. Bair, P. Brockman, R. V. Hess, and E. A. Modlin, Demonstration of Frequency Control and CW Diode Laser Injection Control of a Titanium-Doped Sapphire Ring Laser with No Internal Optical Elements, *IEEE J. Quantum Electron.* QE-24 (1988), 1045.
4. A. S. Barker, Infrared Lattice Vibrations and Dielectric Dispersion in Corundum, *Phys. Rev.* 132 (1963), 1474.
5. J. C. Barnes, N. P. Barnes, and G. E. Miller, Master Oscillator Power Amplifier Performance of $\text{Ti:Al}_2\text{O}_3$, *IEEE J. Quantum Electron.* QE-24 (1988), 1029.
6. N. P. Barnes, J. A. Williams, J. C. Barnes, and G. E. Lockard, A Self-Injection Locked, Q-Switched, Line-Narrowed $\text{Ti:Al}_2\text{O}_3$ Laser, *IEEE J. Quantum Electron.* QE-24 (1988), 1021.
7. W. E. Blumberg, J. Eisinger, and G. S. Geschwind, Cu^{3+} Ion in Corundum, *Phys. Rev.* 130 (1963), 900.
8. O. N. Boksha, T. M. Varina, and A. A. Popova, Optical Spectra of Cr and Mn in Synthetic $\text{MgO-Al}_2\text{O}_3$ Spinels, *Sov. Phys. Crystallogr.* 17 (1973), 940.
9. O. N. Boksha, T. M. Varina, A. A. Popova, and E. F. Smirnova, Conditions for the Synthesis and the Optical Spectra of Crystals Containing Transition Elements: II.--Corundum Containing Ti, *Sov. Phys. Crystallogr.* 17 (1973), 1089.
10. L. D. Calvert, E. J. Gabe, and Y. Le Page, Ruby Spheres for Aligning Single-Crystal Diffractometers, *Acta Crystallogr.* A37 (1981), C314.
11. R. J. Collins, D. F. Nelson, A. L. Schalow, W. Bond, C.G.B. Garret, and W. Kaiser, Coherence, Narrowing, Directionality, and Relaxation Oscillations in the Light Emission From Ruby, *Phys. Rev. Lett.* 5 (1960), 303.
12. D. E. Cox, A. R. Moodenbaugh, A. W. Sleight, and H.-Y. Chen, Structural Refinement of Neutron and X-ray Data by the Rietveld Method: Application to Al_2O_3 and BiVO_4 , *National Bureau Standards (U.S.) Spec. Publ.* No. 567 (1980), 189.

13. J. M. Eggleston, L. G. DeShazer, and K. W. Kangas, Characteristics and Kinetics of Laser Pumped Ti:Sapphire Oscillators, *IEEE J. Quantum Electron.* QE-24 (1988), 1009.
14. W. M. Fairbank, G. K. Klauminzer, and A. L. Schalow, Excited-State Absorption in Ruby, Emerald, and MgO:Cr^{3+} , *Phys. Rev.* B11 (1975), 60.
15. S. Geschwind, P. Kisleuk, M. P. Klein, J. P. Remeika, and D. L. Wood, Sharp-Line Fluorescence, Electron Paramagnetic Resonance and Thermoluminescence of Mn^{4+} in $\text{Mn}^{4+}\text{Al}_2\text{O}_3$, *Phys. Rev.* 126 (1962), 1684.
16. S. Geschwind and J. P. Remeika, Spin Resonance of Transition Metal Ions in Corundum, *J. Appl. Phys. Suppl.* 1 33 (1962), 370.
17. U. Hochli and K. A. Muller, Observations of the John-Teller Splitting of Three-Valent d^7 Ions Via Orbach Relaxation, *Phys. Rev. Lett.* 12 (1964), 730.
18. N. S. Hush and J. M. Hobbs, Absorption Spectra of Crystals Containing Transition Metal Ions, *Prog. Inorgan. Chem.* 10 (1968), 259-186.
19. R. R. Joyce and P. L. Richards, Far-Infrared Spectra of Al_2O_3 Doped with Ti, V, and Cr, *Phys. Rev.* 179 (1969), 375.
20. T. Kushida, Absorption Spectrum of Optically Pumped Ruby: I.--Experimental Studies of Spectrum of Excited States, *J. Phys. Soc. Jpn.* 21 (1966), 1331.
21. R. Lacroix, U. Hochli, and K. A. Muller, Strong Field G-Value Calculation for d^7 Ions in Octahedral Surroundings, *Helv. Phys. Acta* 37 (1964), 627.
22. A. Linz, Jr., and R. E. Newnham, Ultraviolet Absorption Spectra in Ruby, *Phys. Rev.* 123 (1961), 500.
23. R. Louat and E. Duval, Temperature Dependence of the $^1\text{A}_1 \rightarrow ^1\text{E} (^1\text{T}_1)$ Zero Phonon Transition of Co^{3+} in $\alpha\text{-Al}_2\text{O}_3$, *Phys. Status Solidi* 42 (1970), K93.
24. R. M. Macfarlane, On the Ground-State Splitting in Ruby, *J. Chem. Phys.* 42 (1965), 442.
25. R. M. Macfarlane, Optical and Magnetic Properties of Trivalent Vanadium Complexes, *J. Chem. Phys.* 40 (1964), 373.
26. R. M. Macfarlane, Analysis of the Spectrum of d^3 Ions in Trigonal Crystal Fields, *J. Chem. Phys.* 39 (1963), 3118.
27. R. M. Macfarlane, J. Y. Wong, and M. D. Sturge, Dynamic John-Teller Effect in Octahedrally Coordinated d^1 Impurity Systems, *Phys. Rev.* 166 (1968), 250.

Al₂O₃

28. T. H. Maiman, Stimulated Optical Radiation in Ruby, *Nature* 187 (1960), 493.
29. T. H. Maiman, Optical Maser Action in Ruby, *Br. Commun. Electron.* 7 (1960), 674.
30. F. J. McClung, S. E. Schwarz, and F. J. Meyers, R₂ Line Optical Maser Action in Ruby, *J. Appl. Phys.* 33 (1962), 3139.
31. D. S. McClure, Optical Spectra of Transition-Metal Ions in Corundum, *J. Chem. Phys.* 36 (1962), 2757.
32. R. Moncorge, G. Boulon, D. Vivien, A. M. Lejus, R. Collongues, V. Djevahirdjian, K. Djevahirdjian, and R. Cagnard, Optical Properties and Tunable Laser Action of Verneuil-Grown Single Crystals of Al₂O₃:Ti³⁺, *IEEE J. Quantum Electron.* QE-24 (1988), 1049.
33. K. Moorjani and N. McAvoy, Optical Spectra of Trivalent Iron in Trigonal Fields, *Phys. Rev.* 132 (1963), 504.
34. P. F. Moulton, Tunable Solid-State Lasers Targeted for a Variety of Applications, *Laser Focus* 23 (1987), 56.
35. E. D. Nelson, J. Y. Wong, and A. L. Schalow, Far Infrared Spectra of Al₂O₃:Cr³⁺ and Al₂O₃:Ti³⁺, *Phys. Rev.* 56 (1967), 298.
36. E. D. Nelson, J. Y. Wong, and A. L. Schalow, Far Infrared Spectra of Al₂O₃:Cr³⁺ and Al₂O₃:Ti³⁺, in *Optical Properties of Ions in Crystals*, Ed. H. M. Crosswhite and H. W. Moos, Interscience, New York (1967), p 375.
37. R. E. Newnham and Y. M. de Haan, Refinement of the α Al₂O₃, Ti₂O₃, V₂O₃, and Cr₂O₃ Structures, *Z. Kristallogr. Krystallgeom. Krystallphys. Kristallchem.* 117 (1962), 235.
38. A. Pinto, Doubled Titanium Sapphire as Tunable Visible Laser, *Laser Focus* 23 (1987), 58.
39. M.H.L. Pryce and W. A. Runciman, The Absorption Spectrum of Vanadium in Corundum, *Discuss. Faraday Soc.* 26 (1958), 34.
40. S. Sakatsume and I. Tsujikawa, Sharp Absorption Lines of V³⁺-Al₂O₃ in the Near Infrared Region, *J. Phys. Soc. Jpn.* 19 (1964), 1080.
41. A. Sanchez, A. J. Strauss, R. L. Aggarwal, and R. E. Fahey, Crystal Growth, Spectroscopy, and Laser Characteristics of Ti:Al₂O₃, *IEEE J. Quantum Electron.* QE-24 (1988), 995.
42. A. L. Schalow and G. E. Devlin, Simultaneous Optical Maser Action in Two Satellite Lines, *Phys. Rev. Lett.* 6 (1961), 96.

43. P. A. Schulz, Single-Frequency Ti: Al_2O_3 Ring Laser, IEEE J. Quantum Electron. QE-24 (1988), 1039.
44. R. R. Sharma and T. P. Das, Crystalline Fields in Corundum-Type Lattices, J. Chem. Phys. 41 (1964), 3581.
45. M. D. Sturge, F. R. Merritt, L. F. Johnson, H. J. Guggenheim, and J. P. van der Ziel, Optical and Microwave Studies of Divalent Vanadium in Octahedral Fluoride Coordination, J. Chem. Phys. 54 (1971), 405.
46. S. Sugaus and M. Peter, Effect of Configuration Mixing and Covalency on the Energy Spectrum of Ruby, Phys. Rev. 122 (1961), 381.
47. S. Sugaus and M. Shinada, Theoretical Analysis of Absorption Spectrum of Optically Pumped Ruby, in Optical Properties of Ions in Crystals, Ed. H. M. Crosswhite and H. W. Moos, Interscience, New York (1967), p 187.
48. S. Sugano and Y. Tanabe, The Line Spectra of Cr^{3+} Ion in Crystals, Discuss. Faraday Soc. 26 (1958), 43.
49. D. T. Sviridov, R. K. Sviridova, N. I. Kulik, and V. B. Glasko, Optical Spectra of the Isoelectronic Ions V^{2+} , Cr^{2+} , and Mn^{4+} in an Octahedral Coordination, J. Appl. Spectrosc. 30 (1979), 334.
50. T. Tatsukawa, M. Inove, and H. Yagi, Five Structure Constant at V-Band Region of Cr^{3+} in Ruby Crystal, J. Phys. Soc. Jpn. 36 (1974), 908.
51. P. Thompson, D. E. Cox, and J. B. Hastings, Rietveld Refinement of Debye-Scherrer Synchrotron X-Ray Data from Al_2O_3 , J. Appl. Crystallogr. 20 (1987), 79.
52. K. F. Wall, R. L. Aggarwal, R. E. Fahey, and A. J. Strauss, Small-Signal Gain Measurements in a Ti: Al_2O_3 Amplifier, IEEE J. Quantum Electron. QE-24 (1988), 1016.
53. A. Wasiela, D. Block, and Y. M. D'Aubigne, Chromium-Gallium Complexes in Al_2O_3 : II.--Energy Transfer, J. Lumin. 36 (1986), 23.
54. A. Wasiela, Y. M. D'Aubigne, and D. Block, Chromium-Gallium Complexes in Al_2O_3 : I.--Luminescence, J. Lumin. 36 (1986), 11.
55. J. Y. Wong, M. J. Berggren, and A. L. Schalow, Far-Infrared Spectrum of $\text{Al}_2\text{O}_3:\text{V}^{4+}$, J. Chem. Phys. 49 (1968), 835.
56. E. J. Woodbury and W. K. Ng, Ruby Laser Operation in the Near I.R., Proc. I.R.E. 50 (1962), 2367.
57. Y. Y. Yeung and D. J. Newman, Superposition-Model Analysis for the Cr^{3+} , Al_2 Ground State, Phys. Rev. 51 (1969), 4123.

25. **MgAl₂O₄**

25.1 Crystallographic Data on MgAl₂O₄

Cubic O_h⁷ (Fd3m), 227, Z = 8

Ion	Site	Symmetry	x ^a	y	z	q	α (Å ³) ^b
Mg	8(a)	T _d	0	0	0	2	0.0809
Al	16(d)	D _{3d}	5/8	5/8	5/8	3	0.053
O	32(e)	C _{3v}	x	x	x	-2	1.349

^aX-ray data: a = 8.080 Å, x = 0.389 (reference 10).

^bReference 6.

25.2 Crystal-Field Components, A_{nm} (cm⁻¹/Åⁿ)

25.2.1 For Al (D_{3d}) site (rotated so that z-axis is parallel to (111) crystallographic axis)

A _{nm}	Point charge	Self-induced	Dipole	Total
A ₂₀	-2,283	-2008	23,088	18,797
A ₄₀	-20,238	8618	-4,838	-16,458
A ₄₃	23,688	-8781	2,390	17,297

25.2.2 For Mg (T_d) site

A _{nm}	Point-charge	Self-induced	Dipole	Total
A ₃₂	30,202	-8210	-9151	12,840
A ₄₀	-13,597	5447	5350	-2,800
A ₄₄	8,126	-3255	-3197	1,673

25.3 Experimental Parameters (cm⁻¹) for Transition-Metal Ions

Ion	nd ^N	Site	F ⁽²⁾	F ⁽⁴⁾	α	ζ	B ₂₀	B ₄₀	B _{4m} ^a	Ref.
Cr ³⁺	3d ³	Al	56,700	40,320	--	250	4608	-30,625	28,415	9
Cr ³⁺	3d ³	Al	56,700	40,320	--	--	0	-25,550	30,538	9
Fe ²⁺	3d ⁶	Mg	--	--	--	-392	0	-9,387	--	7
Co ²⁺	3d ⁷	Mg	--	--	--	--	0	-8,400	--	1

^aFor Al site B_{4m} = B₄₃, and for Mg site B_{4m} = B₄₄ (B₄₄ = $\sqrt{5/14}$ |B₄₀|).

25.4 Bibliography and References

1. R. D. Gillen and R. E. Solomon, Optical Spectra of Chromium (III), Cobalt (II), and Nickel (II) Ions in Mixed Spinels, *J. Phys. Chem.* 74 (1970), 4252.
2. W. Mikenda, N-Lines in the Luminescence Spectra of Cr^{3+} -Doped Spinels (III) Partial Spectra, *J. Lumin.* 26 (1981), 85-98.
3. W. Mikenda and A. Preisinger, N-Lines in the Luminescence Spectra of Cr^{3+} -Doped Spinels: I.--Identification of N-Lines, *J. Lumin.* 26 (1981), 53-66.
4. W. Mikenda and A. Preisinger, N-Lines in the Luminescence Spectra of Cr^{3+} -Doped Spinels: II.--Origins of N-Lines, *J. Lumin.* 26 (1981), 67-83.
5. R. Pappalardo, D. L. Wood, and R. C. Linares, Jr., Optical Absorption Spectra of Ni-Doped Oxide Systems: I, *J. Chem. Phys.* 35 (1961), 1460.
6. P. C. Schmidt, A. Weiss, and T. P. Das, Effect of Crystal Fields and Self-Consistency on Dipole and Quadrupole Polarizabilities of Closed-Shell Ions, *Phys. Rev.* B19 (1979), 5525.
7. G. A. Slack, F. S. Ham, and R. M. Chrenko, Optical Absorption of Tetrahedral Fe^{2+} ($3d^6$) in Cubic ZnS, CdTe, and MgAl_2O_4 , *Phys. Rev.* 152 (1966), 376-402.
8. H. A. Weakliem, Optical Spectra of Ni^{2+} , Co^{2+} , and Cu^{2+} , *J. Chem. Phys.* 36 (1962), 2117.
9. D. L. Wood, G. F. Imbusch, R. M. McFarlane, P. Kisliuk, and D. M. Larkin, Optical Spectrum of Cr^{3+} Ions in Spinels, *J. Chem. Phys.* 48 (1968), 5255.
10. R.W.G. Wyckoff, Crystal Structures, vol. 3, Interscience, New York (1968), 75.

26. $A_3^{+2}B_2^{+3}Ge_3O_{12}$ (Germanium Garnet)

26.1 Crystallographic Data on $A_3B_2Ge_3O_{12}$

Cubic O_h^{10} (Ia3d), 230, Z = 8

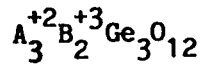
Ion	Site	Symmetry	x	y	z	q	α (\AA^3) ^a
A^{+2}	24(c)	D_2	0	1/4	1/8	2	α_A
B^{+3}	16(a)	C_{3i}	0	0	0	3	α_B
Ge	24(d)	S_4	0	1/4	3/8	4	0.12
O	96(h)	C_1	x	y	z	-2	1.349

^aValues for α are from reference 19, and for values not given there the α are from reference 3.

26.2 X-Ray Data on $A_3B_2Ge_3O_{12}$

A^{+2}	B^{+3}	a	x	y	z	Ref.	α_A ^a	α_B ^a
Ca	Al	12.118	-0.03345	0.0488	0.14753	22	0.564	0.0530
Ca	Ga	12.251	--	--	--	24	0.564	0.19
Ca	Cr	12.262	--	--	--	24	0.564	0.29
Ca	V	12.324	--	--	--	24	0.564	0.31
Ca	Fe	12.325	--	--	--	24	0.564	0.24
Ca	Sc	12.519	-0.0352	0.0524	0.1552	22	0.564	0.540
Ca	Lu	12.590	-0.03538	0.05607	0.15989	22	0.564	0.77
Ca	In	12.735	-0.0363	0.0543	0.15724	22	0.564	0.54
Sr	Sc	12.785	-0.03861	0.04909	0.15339	22	1.039	0.540
Cd	Sc	12.458	-0.03437	0.05300	0.15564	13	0.840	0.540
Cd	Al	12.08	--	--	--	24	0.840	0.0530
Cd	Cr	12.20	--	--	--	24	0.840	0.29
Cd	Fe	12.26	--	--	--	24	0.840	0.24
Cd	Ga	12.19	--	--	--	24	0.840	0.19
Mn	Al	11.902	--	--	--	24	0.460	0.0530
Mn	Cr	12.027	--	--	--	24	0.460	0.29
Mn	Fe	12.087	--	--	--	24	0.460	0.24
Mn	Ga	12.00	--	--	--	24	0.460	0.19

^aValues for α are from reference 19, and for values not given there the α are from reference 3.



26.3 Crystal-Field Components, A_{nm} ($\text{cm}^{-1}/\text{\AA}^n$)

Rotated so that z-axis is parallel to (111) crystallographic axis

26.3.1 For Al ion in 16(a) (C_{3i}) site in $Ca_3Al_2Ge_3O_{12}$

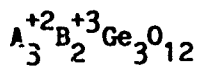
A_{nm}	Point charge	Self-induced	Dipole	Total
A_{20}	11,161	-451.6	-35,565	-24,855
A_{40}	-20,669	8255	9,602	-2,812
ReA_{43}	2,625	-1473	7,554	8,706
ImA_{43}	-22,662	9272	5,206	-8,184
$ A_{43} $	22,814	--	--	11,949

26.3.2 For Sc ion in 16(a) (C_{3i}) site in $Ca_3Sc_2Ge_3O_{12}$

A_{nm}	Point charge	Self-induced	Dipole	Total
A_{20}	9,208	-299.1	-28,304	-19,395
A_{40}	-13,449	4192	5,733	-3,523
ReA_{43}	1,227	-651.0	4,588	5,164
ImA_{43}	-14,541	4678	2,550	-7,313
$ A_{43} $	14,593	--	--	8,953

26.3.3 For Lu ion in 16(a) (C_{3i}) site in $Ca_3Lu_2Ge_3O_{12}$

A_{nm}	Point charge	Self-induced	Dipole	Total
A_{20}	10,201	-354.1	-26,892	-17,044
A_{40}	-11,205	3133	4,153	-3,920
ReA_{43}	525.3	-376.6	3,896	4,044
ImA_{43}	-11,743	3417	1,241	-7,085
$ A_{43} $	11,754	--	--	8,158



26.3.4 For In ion in 16(a) (C_{3i}) site in $Ca_3In_2Ge_3O_{12}$

A_{nm}	Point charge	Self-induced	Dipole	Total
A_{20}	8,212	-237.9	-25,117	-17,143
A_{40}	-11,352	3214	4,616	-3,523
ReA_{43}	612.7	-398.0	3,909	4,123
ImA_{43}	-12,272	3594	1,839	-6,838
$ A_{43} $	12,287	--	--	7,985

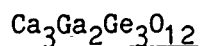
26.3.5 For Sc ion in 16(a) (C_{3i}) site in $Sr_3Sc_2Ge_3O_{12}$

A_{nm}	Point charge	Self-induced	Dipole	Total
A_{20}	2,456	79.17	-22,887	-20,343
A_{40}	-12,168	3,703	6,298	-2,167
ReA_{43}	1,424	-667.5	4,090	4,847
ImA_{43}	-14,278	4,414	3,785	-6,079
$ A_{43} $	14,349	--	--	7,775

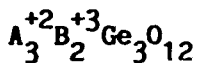
26.3.6 For Sc ion in 16(a) (C_{3i}) site in $Cd_3Sc_2Ge_3O_{12}$

A_{nm}	Point charge	Self-induced	Dipole	Total
A_{20}	10,782	-444.2	-29,570	-19,232
A_{40}	-13,735	4323	5,561	-3,851
ReA_{43}	1,236	-664.4	4,670	5,241
ImA_{43}	-14,599	4729	2,266	-7,605
$ A_{43} $	14,652	--	--	9,236

26.4 Experimental Values (cm^{-1}) of B_{40} , $F^{(2)}$, and $F^{(4)}$ for nd^N Ions in

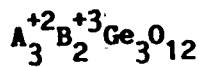


Ion	Site	nd^N	B_{40}	$F^{(2)}$	$F^{(4)}$	Ref.
Cr^{+3}	C_{3i}	$3d^3$	-21,200	66,121	31,102	14



26.5 Bibliography and References

1. K. P. Belov, D. G. Mamsurova, B. V. Mill, and V. I. Sokolov, Ferromagnetism of the Garnet $Mn_3Cr_2Ge_3O_{12}$, *Zh. Eksp. Teor. Fiz. Pis'ma Red.* 16 (1972), 120.
2. K. P. Belov, B. V. Mill, V. I. Sokolov, and O. I. Shevaleevskii, Antiferromagnetic Resonance in the Garnet $Ca_3Fe_2Ge_3O_{12}$, *JETP Lett.* 20 (1974), 42.
3. S. Fraga, J. Karwowski, and K.M.S. Saxena, Handbook of Atomic Data, vol. 5 (1976), 319.
4. S. Geller and C. E. Miller, New Synthetic Garnets, *Acta Crystallogr.* 13 (1960), 179.
5. R. Gieniusz and A. Maziewski, Low Power Light Deflector on Domain Structure in $(Y,Ca)_3(Fe,Ge)_5O_{12}$, *Opt. Commun.* 51 (1984), 167..
6. V. Havlicek, P. Novak, and B. V. Mill, Epr of V^{4+} Ion in Several Garnet Systems, *Phys. Status Solidi* B64 (1974), K19.
7. A. A. Kaminskii, B. V. Mill, and A. V. Butashin, New Possibilities for Exciting Stimulated Emission in Inorganic Crystalline Materials with the Garnet Structure, *Inorg. Mater. USSR* 19 (1983), 1808.
8. Z. A. Kazei, B. V. Mill, and V. I. Sokolov, Peculiarities of the Metamagnetic Transitions of a Garnet Single Crystal $Ca_3Mn_2Ge_3O_{12}$, *JETP Lett.* 31 (1980), 309.
9. Z. A. Kazei, B. V. Mill, and V. I. Sokolov, Cooperative Jahn-Teller Effect in the Garnet $Ca_3^{Mn}Ge_3O_{12}$, *JETP Lett.* 24 (1976), 203.
10. V. F. Kitaeva, E. V. Zharikov, and I. L. Chisty, The Properties of Crystals with Garnet Structure, *Phys. Status Solidi* A92 (1985), 475.
11. G. S. Krimchik, V. D. Gorbunova, V. S. Gushchin, and B. V. Mill, Absorption of Light in One-Sublattice Iron Garnets, *Sov. Phys. Solid State* 22 (1980), 156.
12. M. D. Lind and S. Geller, Crystal Structure of the Garnet $\{Mn_3\}[Fe_2](Ge_3)O_{12}$, *Z. Kristallogr. Kristallgeom. Kristallphys. Kristallchem.* 129 (1969), 427.
13. B. V. Mill, E. L. Belokoneva, M. A. Simonov, and N. V. Belov, Refined Crystal Structures of the Scandium Garnets, *Zh. Strukt. Khim.* 18 (1977), 399.
14. A. E. Nosenko, A. I. Bilyi, L. V. Kostyk, and V. V. Kravchishin, Emission Spectra of Cr^{3+} Ions in $Ca_3Ga_2Ge_3O_{12}$ Single Crystals, *Opt. Spectrosc.* 57 (1984), 510.



15. A. E. Nosenko, B. V. Padlyak, and V. V. Kravchishin, Electron Spin Resonance of Mn^{4+} Ions in $Ca_3Ga_2Ge_3O_{12}$ Single Crystals, Sov. Phys. Solid State 27 (1985), 2083.
16. P. Novak, V. Havlicek, B. V. Mill, V. I. Sokolov, and O. I. Shevaleevskii, EPR of Fe^{3+} Ions in Several Germanate Garnets and Magnetocrystalline Anisotropy of $Ca_3Fe_2Ge_3O_{12}$, Solid State Commun. 19 (1976), 631.
17. R. Pappalardo, D. L. Wood, and R. C. Linares, Jr., Optical Absorption Spectra of Ni-Doped Oxide Systems: I, J. Chem. Phys. 35 (1961), 1460.
18. R. Plumier and M. Sougi, Neutron Diffraction Study in Magnetic Field of Antiferromagnetic Garnet $Ca_3Mn_2Ge_3O_{12}$, J. Phys. Paris Lett. 40 (1979), L-213.
19. P. C. Schmidt, A. Weiss, and T. P. Das, Effect of Crystal Fields and Self-Consistency on Dipole and Quadrupole Polarizabilities of Closed-Shell Ions, Phys. Rev. B19 (1979), 5525.
20. V. I. Sokolov and O. I. Shevaleevskii, Antiferromagnetic Resonance in the Cubic Crystal FeGeG and CrGeG, Sov. Phys. JETP 45 (1977), 1245.
21. T. V. Valyanskaya, B. V. Mill, and V. I. Sokolov, Antiferromagnetic Ordering of Cr^{3+} in Octahedral Garnet Sublattice, Sov. Phys. Solid State 18 (1976), 696.
22. I. Veltrusky, Effects of Covalency on Magnetic Properties of Tetrahedral V^{4+} Ion in Garnets, Czech. J. Phys. B28 (1978), 675.
23. D. Wolf and S. Kemmler-Sack, Cathodo- and Photo-Luminescence in Rare Earth Activated Garnets of Type $Ca_3M_2Ge_{3-x}Si_xO_{12}$ (M = Al, Ga, Sc, Y), Phys. Status Solidi A98 (1986), 567.
24. R.W.G. Wyckoff, Crystal Structures, vol. 3, Interscience, New York (1968), 223.

27. ZnGa_2O_4 27.1 Crystallographic Data on ZnGa_2O_4 Cubic O_h^7 ($\text{Fd}3\bar{m}$), 227, $Z = 8$

Ion	Site	Symmetry	x ^a	y	z	q	α (\AA^3) ^b
Zn	8(a)	T_d	0	0	0	2	0.676
Ga	16(d)	D_{3d}	5/8	5/8	5/8	3	0.458
O	32(e)	C_{3v}	x	x	x	-2	1.349

^aX-ray data: $a = 8.330 \text{ \AA}$, $x = 0.38675$ (reference 5).^bReference 10.27.2 Crystal-Field Components, A_{nm} ($\text{cm}^{-1}/\text{\AA}^n$)27.2.1 For Zn (T_d) site

A_{nm}	Monopole	Dipole	Self-induced	Total
A_{32}	26,942	-7790	-6727	-12,425
A_{40}	-11,793	4419	4333	-3,040
A_{44}	7,047	-2641	-2590	1,817

27.2.2 For Ga (D_{3d}) site (rotated so that z-axis is parallel to (111) crystallographic axis)

A_{nm}	Monopole	Dipole	Self-induced	Total
A_{20}	-2,616	19,928	-1736	15,576
A_{40}	-17,273	-3,972	6713	-14,531
A_{43}	20,288	1,969	-6815	15,442

27.3 Bibliography and References

1. G.G.P. van Gorkom, J.C.M. Henning, and R. P. van Stepele, Optical Spectra at Cr^{3+} Pairs in the Spinel ZnGa_2O_4 , Phys. Rev. B8 (1973), 955.
2. J.C.M. Henning, Weak Exchange Interactions in Chromium-Doped ZnGaO_4 , Phys. Lett. 34A (1971), 215.
3. J.C.M. Henning, J. H. den Boef, and G.G.P. van Gorkom, Electron-Spin-Resonance Spectra of Nearest-Neighbor Cr^{3+} Pairs in the Spinel ZnGaO_4 , Phys. Rev. B7 (1973), 1825.

4. J.C.M. Henning and J.P.M. Damen, Exchange Interactions Within Nearest-Neighbor Cr³⁺ Pairs in Chromium-Doped Spinel ZnGaO₄, Phys. Rev. B3 (1971), 3852.
5. J. Hornstra and E. Keulen, The Oxygen Parameter of the Spinel ZnGa₂O₄, Philips Res. Rep. 27 (1972), 76.
6. O. Kahan and R. M. Macfarlane, Optical and Microwave Spectra of Cr³⁺ in the Spinel ZnGa₂O₄, J. Chem. Phys. 54 (1971), 5197.
7. W. Mikenda, N-Lines in the Luminescence Spectra of Cr³⁺-Doped Spinels: III.--Partial Spectra, J. Lumin. 26 (1981), 85-98.
8. W. Mikenda and A. Preisinger, N-Lines in the Luminescence Spectra of Cr³⁺-Doped Spinels: I.--Identification of N-Lines, J. Lumin. 26 (1981), 53-66.
9. W. Mikenda and A. Preisinger, N-Lines in the Luminescence Spectra of Cr³⁺-Doped Spinels: II.--Origins of N-Lines, J. Lumin. 26 (1981), 67-83.
10. P. C. Schmidt, A. Weiss, and T. P. Das, Effect of Crystal Fields and Self-Consistency on Dipole and Quadrupole Polarizabilities of Closed-Shell Ions, Phys. Rev. B19 (1979), 5525.

28. Cs_2GeF_6

28.1 Crystallographic Data on Cs_2GeF_6

Cubic O_h^5 (Fm3m), 225, $Z = 4$

Ion	Site	Symmetry	x ^a	y	z	q	α (\AA^3)
Ge	4(a)	O_h	0	0	0	4	0.120 ^b
Cs	8(c)	T_d	1/4	1/4	1/4	1	2.492 ^c
F	24(e)	C_{4v}	x	0	0	-1	0.731 ^c

^aX-ray data: $a = 9.021 \text{ \AA}$, $x = 0.20$ (reference 16).

^bReference 3.

^cReference 14.

28.2 Crystal-Field Components, A_{nm} ($\text{cm}^{-1}/\text{\AA}^n$)

28.2.1 For Ge (O_h) site

A_{nm}	Monopole	Self-induced	Dipole	Total
A_{40}	21,689	-10,895	25,645	36,439
A_{44}	12,962	-6,511.5	15,326	21,776

28.2.2 For Cs (T_d) site

A_{nm}	Monopole	Self-induced	Dipole	Total
A_{32}	1162.7	139.27	-2378.4	-1076.4
A_{40}	-181.65	43.06	-174.48	-313.07
A_{44}	108.56	-25.74	104.27	187.10

28.3 Experimental Parameters (cm^{-1})

Ion	nd ^N	$F^{(2)}$	$F^{(4)}$	ζ	B_{40}	Ref
Mn ⁴⁺	3d ³	52,794	50,929	380	45,885	1
Mn ⁴⁺	3d ³	58,489	48,460	363	45,780	17
Re ⁴⁺	5d ³	40,299	22,617	2953	73,143	8
Pt ⁴⁺	5d ⁶	35,133	28,400	3579	66,150	13
Os ⁴⁺	5d ⁴	51,408	37,409	2800	51,450	15
Ir ⁴⁺	5d ⁵	53,389	39,564	3500	51,450	15
Re ⁴⁺	5d ³	40,019	22,554	3094	69,384	9

Cs_2GeF_6

28.4 Index of Refraction

$$n = 1.3920 + 2.26v^2 \times 10^{-11} \quad (v \text{ in cm}^{-1}) \quad (\text{reference 7})$$

28.5 Bibliography and References

1. Ring-Ling Chien, J. M. Berg, and D. S. McClure, Two-Photon Electronic Spectroscopy of $\text{Cs}_2\text{GeF}_6:\text{Mn}^{4+}$, *J. Chem. Phys.* 84 (1986), 4168.
2. S. L. Chodos, A. M. Black, and C. D. Flint, Vibronic Spectra and Lattice Dynamics of Cs_2MnF_6 and $\text{A}_2^1\text{M}^{\text{IV}}\text{F}_6:\text{MnF}_6^2$, *J. Chem. Phys.* 65 (1976), 4816.
3. S. Fraga, K.M.S. Saxena, and J. Karwowski, *Handbook of Atomic Data*, Elsevier, New York (1976).
4. L. Helmholtz and M. E. Russo, Spectra of Manganese (IV) Hexafluoride Ion (MnF_6^-) in Environments of O_h and $\text{D}_{3\text{d}}$ Symmetry, *J. Chem. Phys.* 59 (1973), 5455.
5. L. Kolditz, W. Wilke, and W. Hilmer, Rotgenographische Phasenbestimmungen zur thermischen Dissoziation und das Hydrolyseverhalten von Alkalihexafluororgermanaten bei höheren Temperaturen, *Z. Anorg. Allg. Chem.* 512 (1984), 48.
6. M. P. Laurent, H. H. Patterson, W. Pike, and H. Engstrom, Pure and Mixed Crystal Optical Studies of the Jahn-Teller Effect for the d^6 Hexafluoroplatinate (IV) Ion, *Inorg. Chem.* 20 (1981), 372.
7. T. F. Levchishina and E. F. Yamshchikov, Optical Properties of Some Hexafluoro Compounds, *Inorg. Mater.* (1982), 570.
8. J. LoMenzo, H. Patterson, S. Strobridge, and H. Engstrom, Sharp Line Absorption, Luminescence, Raman Studies for the 5d^3 Hexafluororhenate (IV) Ion in Pure and Host Crystal Environments, *Mol. Phys.* 40 (1980), 1401.
9. J. A. LoMenzo, S. Strobridge, and H. Patterson, Electronic Absorption Spectra of the 5d^3 Hexafluororhenate (IV) Ion, *J. Mol. Phys.* 66 (1977), 150.
10. P. A. Lund, An Analysis of the Low Temperature Zeeman Spectra of $\text{K}_2\text{GeF}_6:\text{Mn}(\text{IV})$ and $\text{Cs}_2\text{GeF}_6:\text{Mn}(\text{IV})$, Ph.D. thesis, Washington University (1977), Univ. Microfilm 77-32, 552.

11. N. B. Manson, Z. Hasan, and C. D. Flint, Jahn-Teller Effect in the ${}^4T_{2g}$ State of Mn^{4+} in Cs_2SiF_6 , J. Phys. C12 (1979), 5483.
12. J. Mrozack, An Analysis of the EPR Spectra of Technetium (IV) Doped Potassium Germanium Hexafluoride and Cesium Germanium Hexafluoride, Ph.D. thesis, Washington University (1976), Univ. Microfilm 7904198.
13. H. Patterson, W. J. DeBerry, J. E. Byrne, M. T. Hsu, and J. A. LoMenzo, Low-Temperature Luminescence and Absorption Spectra of the d^6 Hexafluoroplatinate (IV) Ions Doped in a Cs_2GeF_6 -Type Host Lattice, Inorg. Chem. 16 (1977), 1698.
14. P. C. Schmidt, A. Weiss, and T. P. Das, Effect of Crystal Fields and Self-Consistency on Dipole and Quadrupole Polarizabilities of Closed-Shell Ions, Phys. Rev. B19 (1979), 5525.
15. L. C. Weiss, P. J. McCarthy, J. P. Jasinski, and P. N. Schatz, Absorption and Magnetic Circular Dichroism Spectra of Hexafluoroosmate (IV) and Hexafluoroiridate (IV) in the Cubic Host Cs_2GeF_6 , Inorg. Chem. 17 (1978), 2689.
16. R.W.G. Wyckoff, Crystal Structures, vol. 3, Interscience, New York, (1968), 339.
17. W. C. Yeakel, R. W. Schwartz, H. G. Brittain, J. L. Slater, and P. N. Schatz, Magnetic Circularly Polarized Emission and Magnetic Circular Dichroism of Resolved Vibronic Lines in $\text{Cs}_2\text{GeF}_6:\text{Mn}^{4+}$, Mol. Phys. 32 (1976), 1751.

29. $R_2Ti_2O_7$ ($R \neq Y$)

29.1 Crystallographic Data on $R_2Ti_2O_7$

Cubic O_h^7 ($Fd\bar{3}m$), 227 (second setting), $Z = 8$

Ion	Site	Symmetry	x	y	z	q	α (\AA^3) ^a
R	16(c)	D_{3d}	0	0	0	3	α_R
Ti	16(d)	D_{3d}	1/2	1/2	1/2	4	0.22
O ₁	8(a)	T_d	1/8	1/8	1/8	-2	1.349
O ₂	48(f)	C_{2v}	x	1/8	1/8	-2	1.349
X	8(b)	T_d	3/8	3/8	3/8	--	--

^aReference 5.

29.2 X-Ray Data on $R_2Ti_2O_7$ (reference 4) and Polarizabilities, α_R , of Rare Earth Ions, R^{3+} ($4f^N$) (reference 3)

N	R	a (\AA)	x	α_R (\AA^3)
5	Sm	10.2303	0.4230	1.11
6	Eu	10.1988	--	1.06
7	Gd	10.1857	0.4263	1.01
8	Tb	10.1560	--	0.97
9	Dy	10.1245	--	0.94
10	Ho	10.0979	--	0.90
11	Er	10.0759	0.4194	0.86
12	Tm	10.0533	--	0.83
13	Yb	10.0309	0.4201	0.80
14	Lu	10.0258	--	0.77

29.3 Crystal-Field Components, A_{nm}

Crystal-field components were obtained for $R = Sm, Gd, Er$, and Yb . A least-squares polynomial fit was used to obtain the components for the entire range of R . In 29.3.1 to 29.3.12, the crystal is rotated so that the z-axis is parallel to the (111) crystallographic axis.

29.3.1 A_{20} ($\text{cm}^{-1}/\text{\AA}^2$) for R site 16c (D_{3d})

R	Monopole	Self-induced	Dipole	Total
Sm	8047.5	-1157.9	396.60	8759.2
Eu	8118.3	-1168.8	392.06	6298.6
Gd	8180.3	-1175.9	387.70	4446.7
Tb	8233.2	-1179.3	383.53	3203.4
Dy	8277.3	-1178.8	379.54	2568.9
Ho	8312.5	-1174.6	375.73	2543.1
Er	8338.7	-1166.6	372.10	3125.9
Tm	8356.0	-1154.8	368.66	4317.5
Yb	8364.4	-1139.2	365.41	6117.8
Lu	8363.8	-1119.8	362.33	8526.7

29.3.2 A_{40} ($\text{cm}^{-1}/\text{\AA}^4$) for R site 16c (D_{3d})

R	Monopole	Self-induced	Dipole	Total
Sm	8,295.2	-2797.7	22.651	8132.0
Eu	9,564.4	-2854.0	27.268	8213.1
Gd	10,594	-2913.0	34.538	8296.4
Tb	11,384	-2974.6	44.460	8382.0
Dy	11,934	-3038.7	57.034	8469.8
Ho	12,245	-3105.5	72.261	8559.8
Er	12,316	-3174.9	90.141	8652.1
Tm	12,148	-3246.8	110.67	8746.6
Yb	11,740	-3321.4	133.86	8843.4
Lu	11,092	-3398.6	159.09	8942.3

29.3.3 A_{43} ($\text{cm}^{-1}/\text{\AA}^4$) for R site 16c (D_{3d})

R	Monopole	Self-induced	Dipole	Total
Sm	2378.8	-569.66	-1038.3	770.73
Eu	2405.2	-580.49	-1055.5	769.11
Gd	2454.3	-596.22	-1087.6	770.41
Tb	2526.1	-616.84	-1134.6	774.63
Dy	2620.5	-642.35	-1196.4	781.76
Ho	2737.6	-672.75	-1273.1	791.80
Er	2877.4	-708.05	-1364.6	804.76
Tm	3039.9	-748.24	-1471.0	820.64
Yb	3225.0	-793.33	-1592.2	839.44
Lu	3432.8	-843.31	-1728.3	861.15

$R_2Ti_2O_7$ 29.3.4 A_{60} ($\text{cm}^{-1}/\text{\AA}^6$) for R site 16c (D_{3d})

R	Monopole	Self-induced	Dipole	Total
Sm	1750.0	-840.62	-56.417	852.93
Eu	1781.8	-862.76	-59.013	860.01
Gd	1815.3	-885.71	-63.115	866.49
Tb	1850.6	-909.45	-68.724	872.38
Dy	1887.5	-934.00	-75.838	877.66
Ho	1926.2	-959.36	-84.457	882.35
Er	1966.6	-985.51	-94.583	886.45
Tm	2008.7	-1012.5	-106.21	889.94
Yb	2052.5	-1040.2	-119.35	892.84
Lu	2098.0	-1068.8	-134.00	895.14

29.3.5 A_{63} ($\text{cm}^{-1}/\text{\AA}^6$) for R site 16c (D_{3d})

R	Monopole	Self-induced	Dipole	Total
Sm	-698.03	198.07	182.45	-317.52
Eu	-709.98	203.77	186.39	-319.83
Gd	-726.15	211.36	193.04	-321.76
Tb	-746.55	220.85	202.40	-323.31
Dy	-771.17	232.23	214.47	-324.48
Ho	-800.02	245.51	229.25	-325.28
Er	-833.10	260.69	246.73	-325.70
Tm	-870.40	277.76	266.93	-325.74
Yb	-911.93	296.73	289.83	-325.40
Lu	-957.69	317.59	315.44	-324.69

29.3.6 A_{66} ($\text{cm}^{-1}/\text{\AA}^6$) for R site 16c (D_{3d})

R	Monopole	Self-induced	Dipole	Total
Sm	1014.0	-306.71	-147.86	477.36
Eu	1031.3	-314.60	-150.90	641.04
Gd	1052.3	-324.46	-155.96	735.96
Tb	1076.8	-336.29	-163.05	762.13
Dy	1105.0	-350.09	-172.16	719.55
Ho	1136.8	-365.87	-183.31	608.21
Er	1172.3	-383.62	-196.48	428.11
Tm	1211.3	-403.35	-211.68	179.25
Yb	1254.0	-425.05	-228.91	-138.35
Lu	1300.3	-448.72	-248.16	-524.72

29.3.7 A_{20} ($\text{cm}^{-1}/\text{\AA}^2$) for Ti site 16d (D_{3d})

R	Monopole	Self-induced	Dipole	Total
Sm	-13,382	1444.3	12,981	1043.4
Eu	-13,282	1441.8	13,035	1195.7
Gd	-13,476	1461.6	13,172	1158.1
Tb	-13,965	1503.7	13,391	930.45
Dy	-14,748	1568.2	13,692	512.83
Ho	-15,826	1655.0	14,076	-94.792
Er	-17,199	1764.2	14,542	-892.41
Tm	-18,866	1895.7	15,090	-1880.0
Yb	-20,828	2049.5	15,720	-3057.6
Lu	-23,084	2225.7	16,432	-4425.2

29.3.8 A_{40} ($\text{cm}^{-1}/\text{\AA}^4$) for Ti site 16d (D_{3d})

R	Monopole	Self-induced	Dipole	Total
Sm	-15,449	5539.2	-4263.2	-14,173
Eu	-15,682	5671.4	-4302.6	-14,313
Gd	-15,823	5761.3	-4388.2	-14,450
Tb	-15,872	5809.0	-4520.0	-14,584
Dy	-15,830	5814.5	-4698.0	-14,714
Ho	-15,696	5777.7	-4922.3	-14,841
Er	-15,471	5698.6	-5192.8	-14,965
Tm	-15,153	5577.4	-5509.5	-15,086
Yb	-14,744	5413.8	-5872.4	-15,203
Lu	-14,244	5208.1	-6281.5	-15,317

29.3.9 A_{43} ($\text{cm}^{-1}/\text{\AA}^4$) for Ti site 16d (D_{3d})

R	Monopole	Self-induced	Dipole	Total
Sm	21,584	-8272.2	2158.6	15,464
Eu	21,851	-8445.4	2185.6	15,596
Gd	22,079	-8593.4	2245.2	15,743
Tb	22,268	-8716.2	2337.2	15,906
Dy	22,417	-8814.0	2461.7	16,084
Ho	22,527	-8886.5	2618.7	16,279
Er	22,597	-8933.9	2808.2	16,489
Tm	22,628	-8956.1	3030.2	16,715
Yb	22,619	-8953.1	3284.7	16,956
Lu	22,571	-8925.0	3571.7	17,213

R₂Ti₂O₇

29.3.10 A₆₀ (cm⁻¹/Å⁶) for Ti site 16d (D_{3d})

R	Monopole	Self-induced	Dipole	Total
Sm	3912.5	-2792.4	29.807	1149.9
Eu	3968.2	-2853.9	32.760	1147.0
Gd	4026.5	-2914.2	47.133	1159.4
Tb	4087.6	-2973.5	72.926	1187.0
Dy	4151.3	-3031.6	110.14	1229.8
Ho	4217.7	-3088.5	158.77	1287.9
Er	4286.8	-3144.3	218.82	1361.2
Tm	4358.6	-3199.0	290.30	1449.8
Yb	4433.0	-3252.5	373.19	1553.6
Lu	4510.2	-3304.9	467.50	1672.6

29.3.11 A₆₃ (cm⁻¹/Å⁶) for Ti site 16d (D_{3d})

R	Monopole	Self-induced	Dipole	Total
Sm	-150.68	-9.2581	1199.2	1039.2
Eu	-132.98	-26.031	1213.1	1054.1
Gd	-143.99	-20.254	1231.8	1067.6
Tb	-183.69	8.0703	1255.3	1079.7
Dy	-252.09	58.943	1283.6	1090.4
Ho	-349.20	132.36	1316.7	1099.9
Er	-475.00	228.33	1354.6	1107.9
Tm	-629.51	346.85	1397.3	1114.6
Yb	-812.72	487.92	1444.8	1120.0
Lu	-1024.6	651.53	1497.1	1124.0

29.3.12 A₆₆ (cm⁻¹/Å⁶) for Ti site 16d (D_{3d})

R	Monopole	Self-induced	Dipole	Total
Sm	2346.3	-1665.6	-70.846	609.77
Eu	2384.7	-1706.3	-70.685	607.71
Gd	2425.9	-1747.3	-69.591	609.02
Tb	2469.9	-1788.6	-67.564	613.71
Dy	2516.7	-1830.2	-64.606	621.78
Ho	2566.2	-1874.2	-60.714	633.22
Er	2618.5	-1914.6	-55.890	648.03
Tm	2673.6	-1957.2	-50.134	666.22
Yb	2731.5	-2000.2	-43.445	687.79
Lu	2792.2	-2043.5	-35.824	712.73

29.3.13 A_{32} ($\text{cm}^{-1}/\text{Å}^3$) for vacancy site, X, 8b (T_d)

R	Monopole	Self-induced	Dipole	Total
Sm	-36,871	-538.71	606.15	-36,804
Eu	-37,235	-549.82	612.32	-37,174
Gd	-37,617	-560.68	625.71	-37,553
Tb	-38,017	-571.30	646.31	-37,944
Dy	-38,435	-581.67	674.14	-38,344
Ho	-38,871	-591.80	709.18	-38,756
Er	-39,325	-601.69	751.44	-39,177
Tm	-39,798	-611.33	800.91	-39,610
Yb	-40,288	-620.73	857.61	-40,053
Lu	-40,796	-629.89	921.52	-40,506

29.3.14 A_{40} ($\text{cm}^{-1}/\text{Å}^4$) for vacancy site, X, 8b (T_d)

R	Monopole	Self-induced	Dipole	Total
Sm	34,671	-6813.8	4,549.7	33,401
Eu	35,195	-7002.9	3,407.7	33,797
Gd	35,598	-7125.0	2,704.2	34,162
Tb	35,877	-7180.0	2,439.2	34,496
Dy	36,035	-7168.0	26,12.6	34,798
Ho	36,071	-7089.0	3,224.5	35,069
Er	35,984	-6943.0	4,274.9	35,308
Tm	35,775	-6729.9	5,763.8	35,517
Yb	35,444	-6449.9	7,691.1	35,694
Lu	34,991	-6102.8	10,057	35,839

29.3.15 A_{44} ($\text{cm}^{-1}/\text{Å}^4$) for vacancy site, X, 8b (T_d)

R	Monopole	Self-induced	Dipole	Total
Sm	20,719	-4071.9	3313.3	19,961
Eu	21,033	-4185.0	3349.0	20,198
Gd	21,274	-4257.9	3399.0	20,415
Tb	21,441	-4290.8	3463.5	20,614
Dy	21,536	-4283.7	3542.4	20,795
Ho	21,557	-4236.4	3635.6	20,957
Er	21,505	-4149.2	3743.2	21,100
Tm	21,380	-4021.9	3865.2	21,224.0
Yb	21,181	-3854.5	4001.6	21,330
Lu	20,910	-3647.0	4152.4	21,418

$R_2Ti_2O_7$ 29.3.16 A_{60} ($\text{cm}^{-1}/\text{Å}^6$) for vacancy site, X, 8b (T_d)

R	Monopole	Self-induced	Dipole	Total
Sm	-494.90	-807.28	405.60	896.57
Eu	-496.57	-834.96	412.24	-919.25
Gd	-508.14	-853.75	419.91	-941.93
Tb	-529.63	-863.66	428.60	-964.63
Dy	-561.02	-864.68	438.31	-987.33
Ho	-602.32	-856.83	499.05	-1010.0
Er	-653.53	-840.09	460.81	-1032.8
Tm	-714.64	-814.48	473.59	-1055.5
Yb	-785.67	-779.98	487.39	-1078.2
Lu	-866.60	-736.60	502.22	-1101.0

29.3.17 A_{64} ($\text{cm}^{-1}/\text{Å}^6$) for vacancy site, X, 8b (T_d)

R	Monopole	Self-induced	Dipole	Total
Sm	925.92	1510.2	-758.83	1677.3
Eu	929.02	1562.0	-771.26	1719.7
Gd	950.66	1597.2	-785.60	1762.2
Tb	990.84	1615.8	-801.86	1804.7
Dy	1049.6	1617.7	-820.03	1847.2
Ho	1126.8	1603.0	-840.12	1889.6
Er	1222.6	1571.7	-862.11	1932.1
Tm	1336.9	1523.7	-886.03	1974.6
Yb	1469.8	1459.1	-911.85	2017.1
Lu	1621.2	1377.9	-939.56	2059.6

29.3.18 A_{72} ($\text{cm}^{-1}/\text{Å}^7$) for vacancy site, X, 8b (T_d)

R	Monopole	Self-induced	Dipole	Total
Sm	1034.2	57.289	-0.264	1091.2
Eu	1055.0	58.860	-0.263	1113.6
Gd	1076.4	60.479	-0.258	1136.5
Tb	1098.2	62.148	-0.249	1160.0
Dy	1120.5	63.867	-0.237	1184.0
Ho	1143.2	65.635	-0.220	1208.6
Er	1166.5	67.452	-0.199	1233.7
Tm	1190.3	69.319	-0.174	1259.4
Yb	1214.6	71.236	-0.145	1285.6
Lu	1239.3	73.201	-0.112	1312.4

29.3.19 A_{76} ($\text{cm}^{-1}/\text{A}^7$) for vacancy site, X, 8b (T_d)

R	Monopole	Self-induced	Dipole	Total
Sm	951.31	52.697	-0.243	1003.8
Eu	970.47	54.142	-0.242	1024.4
Gd	990.07	55.632	-0.238	1045.5
Tb	1010.1	57.167	-0.230	1067.1
Dy	1030.6	58.748	-0.218	1089.2
Ho	1051.6	60.374	-0.202	1111.8
Er	1073.0	62.046	-0.183	1134.9
Tm	1094.9	63.763	-0.160	1158.5
Yb	1117.2	65.526	-0.133	1182.6
Lu	1139.9	67.334	-0.102	1207.2

29.4 Experimental Parameters (cm^{-1}) (reference 1)

nd ^N	Ion	F ⁽²⁾	F ⁽⁴⁾	B ^a ₄₀
3d ²	V ³⁺	63,903	41,378	-24,500
3d ³	Cr ³⁺	65,450	42,840	-26,222
3d ³	Mn ⁴⁺	--	--	-31,920
3d ⁴	Mn ³⁺	--	--	-28,406
3d ⁶	Co ³⁺	58,100	34,902	-24,360
3d ⁷	Co ²⁺	66,220	43,344	-8,442
3d ⁷	Ni ³⁺	--	--	--
3d ⁸	Ni ²⁺	84,420	61,110	-12,278

$$^a B_{43} = \sqrt{10/7} |B_{40}|$$

29.5 Bibliography and References

1. V. A. Antonov and P. A. Arsenev, Spectroscopic Properties of Single Crystals of Rare Earth Titanates, Phys. Status Solidi A35 (1976), K169.
2. P.A.M. Berdowski and G. Blasse, Luminescence and Energy Transfer in a Highly Symmetrical System: $Eu_2Ti_2O_7$, J. Solid State Chem. 62 (1986), 317.
3. S. Fraga, K.M.S. Saxena, and J. Karwowski, Handbook of Atomic Data, Elsevier, New York (1976).
4. O. Knop, F. Brisse, and L. Castelliz, Pyrochlores: V.--Thermoanalytic, X-ray, Neutron, Infrared, and Dielectric Studies of $A_2Ti_2O_7$, Can. J. Chem. 47 (1969), 971.

$R_2Ti_2O_7$

5. P. C. Schmidt, A. Weiss, and T. P. Das, Effect of Crystal Fields and Self-Consistency on Dipole and Quadrupole Polarizabilities of Closed-Shell Ions, *Phys. Rev. B19* (1979), 5525.
6. N. A. Zakhoror, V. S. Krikorov, E. F. Kustov, and S. Yu. Stefanovich, New Non-linear Crystals in the $A_2B_2O_7$ Series, *Phys. Status Solidi A50* (1978), K 13. (R = La, Ce, Pr, Nd, Sm, Gd, Y in $R_2Ti_2O_7$ nonlinear properties given.)

30. $Y_2Ti_2O_7$

30.1 Crystallographic Data on $Y_2Ti_2O_7$ for Two Choices of Ion Sites

30.1.1 Cubic O_h^7 (Fd3m), 227 (second setting), $Z = 8$ (see reference 4)

Ion	Site	Symmetry	x ^a	y	z	q	α (\AA^3) ^b
Y	16(c)	D _{3d}	0	0	0	3	0.870
Ti	16(d)	D _{3d}	1/2	1/2	1/2	4	0.22 ^c
O ₁	8(a)	T _d	1/8	1/8	1/8	-2	1.349
O ₂	48(f)	C _{2v}	0.4201	1/8	1/8	-2	1.349
X	8(b)	T _d	3/8	3/8	3/8	0	0

^aX-ray data: $a = 10.095 \text{ \AA}$ (reference 4).

^bReference 6.

^cReference 3.

30.1.2 Cubic O_h^7 (Fd3m), 227 (second setting), $Z = 8$ (see reference 2)

Ion	Site	Symmetry	x ^a	y	z	q	α (\AA^3) ^b
Y	16(d)	D _{3d}	1/2	1/2	1/2	3	0.870
Ti	16(c)	D _{3d}	0	0	0	4	0.22 ^c
O ₁	8(b)	T _d	3/8	3/8	3/8	-2	1.349
O ₂	48(f)	C _{2v}	-0.0788	1/8	1/8	-2	1.349
X	8(a)	T _d	1/8	1/8	1/8	0	0

^aX-ray data: $a = 10.0896 \text{ \AA}$ (reference 2).

^bReference 6.

^cReference 3.

30.2 Crystal-Field Components, A_{nm}

The crystal-field components, A_{nm} ($\text{cm}^{-1}/\text{A}^n$), are calculated through $n = 6$ because of the possibility of rare-earth ions occupying these sites.

30.2.1 For Y ion in 16c (D_{3d}) site of reference 4 (rotated so that z-axis is parallel to (111) crystallographic axis)

A_{nm}	Monopole	Self-induced	Dipole	Total
A_{20}	8,240.0	-1128.5	364.00	7475.8
A_{40}	11,645	-3144.5	109.33	8610.3
A_{43}	3,006.4	-730.62	-1446.6	829.14
A_{60}	1,953.6	-972.14	-103.67	877.82
A_{63}	-850.91	268.34	260.36	-322.20
A_{66}	1,181.5	-389.33	-206.36	585.85

Y₂Ti₂O₇

30.2.2 For Ti ion in 16d (D_{3d}) site of reference 4 (rotated so that z-axis is parallel to (111) crystallographic axis)

A _{nm}	Monopole	Self-induced	Dipole	Total
A ₂₀	-19,051	1887.4	14,909	-2,255.2
A ₄₀	-14,726	5340.5	-5,416.7	-1,4802
A ₄₃	22,131	-8635.8	2,984.9	16,480
A ₆₀	4,242.0	-3071.0	292.87	1,463.5
A ₆₃	-651.50	363.80	1,355.4	1,067.7
A ₆₆	2,602.1	-1878.9	-47.720	675.50

30.2.3 For vacancy site, X, 8b (T_d) of reference 4

A _{nm}	Monopole	Self-induced	Dipole	Total
A ₃₂	-39,176	592.38	-790.43	38,978
A ₄₀	34,880	-6419.5	6321.3	34,782
A ₄₄	-20,845	3836.4	-3777.7	-20,786
A ₆₀	-708.11	-769.29	458.09	-10,19.3
A ₆₄	1,324.7	1439.2	-857.02	1,906.9
A ₇₂	-1,152.4	-66.33	0.164	-1,218.6
A ₇₆	1,060.1	61.01	-0.151	1,127.0

30.2.4 For Y ion in 16d (D_{3d}) site of reference 2 (rotated so that z-axis is parallel to (111) crystallographic axis)

A _{nm}	Monopole	Self-induced	Dipole	Total
A ₂₀	8,287.8	-1156.5	387.95	7519.2
A ₄₀	11,686	-3152.3	83.620	8616.9
A ₄₃	2,885.0	-704.81	-1367.9	812.26
A ₆₀	1,951.9	-974.79	-92.36	884.77
A ₆₃	-830.75	258.58	246.83	-325.34
A ₆₆	1,167.4	-380.73	-196.75	589.93

30.2.5 For Ti ion 16c (D_{3d}) site of reference 2 (rotated so that z-axis is parallel to (111) crystallographic axis)

A _{nm}	Monopole	Self-induced	Dipole	Total
A ₂₀	-17,718	1800.6	14,730	-1,187.9
A ₄₀	-15,256	5588.2	-5,256.1	-14,924.11
A ₄₃	22,458	-8832.3	2,832.7	16,458
A ₆₀	4,281.6	-3127.7	221.09	1,374.9
A ₆₃	-528.42	271.33	1,370.2	1,113.2
A ₆₆	26,070	-1898.32	-57.96	650.70

30.2.6 For vacancy site, X, 8a (T_d) of reference 2

A_{nm}	Monopole	Self-induced	Dipole	Total
A_{32}	39,189	596.74	-757.44	39,028
A_{40}	35,555	-6746.5	6306.3	35,114.626
A_{44}	-21,248	4031.8	-3768.8	-20,985
A_{60}	-668.40	-812.34	462.050	-1,018.7
A_{64}	1,250.5	1519.7	-864.417	1,905.8
A_{72}	-1,157.4	-66.723	0.208	-1,223.9
A_{76}	1,064.6	61.376	-0.191	1,125.8

30.3 Experimental Parameters (cm^{-1}) (reference 1)

Ion	nd^N	$F^{(2)}$	$F^{(4)}$	B_{40}
V^{3+}	$3d^2$	63,217	41,378	-23,590
Cr^{3+}	$3d^3$	59,444	38,909	-25,970
Mn^{3+}	$3d^4$	--	--	-28,168
Co^{3+}	$3d^6$	56,630	34,020	-23,730
Mn^{4+}	$3d^3$	--	--	-31,822
Co^{2+}	$3d^7$	65,835	43,092	-8,330
Ni^{2+}	$3d^8$	84,420	61,110	-12,180

30.4 Bibliography and References

1. V. A. Antonov and P. A. Arsenev, Spectroscopic Properties of Single Crystals of Rare Earth Titanates, *Phys. Status Solidi A35* (1976), K169.
2. W.-J. Becker, Elektronen-Spin-Resonanz und optische Untersuchungen an Cr-Dotierten Y-Ti-Pyrochlor-Einkristall $Y_2Ti_2O_7$, *Z. Naturforsch.* 25a (1970), 642. Also W.-J. Becker and G. Will, Rontgen und Neutronenbeugungsuntersuchungen an $Y_2Ti_2O_7$, *Z. Kristallogr. Kristallgeom. Kristallphys. Kristallchem.* 131 (1970), 278.
3. S. Fraga, K.M.S. Saxena, and J. Karwowski, *Handbook of Atomic Data*, Elsevier, New York (1976).
4. O. Knop, F. Brisse, L. Castelliz, and O. Sutarno, Determination of the Crystal Structure of Erbium Titanate, $Er_2Ti_2O_7$, by X-ray and Neutron Diffraction, *Can. J. Chem.* 43 (1965), 2812. Also, O. Knop, F. Brisse, and L. Castelliz, Pyrochlores: V.--Thermoanalytic, X-ray, Neutron, Infrared, and Dielectric Studies of $A_2Ti_2O_7$ Titanates, *Can. J. Chem.* 47 (1969), 971. Also see R.W.G. Wyckoff, *Crystal Structures*, vol. 3, Interscience, New York (1968), 441.

$Y_2Ti_2O_7$

5. K. A. Kuvshinova, M. L. Meil'man, A. G. Smagin, R. Yu. Abdulseribo, V. A. Antonov, P. A. Ansen'ev, and L. B. Pasternak, Structure of Active Centers in Manganese-Doped Single Crystals of Yttrium Titanate $Y_2Ti_2O_7$, Sov. Phys. Crystallogr. 28 (1983), 198.
6. P. C. Schmidt, A. Weiss, and T. P. Das, Effect of Crystal Fields and Self-Consistency on Dipole and Quadrupole Polarizabilities of Closed-Shell Ions, Phys. Rev. B19 (1979), 5525.

K_2ReCl_6

4. P. C. Schmidt, A. Weiss, and T. P. Das, Effect of Crystal Fields and Self-Consistency on Dipole and Quadrupole Polarizabilities of Closed-Shell Ions, Phys. Rev. B19 (1979), 5525.
5. R.W.G. Wyckoff, Crystal Structures, vol. 3, Interscience, New York, (1968), 339.

31. K_2ReCl_6

31.1 Crystallographic Data on K_2ReCl_6

Cubic O_h^5 (Fm3m), 225, $Z = 4$

Ion	Site	Symmetry	x^a	y	z	q	α (\AA^3)
Re	4a	O_h	0	0	0	4	0.70 ^b
K	8c	T_d	1/4	1/4	1/4	1	0.827 ^c
Cl	24e	C_{4v}	x	0	0	-1	2.694 ^c

^aX-ray data: $a = 9.861 \text{ \AA}$, $x = 0.240$ (reference 5).

^bReference 3.

^cReference 4.

31.2 Crystal-field Components, A_{nm} ($\text{cm}^{-1}/\text{\AA}^n$), for Re (O_h) Site

A_{nm}	Monopole	Self-induced	Dipole	Total
A_{40}	5793.3	-4601.3	9735.1	10,927
A_{44}	3462.2	-2749.8	5817.9	6,530.2

31.3 Experimental Parameters (cm^{-1})

Ion	nd^N	$F^{(2)}$	$F^{(4)}$	ζ	B_{40}	Ref.
Re^{4+}	$5d^3$	31,891	20,928	2328	90,564	2

31.4 Bibliography and References

1. P. B. Dorain, Magnetic and Optical Properties of Transition Metal Ions in Single Crystals, Aerospace Laboratories Report, ARL-73-0139 (October 1973), NTIS AD 769870.
2. J. C. Eisenstein, Magnetic Properties and Optical Absorption Spectrum of K_2ReCl_6 , J. Chem. Phys. 34 (1961), 1628. (This reference gives a large number of constants used in Eisenstein's calculation. We have taken his reported calculation and best fit it to obtain the parameters in sect. 31.3 above.)
3. S. Fraga, K.M.S. Saxena, and J. Karwowski, Handbook of Atomic Data, Elsevier, New York (1976).

32. A_2BF_6 ($\text{A} = \text{K, Rb, Cs}$; $\text{B} = \text{Ge, Zr}$)

32.1 Crystallographic Data on A_2BF_6

Hexagonal D_{3d}^3 ($\text{P}\bar{3}\text{m}1$), 164, $Z = 1$

Ion	Site	Symmetry	x	y	z	q	α (\AA^3)
B	1(a)	D_{3d}	0	0	0	4	α_B
A	2(d)	C_{3v}	1/3	2/3	z	1	α_A
F	6(i)	C_s	x	-x	z	-1	0.731

32.2 X-Ray Data

A	B	a (\AA) ^a	c (\AA)	z_A	x_F	z_F	α_A (\AA^3) ^b	α_B (\AA^3) ^c
K	Ge	5.62	4.65	0.70	0.148	0.220	0.827	0.12
Rb	Ge	5.82	4.79	0.695	0.144	0.213	1.383	0.12
Cs	Zr	6.41	5.01	0.692	0.16	0.198	2.492	0.48
Rb	Zr	6.16	4.82	0.691	0.167	0.206	1.383	0.48

^aReference 7.

^bReference 6.

^cReference 4.

32.3 Crystal-Field Components, A_{nm} ($\text{cm}^{-1}/\text{\AA}^n$)

32.3.1 For Ge (D_{3d}) site of K_2GeF_6

A_{nm}	Monopole	Self-induced	Dipole	Total
A_{20}	3,371.0	-52.7	-2,040.3	1,277.9
A_{40}	-15,618	8,667.1	-18,481	-25,432
A_{43}	19,236	-10,270	23,136	32,103

32.3.2 For Ge site (D_{3d}) site of Rb_2GeF_6

A_{nm}	Monopole	Self-induced	Dipole	Total
A_{20}	2,187.4	89.8	-2,279.8	-2.610
A_{40}	-15,138	8310.5	-17,768	-24,595
A_{43}	18,831	-9956.6	22,422	31,296

A_2BF_6 32.3.3 For Zr (D_{3d}) site of Cs_2ZrF_6

A_{nm}	Monopole	Self-induced	Dipole	Total
A_{20}	-10,846	1089.7	-4014.2	-13,771
A_{40}	-5,354.3	1942.2	-4819.3	-8,231.4
A_{43}	9,810	-3407.0	8328.6	14,732

32.3.4 For Zr (D_{3d}) site of Rb_2ZrF_6

A_{nm}	Monopole	Self-induced	Dipole	Total
A_{20}	-11,003	1047.3	-3653.0	-13,608
A_{40}	-5,288.4	1888.9	-4747.9	-8,147.4
A_{43}	9,737.6	-3347.2	8207.6	14,598

32.4 Bibliography and References

1. A. M. Black and C. D. Flint, Splitting of the Γ_{8g} (4A_2) Ground State in Cs_2ReF_6 , *J. Mol. Phys.* 70 (1978), 481.
2. G. R. Clark and D. R. Russell, Potassium Hexafluororhenate (IV), *Acta Crystallogr.* B34 (1978), 894.
3. R. L. Davidovich and T. A. Kaidalova, Ammonium Hexafluorostannate and Hexafluoroplumbate, *Russ. J. Inorg. Chem.* 16 (1971), 1354.
4. S. Fraga, K.M.S. Saxena, and J. Karwowski, *Handbook of Atomic Data*, Elsevier, New York (1976).
5. F. Hanic, The Crystal Chemistry of Complex Fluorides of General Formula A_2MF_6 , The Refinement of the Structure $(NH_4)_2SiF_6$, *Chem. Zvesti* 20 (1966), 738.
6. P. C. Schmidt, A. Weiss, and T. P. Das, Effect of Crystal Fields and Self-Consistency on Dipole and Quadrupole Polarizabilities of Closed-Shell Ions, *Phys. Rev.* B19 (1979), 5525.
7. R.W.G. Wyckoff, *Crystal Structures*, vol. 3, Interscience, New York (1968), 349.

Rb_2SnCl_6

5. C. D. Flint and A. G. Paulusz, Infrared Luminescence Spectra of Hexabromoiridate (IV) and Hexabrooiridate (IV) in Cubic Crystals, *Inorg. Chem.* 20 (1981), 1768.
6. C. D. Flint and A. G. Paulusz, Infrared Luminescence of the ReBr_6^{2-} Ion, *Chem. Phys. Lett.* 62 (1979), 259.
7. S. Fraga, K.M.S. Saxena, and J. Karwowski, *Handbook of Atomic Data*, Elsevier, New York (1976).
8. P. C. Schmidt, A. Weiss, and T. P. Das, Effect of Crystal Fields and Self-Consistency on Dipole and Quadrupole Polarizabilities of Closed-Shell Ions, *Phys. Rev. B19* (1979), 5525.
9. H.-H. Schmidtke and D. Strand, The Emission Spectrum of OsCl_6^{2-} Doped in Various Cubic Host Lattices, *Inorg. Chim. Acta* 62 (1982), 153.
10. T. Schönherr, R. Wernicke, and H.-H. Schmidtke, *Spectrochim. Acta* 38A (1982), 679.
11. V. Waschk and J. Pelzl, Raman Bands and Phase Transitions in $(\text{A}_x\text{K}_{1-x})\text{SnCl}_6$ Solid Solutions (A = Rb, NH_4), *Raman Spectrosc. Proc. Int. Conf. 8th*, Ed. J. Lascombe et al (1982), 413.
12. R.W.G. Wyckoff, *Crystal Structures*, vol. 3, Interscience, New York, (1968), 339.

33. Rb_2SnCl_6

33.1 Crystallographic Data on Rb_2SnCl_6

Cubic O_h^5 (Fm3m), 225, $Z = 4$

Ion	Site	Symmetry	x ^a	y	z	q	α (\AA^3)
Sn	4(a)	O_h	0	0	0	4	0.37 ^b
Rb	8(c)	T_d	1/4	1/4	1/4	1	1.383 ^c
Cl	24(e)	C_{4v}	x	0	0	-1	2.694 ^c

^aX-ray data: $a = 10.118 \text{ \AA}$, $x = 0.240$ (reference 12).

^bReference 7.

^cReference 8.

33.2 Crystal-Field Components, A_{nm} ($\text{cm}^{-1}/\text{\AA}^n$), for Sn (O_h) Site

A_{nm}	Monopole	Self-induced	Dipole	Total
A_{40}	5094.0	-3739.2	8166.3	9521.1
A_{44}	3044.3	-2234.6	4880.3	5689.9

33.3 Experimental Parameters (cm^{-1})

Ion	nd^N	$F^{(2)}$	$F^{(4)}$	ζ	B_{40}	Ref
Os^{4+}	d^4	28,549	17,365	2606	40,198	9

33.4 Bibliography and References

1. A. Black and C. D. Flint, Luminescence Spectra and Relaxation Processes of ReCl_6^{2-} in Cubic Crystals, J. Chem. Soc. Faraday Trans. 2 73 (1977), 877.
2. A. Black and C. D. Flint, Jahn-Teller Effect in the $\Gamma_8(^2T_{2g}, t_{2g}^3)$ State of ReBr_6^{2-} , J. Chem. Soc. Faraday Trans. 2 71 (1975), 1871.
3. P. B. Dorain, Magnetic and Optical Properties of Transition Metal Ions in Single Crystals, Aerospace Laboratories Report, ARL-73-0139 (October 1973), NTIS AD 769870.
4. C. D. Flint and A. G. Paulusz, High Resolution Infrared and Visible Luminescence Spectra of ReCl_6^{2-} and ReBr_6^{2-} in Cubic Crystals, Mol. Phys. 43 (1981), 321.

Cs_2TeCl_6

7. H.-H. Schmidtke and D. Strand, The Emission Spectrum of OsCl_6^{2-} Doped in Various Cubic Host Lattices, *Inorg. Chim. Acta* 62 (1982), 153.
8. R.W.G. Wyckoff, *Crystal Structures*, vol. 3, Interscience, New York (1968), 339.

34. Cs_2TeCl_6

34.1 Crystallographic Data on Cs_2TeCl_6

Cubic O_h^5 (Fm $\bar{3}m$), 225, $Z = 4$

Ion	Site	Symmetry	x^a	y	z	q	α [\AA^3]
Te	4(a)	O_h	0	0	0	4	1.21 ^b
Cs	8(c)	T_d	1/4	1/4	1/4	1	2.492 ^c
Cl	24(e)	C_{4v}	x	0	0	-1	2.694 ^c

^aX-ray data: $a = 10.447 \text{ \AA}$, $x = 0.240$.

^bReference 5.

^cReference 6, reference 8.

34.2 Crystal-Field Components, A_{nm} ($\text{cm}^{-1}/\text{\AA}^n$) for Te (O_h) Site

A_{nm}	Monopole	Self-induced	Dipole	Total
A_{40}	4340.9	-2885.2	6549.2	8004.9
A_{44}	2594.2	-1724.2	3913.9	4783.9

34.3 Bibliography and References

1. P. B. Dorain, Magnetic and Optical Properties of Transition Metal Ions in Single Crystals, Aerospace Laboratories Report, ARL-73-0139 (October 1973), NTIS AD 769870.
2. C. D. Flint, Luminescence Spectra and Relaxation Processes of ReCl_6^{2-} in Cubic Crystals, J. Chem. Soc. Faraday Trans. 2 74 (1978), 767.
3. C. D. Flint and P. Lang, Infrared and Visible Luminescence of TeX_6^{2-} Cubic Crystals, J. Lumin. 24/25 (1981), 301.
4. C. D. Flint and A. G. Paulusz, High Resolution Infrared and Visible Luminescence Spectra of ReCl_6^{2-} and ReBr_6^{2-} in Cubic Crystals, Mol. Phys. 43 (1981), 321.
5. S. Fraga, K.M.S. Saxena, and J. Karwowski, Handbook of Atomic Data, Elsevier, New York (1976).
6. P. C. Schmidt, A. Weiss, and T. P. Das, Effect of Crystal Fields and Self-Consistency on Dipole and Quadrupole Polarizabilities of Closed-Shell Ions, Phys. Rev. B19 (1979), 5525.

35. K_2ReF_6

35.1 Crystallographic Data on K_2ReF_6

Hexagonal D_{3d}^3 ($P\bar{3}m1$), 164, $Z = 1$

Ion	Site	Symmetry	x ^a	y	z	q	α (\AA^3)
Re	1(a)	D_{3d}	0	0	0	4	0.70 ^b
K	2(d)	C_{3v}	1/3	2/3	0.3007	1	0.827 ^c
F	6(i)	C_s	0.1617	-0.167	0.2276	-1	0.731 ^c

^aX-ray data: $a = 5.879 \text{ \AA}$, $c = 4.611 \text{ \AA}$ (reference 2).

^bReference 3.

^cReference 4.

35.2 Crystal-Field Components, A_{nm} ($\text{cm}^{-1}/\text{\AA}^n$), for Re (D_{3d}) Site

A_{nm}	Monopole	Self-induced	Dipole	Total
A_{20}	-4,231	592.3	-2741	-6380
A_{40}	-8,445	3421	-7791	-12815
A_{43}	-12,038	4732	-11291	-18597

35.3 Experimental Parameters (cm^{-1})

Ion	nd^N	$F^{(2)}$	$F^{(4)}$	ζ	B_{20}	B_{40}	B_{43}	Ref
Re^{4+}	$5d^3$	41,076	25,409	2612	-7136	-33,993	44,925	1

35.4 References

1. M. Bettinelli, L. Di Sipio, G. Ingletto, A. Montenero, and C. D. Flint, Polarized Electronic Absorption Spectra of the Trigonal Crystal K_2ReF_6 , *Mol. Phys.* 56 (1985), 1033.
2. G. R. Clark and D. R. Russell, Potassium Hexafluororhenate (IV), *Acta Crystallogr.* B34 (1978), 894.
3. S. Fraga, K.M.S. Saxena, and J. Karwowski, *Handbook of Atomic Data*, Elsevier, New York (1976).
4. P. C. Schmidt, A. Weiss, and T. P. Das, Effect of Crystal Fields and Self-Consistency on Dipole and Quadrupole Polarizabilities of Closed-Shell Ions, *Phys. Rev.* B19 (1979), 5525.

36. Cs_2ZrCl_6

36.1 Crystallographic Data on Cs_2ZrCl_6

Cubic O_h^5 ($\text{Fm}3m$), 225, $Z = 4$

Ion	Site	Symmetry	x ^a	y	z	q	α (\AA^3)
Zr	4(a)	O_h	0	0	0	4	0.48 ^b
Cs	8(c)	T_d	1/4	1/4	1/4	1	2.492 ^c
Cl	24(e)	C_{4v}	x	0	0	-1	2.694 ^c

^aX-ray data: $a = 10.407 \text{ \AA}$, $x = 0.235$ (reference 13).

^bReference 6.

^cReference 11.

36.2 Crystal-Field Components, A_{nm} ($\text{cm}^{-1}/\text{\AA}^n$), for Zr (O_h) Site

A_{nm}	Monopole	Self-induced	Dipole	Total
A_{40}	4883.9	-3524.3	7742.1	9101.6
A_{44}	2918.7	-2106.2	4626.8	5439.3

36.3 Experimental Parameters (cm^{-1})

Ion	nd^N	$F^{(2)}$	$F^{(4)}$	ζ	B_{40}	Ref.
Ru ⁴⁺	4d ⁴	48,888	17,173	1044	39,732	9
Re ⁴⁺	5d ³	28,749	22,906	2392	63,729	5
Os ⁴⁺	5d ⁴	45,381	16,329	2416	47,229	4

36.4 Bibliography and References

1. J. F. Ackerman, Preparation and Luminescence of Some $[\text{K}_2\text{PtCl}_6]$ Materials, Mater. Res. Bull. 19 (1984), 783.
2. J. C. Collingwood, P. N. Schatz, and P. J. McCarthy, Absorption and Magnetic Circular Dichroism Spectra of Ru⁴⁺ in Cs_2ZrCl_6 and Cs_2SnBr_6 , Mol. Phys. 30 (1975), 269.
3. P. B. Dorain, Magnetic and Optical Properties of Transition Metal Ions in Single Crystals, Aerospace Laboratories Report, ARL-73-0139 (October 1973), NTIS AD 769870.
4. P. B. Dorain, H. H. Patterson, and P. C. Jordan, Optical Spectra of Os⁴⁺ in Single Cubic Crystals at 4.2°, J. Chem. Phys. 49 (1968), 3845.

5. P. B. Dorain and R. G. Wheeler, Optical Spectrum of Re^{4+} in Single Crystals of K_2PtCl_6 and Cs_2ZrCl_6 at $4.2^\circ K$, *J. Chem. Phys.* 45 (1966), 1172.
6. S. Fraga, K.M.S. Saxena, and J. Karwowski, *Handbook of Atomic Data*, Elsevier, New York (1976).
7. S. M. Khan, H. H. Patterson, and H. Engstrom, Multiple State Luminescence for the $d^4 OsCl_6^{2-}$ Impurity Ion in K_2PtCl_6 and Cs_2ZrCl_6 Cubic Crystals, *Mol. Phys.* 35 (1978), 1623.
8. B. A. Kozikowski and T. A. Keiderling, Intraconfigurational Absorption and Magnetic Circular Dichroism Spectra of Os^{4+} in Cs_2ZrCl_6 and in Cs_2ZrBr_6 , *Mol. Phys.* 40 (1980), 477.
9. H. Patterson and P. Dorain, Optical Spectra of Ru^{4+} in Single Crystals of K_2PtCl_6 and Cs_2ZrCl_6 at $4.2^\circ K$, *J. Chem. Phys.* 52 (1970), 849.
10. A. R. Reinberg and S. G. Parker, Sharp-Line Luminescence of Re^{4+} in Cubic Single Crystals of Cs_2ZrCl_6 and Cs_2HfCl_6 , *Phys. Rev. B* 1 (1970), 2085.
11. P. C. Schmidt, A. Weiss, and T. P. Das, Effect of Crystal Fields and Self-Consistency on Dipole and Quadrupole Polarizabilities of Closed-Shell Ions, *Phys. Rev. B* 19 (1979), 5525.
12. H.-H. Schmidtke and D. Strand, The Emission Spectrum of $OsCl_6^{2-}$ Doped in Various Cubic Host Lattices, *Inorg. Chim. Acta*, 62 (1982), 153.
13. R.W.G. Wyckoff, *Crystal Structures*, vol. 3, Interscience, New York (1968), 339..
14. R. K. Yoo and T. A. Keiderling, Intraconfigurational Absorption Spectroscopy of $IrCl_6^{2-}$ and $IrBr_6^{2-}$ in A_2MX_6 -Type Host Crystals, *Chem. Phys.* 108 (1986), 317.

Acknowledgements

We thank Norman Brandt of the HDL library for his timely and cheerful response to our many requests for information searches and copies of documents from obscure sources. We wish to thank Art Linz, Hans Janssen, and Brian Aull of MIT for suggestions of a number of materials referenced here. Particular thanks are due to Dave Gabbe of MIT for suggesting and supplying information on the fluoride garnets. Rudy Buser and Al Pinto of NVEOL, Fort Belvoir, are thanked for support and suggesting materials. Suggestions of host materials were made by John Gruber of San Jose State University, Leon Esterowitz of the Naval Research Laboratory, Toom Allik of SAIC, and Norman Barnes of NASA Langley Research Center.

I would like to thank the high school students whose companionship during the summer months was much fun and who did much of the labor included here: Betsy Wong, Susan Wong, Ken Wong, Ronald Lee, Glen Lee, Mandy Hansen, and Barry Reich.

Lastly many thanks are due my coworkers, Rich Leavitt, John Bruno, and Greg Turner.

DISTRIBUTION

ADMINISTRATOR DEFENSE TECHNICAL INFORMATION CENTER ATTN DTIC-DDA (12 COPIES) CAMERON STATION, BUILDING 5 ALEXANDRIA, VA 22314	DIRECTOR US ARMY ELECTRONICS WARFARE LABORATORY ATTN J. CHARLTON ATTN DELET-DD FT MONMOUTH, NJ 07703
DIRECTOR NIGHT VISION & ELECTRO-OPTICS LABORATORY ATTN TECHNICAL LIBRARY ATTN R. BUSER ATTN A. PINTO ATTN J. HABERSAT ATTN R. RHODE ATTN W. TRESSEL FT BELVOIR, VA 22060	COMMANDING OFFICER USA FOREIGN SCIENCE & TECHNOLOGY CENTER FEDERAL OFFICE BUILDING ATTN DRXST-BS, BASIC SCIENCE DIV CHARLOTTESVILLE, VA 22901
DIRECTOR DEFENSE ADVANCED RESEARCH PROJECTS AGENCY ATTN J. FRIEBELE 1400 WILSON BLVD ARLINGTON, VA 22209	COMMANDER US ARMY MATERIALS & MECHANICS RESEARCH CENTER ATTN DRXMR-TL, TECH LIBRARY WATERTOWN, MA 02172
DIRECTOR DEFENSE NUCLEAR AGENCY ATTN TECH LIBRARY WASHINGTON, DC 20305	US ARMY MATERIEL COMMAND 5001 EISENHOWER AVE ALEXANDRIA, VA 22333-0001
UNDER SECRETARY OF DEFENSE RES & ENGINEERING ATTN TECHNICAL LIBRARY, 3C128 WASHINGTON, DC 20301	US ARMY MATERIEL SYSTEMS ANALYSIS ACTIVITY ATTN DRXSY-MP (LIBRARY) ABERDEEN PROVING GROUND, MD 21005
OFFICE OF THE DEPUTY CHIEF OF STAFF, FOR RESEARCH, DEVELOPMENT, & ACQUISITION DEPARTMENT OF THE ARMY ATTN DAMA-ARZ-B, I. R. HERSHNER WASHINGTON, DC 20310	COMMANDER US ARMY MISSILE & MUNITIONS CENTER & SCHOOL ATTN ATSK-CTD-F ATTN DRDMM-TB, REDSTONE SCI INFO CENTER REDSTONE ARSENAL, AL 35809
COMMANDER US ARMY ARMAMENT MUNITIONS & CHEMICAL COMMAND (AMCCOM) US ARMY ARMAMENT RESEARCH & DEVELOPMENT CENTER ATTN DRDAR-TSS, STINFO DIV DOVER, NJ 07801	COMMANDER US ARMY RESEARCH OFFICE (DURHAM) PO BOX 12211 ATTN ROBERT J. LONTZ ATTN M. STROSIO ATTN M. CIFTAN ATTN B. D. GUENTHER ATTN CHARLES BOGOSIAN RESEARCH TRIANGLE PARK, NC 27709
COMMANDER ATMOSPHERIC SCIENCES LABORATORY ATTN TECHNICAL LIBRARY WHITE SANDS MISSILE RANGE, NM 88002	COMMANDER US ARMY RSCH & STD GRP (EUROPE) FPO NEW YORK 09510
DIRECTOR US ARMY BALLISTIC RESEARCH LABORATORY ATTN SLCBR-DD-T (STINFO) ABERDEEN PROVING GROUND, MD 21005	COMMANDER US ARMY TEST & EVALUATION COMMAND ATTN D. H. SLINEY ATTN TECH LIBRARY ABERDEEN PROVING GROUND, MD 21005

DISTRIBUTION (cont'd)

COMMANDER US ARMY TROOP SUPPORT COMMAND ATTN DRXRES-RTL, TECH LIBRARY NATICK, MA 01762	AEROSPACE CORPORATION PO BOX 92957 ATTN M. BIRNBAUM ATTN N. C. CHANG ATTN T. S. ROSE LOS ANGELES, CA 90009
OFFICE OF NAVAL RESEARCH ATTN J. MURDAY ARLINGTON, VA 22217	ALLIED ADVANCED APPLICATION DEPT ATTN A. BUDGOR 31717 LA TIENDA DRIVE WESTLAKE VILLAGE, CA 91362
DIRECTOR NAVAL RESEARCH LABORATORY ATTN CODE 2620, TECH LIBRARY BR ATTN G. QUARLES ATTN G. KINTZ ATTN A. ROSENBAUM ATTN G. RISENBLATT ATTN CODE 5554, F. BARTOLI ATTN CODE 5554, L. ESTEROWITZ ATTN CODE 5554, R. E. ALLEN WASHINGTON, DC 20375	ALLIED SIGNAL INC. ATTN Y. BAND ATTN R. MORRIS POB 1021R MORRISTOWN, NJ 07960
COMMANDER NAVAL WEAPONS CENTER ATTN CODE 3854, R. SCHWARTZ ATTN CODE 3854, M. HILLS ATTN CODE 3844, M. NADLER ATTN CODE 385, R. L. ATKINS ATTN CODE 343, TECHNICAL INFORMATION DEPARTMENT CHINA LAKE, CA 93555	AMES LABORATORY DOE IOWA STATE UNIVERSITY ATTN K. A. GSCHNEIDNER, JR. (2 COPIES) AMES, IA 50011
AIR FORCE OFFICE OF SCIENTIFIC RESEARCH ATTN MAJOR H. V. WINSOR, USAF BOLLING AFB WASHINGTON, DC 20332	ARGONNE NATIONAL LABORATORY ATTN W. T. CARNALL 9700 SOUTH CASS AVENUE ARGONNE, IL 60439
HQ, USAF/SAMI WASHINGTON, DC 20330	BOOZ, ALLEN AND HAMILTON ATTN W. DROZDOSKI 4330 EAST WEST HWY BETHESDA, MD 20814
DEPARTMENT OF COMMERCE NATIONAL BUREAU OF STANDARDS ATTN LIBRARY WASHINGTON, DC 20234	BRIMROSE CORP OF AMERICA ATTN R. G. ROSEMEIER 7527 BELAIR ROAD BALTIMORE, MD 21236
NASA Langley Research Center ATTN N. P. BARNES (2 COPIES) ATTN G. ARMAGAN ATTN P. CROSS ATTN D. GETTENY ATTN J. BARNES ATTN E. FILER ATTN C. BAIR ATTN N. BOUNCRISHANI HAMPTON, VA 23665	DRAPER LAB ATTN F. HAKIMI MS 53 555 TECH. SQ CAMBRIDGE, MA 02139
DIRECTOR ADVISORY GROUP ON ELECTRON DEVICES ATTN SECTRY, WORKING GROUP D 201 VARICK STREET NEW YORK, NY 10013	ENGINEERING SOCIETIES LIBRARY ATTN ACQUISITIONS DEPT 345 EAST 47TH STREET NEW YORK, NY 10017
	FIBERTECH INC. ATTN H. R. VERDIN (3 COPIES) 510-A HERNDON PKWY HERNDON, VA 22070
	HUGHES AIRCRAFT COMPANY ATTN D. SUMIDA 3011 MALIBU CANYON RD MALIBU, CA 90265

DISTRIBUTION (cont'd)

IBM RESEARCH DIVISION
 ALMADEN RESEARCH CENTER
 ATTN R. M. MACFARLANE
 MAIL STOP K32 802(D)
 650 HARRY ROAD
 SAN JOSE, CA 95120

DIRECTOR
 LAWRENCE RADIATION LABORATORY
 ATTN MARVIN J. WEBER
 ATTN HELMUT A. KOEHLER
 ATTN W. KRUPKE
 LIVERMORE, CA 94550

MARTIN MARIETTA
 ATTN F. CROWNE
 ATTN J. LITTLE
 ATTN T. WORCHESKY
 ATTN D. WORTMAN
 1450 SOUTH ROLLING ROAD
 BALTIMORE, MD 21227

MIT LINCOLN LAB
 PO BOX 73
 ATTN B. AULL
 LEXINGTON, MA 02173

DEPARTMENT OF MECHANICAL, INDUSTRIAL,
 & AEROSPACE ENGINEERING
 PO BOX 909
 ATTN S. TEMKIN
 PISCATAWAY, NJ 08854

NATIONAL OCEANIC & ATMOSPHERIC ADM
 ENVIRONMENTAL RESEARCH LABS
 ATTN LIBRARY, R-51, TECH RPTS
 BOULDER, CO 80302

OAK RIDGE NATIONAL LABORATORY
 ATTN R. G. HAIRE
 OAK RIDGE, TN 37830

W. J. SCHAFER ASSOC.
 ATTN J. W. COLLINS
 321 BILLERICA ROAD
 CHELMSFORD, MA 01824

SCIENCE APPLICATIONS, INTERNATIONAL CORP.
 ATTN T. ALLIK
 1710 GOODRIDGE DRIVE
 McLEAN, VA 22102

UNION CARBIDE CORP
 ATTN M. R. KOKTA
 ATTN J. H. W. LIAW
 750 SOUTH 32ND STREET
 WASHOUGAL, WA 98671

ARIZONA STATE UNIVERSITY
 DEPT OF CHEMISTRY
 ATTN L. EYRING
 TEMPE, AZ 85281

CARNEGIE MELLON UNIVERSITY
 SCHENLEY PARK
 ATTN PHYSICS & EE, J. O. ARTMAN
 PITTSBURGH, PA 15213

COLORADO STATE UNIVERSITY
 PHYSICS DEPARTMENT
 ATTN S. KERN
 FORT COLLINS, CO 80523

UNIVERSITY OF CONNECTICUT
 DEPARTMENT OF PHYSICS
 ATTN R. H. BARTRAM
 STORRS, CT 06269

UNIVERSITY OF SOUTH FLORIDA
 PHYSICS DEPT
 ATTN R. CHANG
 ATTN SENGUPTA
 TAMPA, FL 33620

JOHNS HOPKINS UNIVERSITY
 DEPT OF PHYSICS
 ATTN B. R. JUDD
 BALTIMORE, MD 21218

KALAMAZOO COLLEGE
 DEPT OF PHYSICS
 ATTN K. RAJNAK
 KALAMAZOO, MI 49007

MASSACHUSETTS INSTITUTE OF TECHNOLOGY
 CRYSTAL PHYSICS LABORATORY
 ATTN H. P. JENSEN
 ATTN A. LINZ
 CAMBRIDGE, MA 02139

MASSACHUSETTS INSTITUTE OF TECHNOLOGY
 77 MASS AVE
 ROOM 26-251
 ATTN V. BAGNATO
 CAMBRIDGE, MA 02139

UNIVERSITY OF MINNESOTA, DULUTH
 DEPARTMENT OF CHEMISTRY
 ATTN L. C. THOMPSON
 DULUTH, MN 55812

OKLAHOMA STATE UNIVERSITY
 DEPT OF PHYSICS
 ATTN R. C. POWELL
 STILLWATER, OK 74078

DISTRIBUTION (cont'd)

PENNSYLVANIA STATE UNIVERSITY
MATERIALS RESEARCH LABORATORY
ATTN W. B. WHITE
UNIVERSITY PARK, PA 16802

PRINCETON UNIVERSITY
DEPARTMENT OF CHEMISTRY
ATTN D. S. McCCLURE
PRINCETON, NJ 08544

SAN JOSE STATE UNIVERSITY
DEPARTMENT OF PHYSICS
ATTN J. B. CRUBER
SAN JOSE, CA 95192

SETON HALL UNIVERSITY
CHEMISTRY DEPARTMENT
ATTN H. BRITTAINE
SOUTH ORANGE, NJ 07099

UNIVERSITY OF VIRGINIA
DEPT OF CHEMISTRY
ATTN DR. F. S. RICHARDSON (2 COPIES)
ATTN DR. M. REID
CHARLOTTESVILLE, VA 22901

UNIVERSITY OF WISCONSIN
CHEMISTRY DEPARTMENT
ATTN J. WRIGHT
ATTN B. TISSUE
MADISON, WI 53706

US ARMY LABORATORY COMMAND
ATTN TECHNICAL DIRECTOR, AMSLC-CT

INSTALLATION SUPPORT ACTIVITY
ATTN LEGAL OFFICE, SLCIS-CC
ATTN S. ELBAUM, SLCIS-CC

USAISC
ATTN TECHNICAL REPORTS BRANCH,
AMSLC-IM-TR (2 COPIES)

HARRY DIAMOND LABORATORIES
ATTN D/DIVISION DIRECTORS
ATTN HDL LIBRARY, SLCHD-TL (3 COPIES)
ATTN HDL LIBRARY, SLCHD-TL (WOODBRIDGE)

HARRY DIAMOND LABORATORIES

(cont'd)

ATTN CHIEF, SLCHD-NW-E
ATTN CHIEF, SLCHD-NW-EP
ATTN CHIEF, SLCHD-NW-EH
ATTN CHIEF, SLCHD-NW-ES
ATTN CHIEF, SLCHD-NW-R
ATTN CHIEF, SLCHD-NW-TN
ATTN CHIEF, SLCHD-NW-RP
ATTN CHIEF, SLCHD-NW-CS
ATTN CHIEF, SLCHD-NW-TS
ATTN CHIEF, SLCHD-NW-RS
ATTN CHIEF, SLCHD-NW-P
ATTN CHIEF, SLCHD-PO
ATTN CHIEF, SLCHD-ST-C
ATTN CHIEF, SLCHD-ST-RS
ATTN CHIEF, SLCHD-ST-RP
ATTN CHIEF, SLCHD-TT

ATTN WILLIS, B., SLCHD-TA-ET
ATTN ZABLUDOWSKI, B., SLCHD-TA-ET
ATTN KENYON, C. S., SLCHD-NW-EP
ATTN MILETTA J. R., SLCHD-NW-EP
ATTN MCLEAN, F. B., SLCHD-NW-RP
ATTN LIBELO, L., SLCHD-ST-MW
ATTN BENCIVENGA, A. A., SLCHD-ST-SP
ATTN SATTLER, J., SLCHD-PO-P
ATTN NEMARICH, J., SLCHD-ST-CB
ATTN WEBER, B., SLCHD-ST-CB
ATTN BAHDER, T., SLCHD-ST-AP
ATTN BENCIVENGA, B., SLCHD-TA-AS
ATTN BRODY, P., SLCHD-ST-AP
ATTN BRUNO, J., SLCHD-ST-AP
ATTN DROPKIN, H., SLCHD-ST-SP
ATTN EDWARDS, A., SLCHD-ST-AP
ATTN HAY, G., SLCHD-ST-AP
ATTN LEAVITT, R., SLCHD-ST-AP
ATTN SIMONIS, G., SLCHD-ST-AP
ATTN STEAD, M., SLCHD-ST-AP
ATTN STELLATO, J., SLCHD-ST-AP
ATTN TOBIN, M., SLCHD-ST-AP
ATTN TURNER, G., SLCHD-ST-AP
ATTN WORTMAN, D., SLCHD-ST-AP
ATTN GARVIN, C., SLCHD-ST-SS
ATTN GOFF, J., SLCHD-ST-SS
ATTN MORRISON, C., SLCHD-ST-AP (30 COPIES)

The findings in this report are not to be construed as an official Department of the Army position unless so designated by other authorized documents.

Citation of manufacturers' or trade names does not constitute an official endorsement or approval of the use thereof.

Destroy this report when it is no longer needed. Do not return it to the originator.